Alma Mater Studiorum · Università di Bologna

Scuola di Scienze
Dipartimento di Fisica e Astronomia
Corso di Laurea Magistrale in Fisica

High-energy behaviour of scattering amplitudes in the Standard Model Effective Field Theory

Relatore:
Prof. Fabio Maltoni

Correlatore:
Dott. Ken Mimasu

Presentata da:
Federico De Lillo

Anno Accademico 2018/2019

Sommario

L'attuale comprensione delle interazioni fondamentali tra i costituenti elementari della materia è contenuta all'interno di un quadro teorico denominato modello standard. La maggior parte delle sue predizioni è stata verificata anche a grandi precisioni nel corso dei decenni, grazie ad uno straordinario sforzo sperimentale e collettivo, a differenti scale energetiche. Incuranti di questo incredibile successo, osservazioni sperimentali insieme a motivazioni teoriche indicano l'esistenza di nuova fisica a scale più alte. Un approccio consistente che non dipende dal modello utilizzato per andare a sondare tali interazioni ad alte energie in maniera sistematica viene offerto dalle teorie efficaci di campo.
In questo lavoro, si studia un insieme di processi d'urto ad alte energie, nei quali sono coinvolte le particelle più pesanti del modello standard, quali il quark top, i bosoni vettori W e Z ed infine il bosone di Higgs. Il tutto viene fatto all'interno della teoria di campo efficace del modello standard, nella quale si estende il modello standard per mezzo di operatori di dimensione sei che rispettano le simmetrie di quelli a dimensione quattro. In particolare, si è interessati a valutare se i processi d'urto 2 in N possano fornire una maggiore sensibilità a nuova fisica, rispetto a processi 2 in 2 già ampiamente studiati.
L'analisi è suddivisa in due parti. Nella prima, di carattere maggiormente teorico, si determina per ogni processo il comportamento ad alte energie delle ampiezze di elicità, cercando segni di violazione di unitarietà della matrice S. Nella seconda parte, di carattere fenomenologico, i processi vengono immersi in degli stati iniziali-finali plausibili per un futuro collisore leptonico ad alte energie. Ciò permette di ottenere una stima della loro sensibilità ad una particolare classe di operatori e determinare se essi possano risultare utili nel migliorare gli attuali (o attesi) vincoli sui coefficienti di Wilson corrispondenti.

Abstract

Our current understanding of the fundamental interactions among the elementary constituents of matter is encapsulated in a theoretical framework called the standard model. Most of its predictions have been experimentally verified, some to a very high degree of accuracy, in an experimental effort which spans a large number of experiments conducted over several decades at different scales. Notwithstanding its amazing success, observations as well as theoretical arguments point to the existence of new physics at higher scales. A consistent and model-independent approach that can be used to systematically study interactions at very short distances, i.e. at high energy, is that of an effective field theory.

In this work, I present the study of several scattering processes at very high energy involving the heaviest degrees of freedom of the standard model, i.e. the top quark, the vector bosons W and Z, and the Higgs boson. I employ the framework of the standard model effective field theory, where the standard model is extended to include higher order operators of dimension six which are compatible with the local and global symmetries at dimension four. The main motivation for this work is to explore the possibly increased sensitivity to new physics of $2 \to N$ scattering amplitudes with respect to $2 \to 2$ processes which have been already considered.

The analysis is divided in two parts. In the first more theoretical part, the high-energy behaviour of the helicity amplitudes is evaluated for every core process, looking for footprints of S-matrix unitarity violation. In the second more phenomenological part, core processes are embedded in realistic initial-final states that can appear at future very high-energy lepton collider. This allows to estimate their sensitivity to a selected set of the standard model effective field theory operators and determine whether they can be useful to improve on the current (or expected) constraints on the corresponding Wilson coefficients.

Contents

Introduction

The discovery of the Higgs boson in 2012 has completed the Standard Model (SM), finding the last missing particle whose existence was foreseen almost 50 years ago.
The SM is a gauge theory based on $SU(3)_C \times SU(2)_L \times U(1)_Y$ local symmetries. It is renormalisable and describes the interactions among elementary particles, fermions and bosons, at the microscopic level. This theory is self consistent up to very high energy and it is in agreement with all the experimental data collected so far in terrestrial experiments. In fact, a wealth of data has been confronted with its predictions, always leading to an agreement at various level of accuracy, sometimes astonishing.
Nevertheless, several open problems exist that have lead the scientific community to speculate and argue about the existence of physics Beyond the Standard Model (BSM). One of the historical strengths of the SM, i.e. its renormalisability and unitarity up to arbitrary scales, actually leaves us in the dark with respect to what the nature of new physics might be and where it might reside. In this respect, the discovery of the Higgs boson has opened up a completely new era in particle physics, where theory cannot point to any specific energy scale and a new exploratory phase has started covering many different directions.
The simplest, at least conceptually, search for new physics which has been going on for years at colliders, entails looking for degrees of freedom associated to new physics. Such degrees of freedom would manifest as new resonances if the energy of the colliders were high enough to produce them on shell. Many extensions of the SM exist that feature new resonant states, even though with characteristics that are strongly dependent on the UV dynamics/assumptions, manifesting quite differently at current colliders. Moreover, in some cases (e.g. GUT), due to the large masses and weak interactions, one expects not to be possible to directly or indirectly detect the effect of very heavy resonances at the current accessible energy scales. Finally, new resonances could still be light enough to be accessible at the present collider energies, but interact too weakly to be produced/detected at observable rates. In this case dedicated experiments at high-intensity can be employed.
A different strategy is based on a programme of precision measurements. This is one of the most promising strategies to detect new physics and it relies on the ability to detect small deviations in the interactions among the known SM particles. As it turns out, this

strategy is extremely powerful because it can be formulated in a model independent way. In this case new physics effects can be systematically parameterised by making use of the formalism of Effective Field Theories (EFTs), which allows to organise them through the inclusion of higher dimension operators and the corresponding Wilson's coefficients. The EFT considered for the SM in this work is the the so-called Standard Model Effective Field Theory (SMEFT).
As already mentioned, the SM is a renormalisable/unitary gauge theory. This fundamental property implies constraints on the structure/behaviour of scattering amplitudes: intricate cancellations, especially in presence of spontaneous symmetry breaking, take place that guarantee unitarity (e.g., as in the case of the fully longitudinal WW scattering). The addition of higher dimensional operators in the SM Lagrangian may give rise to interactions which spoil the cancellations present in the SM and cause unitarity-breaking behaviours of the scattering amplitudes at high-energies.
Such unitarity breaking behaviours have been exploited in the past to formulate "no-lose" theorems on the existence of "new physics" before reaching the energy scale at which the theory becomes non-unitary (the Fermi's theory for weak interaction is the most glaring example).
Systematic studies have appeared in the literature regarding the behaviour of scattering amplitudes for $2 \to 2$ processes involving the heaviest states in the SM (weak bosons and the top quark). The starting point of this investigation is the question whether amplitudes with more particles in the final state, i.e. $2 \to N$ could have a better sensitivity to new physics than the $2 \to 2$ ones. We have therefore considered unitary violating behaviour of specific classes of core $2 \to 3$ scattering amplitudes in presence of a restricted class of dimension six operators of the SMEFT and carefully studied their behaviour at high energy. The core processes have then been embedded in realistic initial-final states at future lepton colliders and their sensitivity to various operators estimated.
The thesis is structured as follows:

- In Chapter 1, a brief review of the SM is provided, starting from the concept of spontaneous symmetry breaking and the implementation of the Brout-Englert-Higgs mechanism. A summary of the open questions and the arguments supporting the existence of new physics is given;

- In Chapter 2, the philosophy and main techniques of effective field theories are illustrated and the SMEFT is introduced together with some phenomenological implications;

- In Chapter 3, some technical topics such as the ξ gauge, tree-level unitarity and the Goldstone boson equivalence theorem are presented and an application showing the intricate cancellations that take place in the SM is discussed, studying fully longitudinal WW scattering;

- In Chapter 4, the original part of this work is reported: the processes and the operators considered are presented; from a previous 2 to 2 scattering study, some helicity selection rules for the SM are deduced and then extended to 2 to N scattering amplitudes; the helicity amplitude structure of several processes is analysed, looking for unitarity-breaking behaviour at high energy; a brief introduction to future lepton colliders such as CLIC and the muon collider is given and a simple sensitivity study is performed in the muon collider case with center of mass energies of 3, 14 and 30 TeV.

Also, this work presents two appendices:

- In Appendix A, the dimension six basis of operators (known as the Warsaw basis) for the SMEFT is derived illustrating the main point and reasoning.
- In Appendix B, the helicity tables containing the high-energies behaviours of the helicity amplitudes of every process and the impact of the operators involved are illustrated.

Chapter 1

The Standard Model: a brief review

In this chapter a brief review of the main features of the Standard Model (SM) is reported.
In the first section the concept of Spontaneous Symmetry Breaking (SSB) in a theory and the Goldstone's theorem for the SSB of a global symmetry are presented.
In the second section the Higgs mechanism for SSB of local gauge symmetries is explained with a simple application to an abelian case and its generalization to the non-abelian case.
In the third section the SM makes its appearance and its key features are described.

1.1 SSB and Goldstone's theorem

The concept of symmetry has always played a central role in physics in order to understand the laws of nature. Symmetries are associated to quantities which are not measurable. As a consequence, in a physical theory the equations of motion should not depend on such quantity[3]. Moreover, it is well known from the Noether theorem that the invariance of a lagrangian under continuous symmetries implies a conservation law for some quantities.
These quantities are associated to properties of the space-time (e.g. the non-measurability of the origin of a reference frame and the consequent invariance under spatial translations bring about the conservation of linear momentum) or internal properties of the physical system (e.g. quantum numbers).
Nowadays, when building a model, a lagrangian respecting certain symmetries has become mandatory in order to have consistent theories with laws of Nature: the requirement of Lorentz invariance is the most clear example of this approach, when dealing with Field Theories; another well known example is the gauge principle.
Symmetries can be discrete or continuous and these can, in turn, be global or local (gauge). When considering a lagrangian L and a symmetry, this can be explicitly broken if $L \to L' \neq L$ under the "symmetry" transformation or can be a symmetry of the

lagrangian if $L \to L' = L$ under such a transformation. However, in the second case the symmetry can still be broken, while leaving the lagrangian invariant but not the ground state of the system: this is what is called Spontaneous Symmetry Breaking. The most glaring examples of SSB in Nature are ferromagnetic systems.
If one wants to translate this to the language of the field theories, there exists a nonzero vev (vacuum expectation value) of the field which minimizes the potential of the theory but that is not invariant under the symmetry transformation that leaves the lagrangian density invariant.
The simplest model that one can consider is $\lambda\phi^4$ theory, whose lagrangian is invariant under a Z_2 symmetry $\phi \to -\phi$

$$\mathcal{L} = \frac{\partial_\mu \phi \partial^\mu \phi}{2} + \frac{\mu^2}{2}\phi^2 - \frac{\lambda}{4!}\phi^4, \tag{1.1.1}$$

where $\lambda \geq 0$ and $\mu^2 \geq 0$. The hamiltonian is

$$H = \int \left[\frac{\pi^2}{2} + \frac{(\nabla\phi)^2}{2} - \frac{\mu^2\phi^2}{2} + \frac{\lambda\phi^4}{4!} \right] d^3x, \quad \pi = \dot{\phi} \tag{1.1.2}$$

from which it is clear that one needs a constant field $\phi(x) = \phi_0$ to extremise the potential

$$V[\phi] = -\frac{\mu^2\phi^2}{2} + \frac{\lambda\phi^4}{4!}. \tag{1.1.3}$$

In particular, one finds that the potential has a minimum for

$$\phi_0 = \pm\sqrt{\frac{6}{\lambda}}\mu \equiv \pm v, \tag{1.1.4}$$

where v is the vev of ϕ.
In order to elucidate the meaning of what was found above, one needs to expand the theory around the vev, defining

$$\phi(x) = v + \sigma(x) \tag{1.1.5}$$

and using σ as dynamical field. The lagrangian becomes

$$\mathcal{L} = \frac{\partial_\mu \sigma \partial^\mu \sigma}{2} - \frac{(2\mu^2)}{2}\sigma^2 - \sqrt{\frac{\lambda}{6}}\mu\sigma^3 - \frac{\lambda}{4!}\sigma^4, \tag{1.1.6}$$

which describes a scalar field of mass $\sqrt{2}\mu$ with cubic and quartic self-interactions. The Z_2 symmetry has been spontaneously broken: the selection of the vev value $+v$ ($-v$ could have been chosen as well) has as a consequence that $\sigma(x) \to -\sigma(x)$ is not a symmetry of the lagrangian anymore.

The above example was about a discrete symmetry: what happens for a continuous global symmetry? When a continuous global symmetry undergoes SSB, massless particles appear in the spectrum of the theory. This is encoded in the **Goldstone's theorem**:

"Let G be a continuous group associated with a global symmetry of the lagrangian subject to SSB with H the group of the residual symmetry. Then the number of massless particles which appear in the mass spectrum of the theory is $dim(G) - dim(H) = dim(G/H)$, with $dim(G/H)$ the number of broken generator of the group G."

The massless particles originating from SSB take the name of *Nambu-Goldstone bosons* ([4, 5]).
Let one consider a theory involving several scalar fields ϕ^a with an unspecified potential $V[\phi]$ such that is minimised by the constant field $\phi^a(x) = \phi_0^a$:

$$\frac{\partial V}{\partial \phi^a}\Big|_{(\phi^a(x)=\phi_0^a)} = 0.$$

Next, if one expands the potential around the minimum, one finds

$$V(\phi) = V(\phi_0) + \frac{1}{2}(\phi - \phi_0)^a(\phi - \phi_0)^b \left(\frac{\partial^2 V(\phi)}{\partial\phi^a \partial\phi^b}\right)_{\phi_0} + ...$$

and the coefficient of the quadratic term

$$\left(\frac{\partial^2 V(\phi)}{\partial\phi^a \partial\phi^b}\right)_{\phi_0} \equiv m_{ab}^2$$

is the mass matrix, whose eigenvalues are the masses of the fields of the theory. Let one consider now a continuous symmetry of the form $\phi^a \to \phi^a + \alpha\Delta^a(\phi)$, with α an infinitesimal parameter and $\Delta(\phi)$ a function of the fields.
If the lagrangian is unchanged under this transformation, this means in particular that

$$V(\phi^a) = V(\phi^a + \alpha\Delta^a(\phi)) \Rightarrow \Delta^a(\phi)\frac{\partial V(\phi)}{\partial\phi^a} = 0.$$

And differentiating with respect to ϕ^b, setting $\phi = \phi_0$, one finally gets

$$0 = \left(\frac{\partial\Delta^a}{\partial\phi^b}\right)_{\phi_0}\left(\frac{\partial V}{\partial\phi^a}\right)_{\phi_0} + \Delta^a(\phi_0)\left(\frac{\partial^2 V}{\partial\phi^a\partial\phi^b}\right)_{\phi_0} = \Delta^a(\phi_0)\left(\frac{\partial^2 V}{\partial\phi^a\partial\phi^b}\right)_{\phi_0}, \qquad (1.1.7)$$

where the first term vanishes, since ϕ_0 a minimum of V. If the transformation is a symmetry for ϕ_0, one has the trivial result $\Delta^a(\phi_0) = 0$. If not, one has $\Delta^a(\phi_0) \neq 0$ and because of Eq. (1.1.7) the mass matrix has a null eigenvalue, i.e. a null mass particle exists in the mass spectrum of the theory. The existence of this eigenvector with null

eigenvalue proves the Goldstone theorem (for the general formal proof, see [6]).

Until now, only the global symmetries have been considered: as illustrated in the next section, the consequences of a SSB are much richer if one considers local (gauge) symmetry.

1.2 The Higgs Mechanism

The simplest example of SSB with a local continuous gauge symmetry that one can encounter is the scalar QED lagrangian with a quartic interaction and a negative mass term (in the potential $V[\phi]$)

$$\mathcal{L} = -\frac{1}{4}F^{\mu\nu}F_{\mu\nu} + (\mathcal{D}^{\mu}\phi)^{*}\mathcal{D}_{\mu}\phi + \mu^{2}\phi^{*}\phi - \lambda(\phi^{*}\phi)^{2}, \tag{1.2.1}$$

where $\mathcal{D}_{\mu} \equiv \partial_{\mu} + ieA_{\mu}$ ($q = -e$) is the covariant derivative for the electromagnetic interaction and A_{μ} is the corresponding massless gauge vector boson, while $\mu^{2} > 0$ and $\lambda > 0$.
The lagrangian is clearly invariant under the following local/gauge $U(1)$ transformation:

$$\phi(x) \to e^{-ie\alpha(x)}\phi, \qquad A_{\mu}(x) \to A_{\mu}(x) + \partial_{\mu}\alpha(x).$$

If $\mu^{2} > 0$, the minimum of the potential

$$V(\phi) = -\mu^{2}\phi^{*}\phi + \lambda(\phi^{*}\phi)^{2}$$

is given by the vev (modulo the above U(1) gauge transformation)

$$\langle\phi\rangle = \phi_{0} = \sqrt{\frac{\mu^{2}}{2\lambda}} \equiv \frac{v}{\sqrt{2}}. \tag{1.2.2}$$

It follows that, expanding the lagrangian around the vev using

$$\phi(x) = \frac{v + H(x)}{\sqrt{2}}e^{-i\frac{\chi(x)}{v}},$$

one gets the following potential:

$$\begin{aligned} V[\phi] &= -\mu^{2}|\phi(x)|^{2} + \lambda|\phi(x)|^{4} = -\mu^{2}\frac{(v + H(x))^{2}}{2} + \lambda\frac{(v + H(x))^{4}}{4} \\ &= -\frac{\mu^{4}}{4\lambda} + \mu^{2}H^{2}(x) + \sqrt{\lambda}\mu H^{3}(x) + \frac{\lambda}{4}H^{4}(x). \end{aligned} \tag{1.2.3}$$

The new potential after SSB describes a real scalar field with mass $m_{H} = \sqrt{2}\mu$ and a cubic and quartic self-interaction. Like in the global case, there is no trace of Goldstone

bosons in the scalar potential and a non-zero vacuum energy $V_0 = -\frac{\mu^4}{4\lambda}$ appears. Until now, nothing has changed compared to the global case. The new aspects come from the "kinetic term".

If one focuses on the covariant derivative, one gets

$$\mathcal{D}_\mu\phi(x) = \mathcal{D}_\mu\Big(v + H(x)\Big) = \frac{1}{\sqrt{2}}\left[\partial_\mu H(x) + \Big(v + H(x)\Big)\left(-\frac{i}{v}\partial_\mu\chi(x) + ieA_\mu(x)\right)\right] e^{-\frac{i\chi(x)}{v}}$$

so that one ends with

$$\begin{aligned}&\mathcal{D}_\mu\phi(x)\mathcal{D}^\mu\phi(x) = \\ &= \frac{1}{2}\partial_\mu H(x)\partial^\mu H(x) + \frac{e^2\left(v + H(x)\right)^2}{2}\left[A_\mu(x) - \frac{1}{ev}\partial_\mu\chi(x)\right]\left[A^\mu(x) - \frac{1}{ev}\partial^\mu\chi(x)\right].\end{aligned} \tag{1.2.4}$$

What one immediately notices, is the presence of a mass term for the vector gauge boson of the form $\frac{(ev)^2}{2}A_\mu(x)A^\mu(x)$, from which results the mass $m_A \equiv ev = \frac{e\mu}{\sqrt{\lambda}}$.
However, something is apparently not right : the presence of the Goldstone boson in kinetic and interaction terms ruins the degrees of freedom counting. Before the SSB, one had four d.o.f.: two from the complex scalar field and two from the transverse polarizations of the massless gauge vector boson. After the SSB, it seems there are five d.o.f. instead: one from the scalar field, three from the polarizations of the massive gauge vector boson and one from the Goldstone boson. This is a hint about the unphysical nature of the latter. This is confirmed by the fact that one can eliminate the Goldstone boson from the dynamics using the gauge transformation (the gauge freedom has not been used yet)

$$V_\mu(x) \equiv A'_\mu(x) = A_\mu(x) - \frac{1}{ev}\partial_\mu\chi(x), \tag{1.2.5}$$

corresponding to the gauge parameter choice $\alpha(x) = -\frac{\chi(x)}{ev}$. In this way the "kinetic term" becomes

$$\mathcal{D}_\mu\phi(x)\mathcal{D}^\mu\phi(x) = \frac{1}{2}\partial_\mu H(x)\partial^\mu H(x) + \frac{e^2\left(v + H(x)\right)^2}{2}V_\mu(x)V^\mu(x), \tag{1.2.6}$$

and one recovers the correct number of d.o.f.
Eventually, one can write the lagrangian of the model in the form

$$\mathcal{L} = \mathcal{L}_0 + \mathcal{L}_I - V_0,$$

where

$$\mathcal{L}_0 = -\frac{1}{4}F_{\mu\nu}(x)F^{\mu\nu}(x) + \frac{m_V^2}{2}V_\mu(x)V^\mu(x) + \frac{1}{2}\partial_\mu H(x)\partial^\mu H(x) - \frac{m_H^2}{2}H^2(x) \tag{1.2.7}$$

and

$$\mathcal{L}_I = -\frac{e^2(2vH(x) + H^2(x))}{2} V_\mu V^\mu - \mu\sqrt{\lambda} H^3(x) - \frac{\lambda}{4} H^4(x). \tag{1.2.8}$$

This is the abelian case of the *Brout-Englert-Higgs mechanism* [7, 8] that generates the gauge vector boson masses starting from the SSB of a gauge symmetry.

Before starting to analyse the non-abelian case, it is useful to make a remark. What has been written before, concerns a classical theory which has to be quantised. In order to do this, one can use the Faddeev-Popov approach for the quantization of a gauge theory (see Chapter 3.1). The consequence of the Faddeev-Popov procedure is the appearance of the gauge fixing lagrangian

$$\mathcal{L}_{g.f.} = V^\mu(x)\partial_\mu B(x) + \frac{1}{2}\xi B^2(x) = \left(A^\mu(x) - \frac{\sqrt{\lambda}}{e\mu}\partial^\mu \chi(x) \right) \partial_\mu B(x) + \frac{1}{2}\xi B^2(x) \tag{1.2.9}$$

where B is the unphysical Stückelberg ghost field and ξ the *gauge fixing parameter*. Moreover, one has to impose the subsidiarity condition on the physical states

$$\hat{B}^{(-)}(x)\,|phys\rangle = 0$$

in order to avoid the presence of negative norm states in the Fock space.
This is what is called ξ-*gauge* and allows one to derive the vector boson propagator in the form

$$\widetilde{D}_{\mu\nu}(k, m_V, \xi) = \frac{i}{k^2 - m_V^2 + i\epsilon} \left[-g_{\mu\nu} + \frac{(1-\xi)k_\mu k_\nu}{k^2 - \xi m_V^2 - i\epsilon'} \right], \tag{1.2.10}$$

which ensures the correct behaviour for large momenta when one has to check the renormalisability of the theory. The choice $\xi = 1$ is called Feynman gauge and simplifies the calculations, whereas in the limit $\xi \to \infty$ one recovers the so called *unitary gauge* (not used here), which allows to work with the physical d.o.f. from the beginning but makes it more difficult to demonstrate the renormalisability of the theory.

1.2.1 The Higgs Mechanism in non-abelian case: systematics

Here one wants to generalise the Higgs mechanism to a non-abelian symmetry group transformation.
Suppose to have a lagrangian invariant under a global symmetry group G that describes a multiplet of real scalar fields which transform as

$$\phi_i(x) \to \phi_i'(x) = \phi_i(x) - \theta^a T^a_{ij} \phi_j, \quad i = 1, 2, ...dim(G) \tag{1.2.11}$$

where T^a are the real and antisymmetric group representation matrices.
Suppose we now promote the symmetry from global to local and define the covariant

derivative acting on ϕ as follows

$$\mathcal{D}_\mu \phi(x) = (\partial_\mu + g A^a_\mu(x) T^a)\phi(x),$$

where A^a_μ are the gauge bosons and g the gauge coupling.
If one considers the "kinetic" term of the lagrangian, one has

$$\begin{aligned}\mathcal{L}_{kin} &= \frac{1}{2}\mathcal{D}_\mu\phi_i(x)\mathcal{D}^\mu\phi_i(x) = \\ &= \frac{1}{2}\partial_\mu\phi_i(x)\partial^\mu\phi^i(x) + gA^{a\mu}(x)(\partial_\mu\phi_i(x)T^a_{ij}\phi_j) + \frac{g^2}{2}A^a_\mu(x)A^{b\mu}(x)(T^a\phi(x))_i(T^b\phi(x))^i.\end{aligned} \tag{1.2.12}$$

Imagine that the ϕ_is have the vevs

$$\langle\phi_i(x)\rangle_0 = \phi_{0i}$$

and expand the lagrangian around these values. The last term of Eq. (1.2.12) gives rise to a term with a structure which can be identified with the mass term for the gauge bosons

$$\mathcal{L}_{kin} \supset \frac{1}{2}m^2_{ab}A^a_\mu(x)A^{b\mu}(x),$$

where

$$m^2_{ab} = g^2(T^a\phi_0)_i(T^b\phi_0)_i \tag{1.2.13}$$

is the positive semidefined mass matrix. This means that generally not all of the gauge bosons will get a mass because the SSB can be partial: in that case, some unbroken generators T^a do exist and

$$T^a\phi_0 = 0.$$

Now consider the second term of Eq. (1.2.12). Expanding around the vev, it gives rise to the interaction term

$$\mathcal{L}_{kin} \supset gA^a_\mu(x)\partial_\mu\phi_i(T^a\phi_0)_i,$$

which involves only the ϕ components parallel to the vector $T^a\phi_0$, i.e. the Goldstone's bosons, which are massless. Using this fact one can build the following diagram

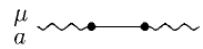

$$= [gk^\mu(T^a\phi_0)_j]\frac{i}{k^2}[gk_\nu(T^b\phi_0)_j], \tag{1.2.14}$$

where the sum over the j index is understood. The diagram is proportional to the mass matrix and contributes to the vacuum polarization amplitude, which becomes

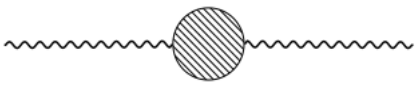

that is the necessary Goldstone boson contribution to the gauge boson propagator in order to have a transverse vacuum polarization amplitude.

1.3 The Standard Model

1.3.1 The Glashow-Weinberg-Salam Model of the Electroweak Interactions

The standard model of the electroweak interactions proposed by Glashow, Weinberg and Salam is a field theory with a $SU(2)_L \times U(1)_Y$ gauge symmetry group. L and Y refer to "left" and "hypercharge" respectively. This nomenclature will become clear in the following. The gauge group undergoes a partial SSB and becomes the residual gauge symmetry group $U(1)_{EM}$, where EM stands for "electromagnetic".
The GWS model describes the weak and the electromagnetic interactions, which unify as the electroweak interaction for energies above the vev of the theory $v = 246$ GeV. Above that energy scale the four gauge vector bosons, the quarks and the leptons are massless and a scalar bosonic field makes its appearance: the Higgs field, which is involved in the SSB process. This process takes place below the *electroweak scale* v and three out of four gauge vector bosons acquire mass through the Brout-Englert-Higgs mechanism. Moreover fermions and leptons acquire mass after the SSB by interacting with the Higgs vev.
Before proceeding in building the lagrangian, it is important to make some remarks. Because of the chiral nature of the weak interactions, under which only left handed particles are charged, quarks and leptons are organised in left-handed doublets of $SU(2)_L$ and right-handed singlet of the same group. Moreover, these doublets are divided in three generations and have a precise structure: a lepton doublet is formed by a left-handed neutrino and a left-handed "electron", whereas a quark doublet is formed by a left-handed "up" quark and a left-handed "down" quark. With the exception of neutrinos (whose right handed-counterpart seem not to exist), the right-handed versions of those particle appear in the theory as isospin singlets.
In order to build a gauge invariant lagrangian, it is important to define how a quantity X transforms under a local $SU(2)_L \times U(1)_Y$ transformation

$$X(x) \to X'(x) = e^{i\hat{T}^a \alpha^a(x)} e^{i\frac{\hat{Y}}{2}\beta(x)} X(x), \tag{1.3.1}$$

where $\hat{T}^a$ (a=1,2,3) and $\hat{Y}$ are the $SU(2)_L$ and $U(1)_Y$ generators. Their meaning emerges on how they act on X

$$\hat{T}^a X(x) = T^a X(x), \qquad \hat{Y} X(x) = Y X(x), \tag{1.3.2}$$

in which T is the *isospin* of X ($T = \frac{1}{2}$ if X is a $SU(2)_L$ doublet and $T = 0$ if X is a singlet) and $Y$is the *hypercharge* of X. The isospin components T_1, T_2 and T_3, together with the hypercharge Y are the conserved in time $SU(2)_L \times U(1)_Y$ charges and quantum numbers. Usually $T_\pm \equiv T_1 \pm iT_2$ are used instead of T_1 and T_2. Moreover, the following relation

among the electric charge Q, the third isospin component T_3 and the hypercharge Y holds:

$$Q = T_3 + \frac{Y}{2}. \tag{1.3.3}$$

The fields of the GWS Model are reported together with their quantum numbers and $SU(2)_L$ structure in Table 1.1.
Now one can start building systematically a gauge invariant lagrangian and study how its parts changes after the SSB.

	Q	T_3	Y
$\begin{pmatrix}\nu_{\ell_L}\\ \ell_L\end{pmatrix}$	0 -1	1/2 -1/2	-1 -1
$\begin{pmatrix}u_L\\ d_L\end{pmatrix}$	2/3 -1/3	1/2 -1/2	1/3 1/3
u_R	2/3	0	4/3
d_R	-1/3	0	-2/3
ℓ_R	-1	0	-2
$\begin{pmatrix}\phi_+\\ \phi_0\end{pmatrix}$	1 0	1/2 -1/2	1 1

Table 1.1: Particles of the Standard Model with charge Q, weak isospin T_3 and hypercharge Y quantum numbers ($u \equiv u_i = u, c, t$, $d \equiv d_i = d, s, b$, $\ell \equiv \ell_i = e^-, \mu^-, \tau^-$).

The Higgs Mechanism: a non-abelian case

Here the Higgs lagrangian is built and the SSB is studied. Remembering that before the SSB the Higgs field is a complex isoscalar doublet of $SU(2)_L$ with hypercharge $Y = 1$ and a $\lambda\phi^4$ interaction, the gauge invariant lagrangian follows to be

$$\mathcal{L}_{Higgs} = \left(\mathcal{D}_\mu \phi(x)\right)^\dagger \left(\mathcal{D}^\mu \phi(x)\right) - V[\phi^\dagger \phi], \tag{1.3.4}$$

where

$$V[\phi^\dagger \phi] = -\mu^2 \phi^\dagger \phi + \lambda \left(\phi^\dagger \phi\right)^2, \tag{1.3.5}$$

with μ^2, $\lambda > 0$, while the covariant derivative reads

$$\mathcal{D}_\mu \phi(x) = \left(\partial_\mu - ig\frac{\sigma^a}{2} A^a_\mu(x) - i\frac{g'}{2} B_\mu(x)\right)\phi(x), \tag{1.3.6}$$

with $A^a_\mu(x)$ and $B_\mu(x)$ the massless gauge bosons of $SU(2)_L$ and $U(1)_Y$ respectively.
It is easy to see that the potential is minimised by

$$\phi^\dagger_o \phi_o = \frac{\mu^2}{2\lambda} \equiv \frac{v^2}{2}, \tag{1.3.7}$$

where $v \simeq 246$ GeV is called the *electroweak scale* and the symmetry is spontaneously broken with the vev choice

$$\langle 0|\phi|0\rangle = \frac{1}{\sqrt{2}}\begin{pmatrix}0\\ v\end{pmatrix}. \tag{1.3.8}$$

Now one proceeds by expanding the Higgs lagrangian around the vev, writing

$$\phi(x) = e^{i\frac{\chi_a(x)\sigma^a}{2v}}\left(\frac{v+H(x)}{\sqrt{2}}\right)\begin{pmatrix}0\\ 1\end{pmatrix} \equiv U_\chi(x)\left(\frac{v+H(x)}{\sqrt{2}}\right)\begin{pmatrix}0\\ 1\end{pmatrix}, \tag{1.3.9}$$

and using the gauge transformation

$$A_\mu(x) = U_\chi(x)W_\mu(x)U_\chi^\dagger(x) - \frac{i}{g}\left[\partial_\mu U_\chi(x)\right]U^\dagger\chi(x) \tag{1.3.10}$$

in order to eliminate the non physical degrees of freedom (an alternative way would have been to start working directly in the unitary gauge).
By doing so, the covariant derivative becomes

$$\begin{aligned}
&\sqrt{2}\mathcal{D}_\mu\phi(x) = \\
&= \left\{\partial_\mu U_\chi(x)\big(v+H(x)\big) + \left[\partial_\mu H(x) - \left(\frac{ig'}{2}B_\mu(x) + \frac{ig}{2}\sigma^a A_\mu^a(x)\right)\big(v+H(x)\big)\right]U_\chi(x)\right\}\begin{pmatrix}0\\ 1\end{pmatrix} \\
&= U_\chi(x)\left[\partial_\mu - i\frac{g'}{2}B_\mu(x) - ig\frac{\sigma^a}{2}W_\mu^a(x)\right]\begin{pmatrix}0\\ v+H(x)\end{pmatrix}.
\end{aligned} \tag{1.3.11}$$

It is useful to observe

$$\frac{\sigma^a}{2}W_\mu^a(x) = \frac{1}{2}\begin{pmatrix}W_\mu^3(x) & W_\mu^+(x)\sqrt{2}\\ W_\mu^-(x)\sqrt{2} & -W_\mu^3(x)\end{pmatrix},$$

where

$$W_\mu^\pm(x) \equiv \frac{W_\mu^1(x) \mp iW_\mu^2(x)}{\sqrt{2}}. \tag{1.3.12}$$

In this way, the "kinetic" term becomes

$$\begin{aligned}
&\left(\mathcal{D}_\mu\phi(x)\right)^\dagger\left(\mathcal{D}_\mu\phi(x)\right) = \\
&= \frac{1}{2}\begin{pmatrix}0 & v+H(x)\end{pmatrix}\left[\partial_\mu + i\frac{g'}{2}B_\mu(x) + ig\frac{\sigma^a}{2}W_\mu^a(x)\right] \\
&\times\left[\partial^\mu - i\frac{g'}{2}B^\mu(x) - ig\frac{\sigma^a}{2}W^{a\mu}(x)\right]\begin{pmatrix}0\\ v+H(x)\end{pmatrix} = \\
&= \frac{1}{2}\partial_\mu H(x)\partial^\mu H(x) + \frac{g^2}{4}\left[v+H(x)\right]^2 W_\mu^+(x)W^{-\mu}(x) + \\
&+ \frac{\left[v+H(x)\right]^2}{8}\left[gW_\mu^3(x) - g'B_\mu(x)\right]\left[gW^{3\mu}(x) - g'B^\mu(x)\right].
\end{aligned} \tag{1.3.13}$$

From this formula, one observes that the gauge vector bosons $W^{\pm}_{\mu}(x)$ are mass eigenstates with mass

$$m_W = \frac{vg}{\sqrt{2}} = \frac{\mu g}{2\sqrt{\lambda}}, \tag{1.3.14}$$

whereas there is no diagonal mass term for the gauge eigenstates W^3_{μ} and B_{μ} (however one can notice the existence of a mass term for the combination $gW^3_{\mu}(x) - g'B_{\mu}(x)$, while $gW^3_{\mu}(x) + g'B_{\mu}(x)$ is massless: a hint that only three out four gauge bosons have become massive).
To find the last two mass eigenstates, it is useful to link them to the gauge eigenstates through the rotation [9]

$$\begin{pmatrix} W^3_{\mu}(x) \\ B_{\mu}(x) \end{pmatrix} = \begin{pmatrix} \cos\theta_W & \sin\theta_W \\ -\sin\theta_W & \cos\theta_W \end{pmatrix} \begin{pmatrix} Z^0_{\mu}(x) \\ A^{\gamma}_{\mu}(x) \end{pmatrix}, \tag{1.3.15}$$

where θ_W is called *Weinberg's angle*. Moreover, one has to identify

$$\tan\theta_W = \frac{g'}{g} \Rightarrow \sin\theta_W = \frac{g'}{\sqrt{g^2 + g'^2}};\ \cos\theta_W = \frac{g}{\sqrt{g^2 + g'^2}}, \tag{1.3.16}$$

in order to get

$$\begin{aligned} &\frac{\left[v + H(x)\right]^2}{8} \left[gW^3_{\mu}(x) - g'B_{\mu}(x)\right] \left[gW^3\mu(x) - g'B^{\mu}(x)\right] = \\ &= \frac{\left[v + H(x)\right]^2}{8} \left(g^2 + g'^2\right) Z^0_{\mu}(x) Z^{0\mu}(x). \end{aligned} \tag{1.3.17}$$

From this last formula, we obtain

$$m_Z = \frac{v}{2}\sqrt{g^2 + g'^2} = \frac{m_W}{\cos\theta_W}, \qquad m_A = 0, \tag{1.3.18}$$

which shows that one out four gauge vector bosons is still massless (it will be seen that this can be interpreted as the electromagnetic photon) and that the mass of Z^0 is related to the mass of $W^{\pm}$ through $\cos\theta_W$ (this relationship derives from a much deeper property called *custodial symmetry*).
Concerning the Higgs potential, after the expansion around the vev one can easily find

$$\begin{aligned} V[\phi^{\dagger}\phi] &= -\frac{\mu^2}{2}\left[v + H(x)\right]^2 + \frac{\lambda}{4}\left[v + H(x)\right]^4 \\ &= -\frac{\mu^4}{4\lambda} + \mu^2 H^2(x) + \mu\sqrt{\lambda} H^3(x) + \frac{\lambda}{4} H^4(x). \end{aligned} \tag{1.3.19}$$

It follows from this that one of the four scalar fields of the isospin doublet is actually physical and has a mass term $m_H = \sqrt{\mu} = \sqrt{2\lambda}v$. This is the Higgs boson scalar field: its

potential allows cubic and quartic self-interactions and has a vacuum energy $V_0 = -\frac{\mu^4}{4\lambda}$, which has important consequences when one considers the gravitational interaction. Finally, the full Higgs lagrangian after the SSB reads

$$\mathcal{L}_H = \mathcal{L}_{0_H} + \mathcal{L}_{int_H}$$

where

$$\mathcal{L}_{0_H} = \frac{1}{2}\left[\partial_\mu H(x)\partial^\mu H(x) - m_H^2 H^2(x)\right] \tag{1.3.20}$$

$$\mathcal{L}_{int_H} = \frac{\lambda}{4}v^2 - \lambda v H^3(x) - \frac{\lambda}{4}H^4(x) + \left[m_W^2 W^{+\mu}W_\mu^- + \frac{m_Z^2}{2}Z^{0\mu}Z_\mu^0\right]\left(1 + \frac{H(x)}{v}\right)^2. \tag{1.3.21}$$

This ends the study of the Higgs lagrangian and of the SSB $SU(2)_L \times U(1)_Y \to U(1)_{EM}$ mechanism. Now one has to understand how to include fermions in this picture: one must build gauge invariant lagrangians before the SSB, understand how the fermion acquires mass through this process and recover the weak and electromagnetic interactions.

Including the fermions

Before proceeding further, it is useful to study the action of the covariant derivative on a fermion field and rewrite it in such a way to show how the electromagnetic interaction is included inside it.
For simplicity's sake, suppose to work first with the gauge eigenstates in a $SU(2)_L$ representation T^a and pass to the mass eigenstates using Eqs. (1.3.15) and (1.3.16). One then gets

$$\begin{aligned}\mathcal{D}_\mu &= \left(\partial_\mu - igA_\mu^a T^a - ig'\frac{Y}{2}B_\mu\right) = \partial_\mu - i\frac{g}{\sqrt{2}}\left(W_\mu^+ T^+ + W_\mu^- T^-\right) \\ &- \left(ig\cos\theta_W T^3 - ig'\frac{Y}{2}\sin\theta_W\right)Z_\mu^0 - ig\sin\theta_W\left(T^3 + \frac{Y}{2}\right)A_\mu \\ &= \partial_\mu - i\frac{g}{\sqrt{2}}\left(W_\mu^+ T^+ + W_\mu^- T^-\right) - \left(ig\cos\theta_W T^3 - ig'\frac{Y}{2}\sin\theta_W\right)Z_\mu^0 - iqQA_\mu, \end{aligned} \tag{1.3.22}$$

where one has identified the unbroken $U(1)_{EM}$ charge operator $Q = T^3 + \frac{Y}{2}$ and the (electric) charge quantum number $q = g\sin\theta_W$ in the last passage.
One can now proceed in building the gauge invariant lagrangian for leptons and quarks. The two will be analyzed separately in order to highlight their specific features. What is noticeable, is that mass terms for fermions are forbidden by gauge invariance before SSB, therefore fermions are massless in GWS model. However, it will be seen that mass

terms originate through the coupling between fermions and Higgs' vev after SSB. Considering the lepton case, the lagrangian before SSB takes the form

$$\mathcal{L}_{Lept} = \sum_{i=e,\mu,\tau} \left[\begin{pmatrix} \bar{\nu}_{\ell_L} & \bar{\ell}_L \end{pmatrix} i\not{D} \begin{pmatrix} \nu_{\ell_L} \\ \ell_L \end{pmatrix} + i\bar{\ell}_L \not{D} \ell_R - y_\ell \left(\begin{pmatrix} \bar{\nu}_{\ell_L} & \bar{\ell}_L \end{pmatrix} \begin{pmatrix} \phi_+ \\ \phi_0 \end{pmatrix} \ell_R + h.c. \right) \right]. \tag{1.3.23}$$

After SSB, expanding about the vev and using what was learnt in Eq. (1.3.22) ($q = -e$ for "electrons"), one finds:

$$\begin{aligned} \mathcal{L}_{Lept} = \sum_\ell \left[\begin{pmatrix} \bar{\nu}_{\ell_L} & \bar{\ell}_L \end{pmatrix} i\not{\partial} \begin{pmatrix} \nu_{\ell_L} \\ \ell_L \end{pmatrix} + i\bar{\ell}_L \not{\partial} \ell_R - \frac{v y_\ell}{\sqrt{2}} \left(1 + \frac{H}{v} \right) \bar{\ell}\ell \right] + \\ + g \left(W^+_\mu J^\mu_+ + W^-_\mu J^\mu_- + Z^0_\mu J^\mu_0 \right) - e A_\mu J^\mu_{em}. \end{aligned} \tag{1.3.24}$$

In this way, one can identify the lepton masses with the terms $m_\ell = \frac{v y_\ell}{\sqrt{2}}$: neutrinos are assumed to be massless, therefore they do not interact with the Higgs. Moreover, the currents have been defined as follows

$$J^\mu_+(x) = \frac{1}{\sqrt{2}} \sum_\ell \bar{\nu}_{\ell_L}(x) \gamma^\mu \ell_R(x) = [J^\mu_-(x)]^\dagger \tag{1.3.25}$$

$$J^\mu_0(x) = \frac{1}{\cos\theta_W} \sum_\ell \frac{1}{2} \bar{\nu}_{\ell_L}(x) \gamma^\mu \nu_{\ell_L}(x) - \frac{1}{2} \bar{\ell}_R(x) \gamma^\mu \ell_R(x) + \sin^2\theta_W \bar{\ell}(x) \gamma^\mu \ell(x) \tag{1.3.26}$$

$$J^\mu_{em}(x) = \sum_\ell \bar{\ell}(x) \gamma^\mu \ell(x), \tag{1.3.27}$$

where $J^\pm$ and J^0 are called *charged* and *neutral* currents of the weak interactions for the leptonic sector.

Now one wants to extend this to the quark sector and some subtleties arise. All quarks are massive and a lagrangian like the leptonic one would explain only the masses of the "down" quarks. In order to build the lagrangian gauge invariant terms which give mass to the "up" quarks, one needs to introduce the charge conjugate of the Higgs doublet ($\phi_-(x) \equiv \phi^*_+$)

$$\tilde{\phi}(x) = i\sigma_2 \phi^*(x) = \begin{pmatrix} \phi^*_0(x) \\ -\phi_-(x) \end{pmatrix}, \tag{1.3.28}$$

which has hypercharge $Y = -1$.
This allows to build the following lagrangian for the quarks sector (the sum over colours

is understood) before SSB ($\vec{u} = (u\ c\ t), \vec{d} = (d\ s\ b)$):

$$\mathcal{L}_{quarks} = \sum_{j=1,2,3} \left(i\bar{u}_j \not{\mathcal{D}} u_j + i\bar{d}_j \not{\mathcal{D}} d_j \right) - \\ - \sum_{i,j=1,2,3} \left[\begin{pmatrix} \bar{u}_{i_L} & \bar{d}_{i_L} \end{pmatrix} \begin{pmatrix} \phi_+ \\ \phi_0 \end{pmatrix} Y^d_{ij} d_{j_R} + \begin{pmatrix} \bar{u}_{i_L} & \bar{d}_{i_L} \end{pmatrix} \begin{pmatrix} \phi_0^* \\ -\phi_- \end{pmatrix} Y^u_{ij} u_{j_R} + h.c \right]. \quad (1.3.29)$$

As one can see, the situation is rather different from the leptonic case. The non conservation of quark quantum numbers (e.g. strangeness) in the electroweak interactions leads to a mixing among the quark families. This mixing is reproduced by the choice of two complex non-diagonal Yukawa matrices in family space.
After SSB, leaving the "kinetic term" unexpanded, the lagrangian becomes

$$\mathcal{L}_{quarks} = \sum_{j=1,2,3} \left(i\bar{u}_j \not{\mathcal{D}} u_j + i\bar{d}_j \not{\mathcal{D}} d_j \right) - \\ - \sum_{i,j=1,2,3} \frac{v}{\sqrt{2}} \left[\bar{d}_{i_L} Y^d_{ij} d_{j_R} + \bar{u}_{i_L} Y^u_{ij} u_{j_R} + h.c \right] (1 + \frac{H}{v}). \quad (1.3.30)$$

Focusing on the mass term of Eq. (1.3.30), before putting it in diagonal form, one notices that this term is CP-invariant if and only if $(Y^q_{ij})^* = Y^q_{ij}$, $q = u, d$, $i, j = 1, 2, 3$ [10]. In order to pass to quark mass eigenstates, one needs to diagonalise the Yukawa matrices. This can always be done by means of a biunitary transformation:

$$\frac{v}{\sqrt{2}} V_L^{d\dagger} Y^d V_R^d = diag(m_d, m_s, m_b) \\ \frac{v}{\sqrt{2}} V_L^{u\dagger} Y^u V_R^u = diag(m_u, m_c, m_t),$$

where the Vs are four 3×3 unitary matrices and $m_i = y_i \frac{v}{\sqrt{2}}$, $i = u, d, s, c, b, t$. In addition, one has also the following relation between gauge and mass eigenstates:

$$\vec{u}_{L/R}(x) = V^u_{L/R} \vec{U}_{L/R}(x) \qquad \vec{d}_{L/R}(x) = V^d_{L/R} \vec{D}_{L/R}(x). \quad (1.3.31)$$

In this way, the mass term becomes diagonal in flavour space and is invariant under C,P,T transformations (this also holds true for the colour covariant derivatives term in QCD)

$$- \left(1 + \frac{H(x}{v} \right) \left(\sum_{i=u,c,t} m_i \bar{U}_i(x) U_i(x) + \sum_{i=d,s,b} m_i \bar{D}_i(x) D_i(x) \right). \quad (1.3.32)$$

However, this basis does not allow a diagonal term when one considers the covariant derivative terms of the quarks lagrangian. The charged, neutral and electromagnetic currents assume the following forms in the hadronic sector:

$$J^\mu_+(x) = \sum_{i=1,2,3} \bar{U}_{i_L}(x) \gamma^\mu \left(V_L^{u\dagger} V_L^d \right)_{ij} D_{i_L}(x) = [J^\mu_-(x)]^* \quad (1.3.33)$$

$$J_0^\mu(x) = \frac{1}{\cos\theta_W}\Bigg\{\sum_{i=1,2,3}\frac{1}{2}\bar{u}_{i_L}(x)\gamma^\mu u_{i_L}(x) - \frac{1}{2}\bar{d}_{i_L}(x)\gamma^\mu d_{i_L}(x) + \\ + \sin^2\theta_W\left[-\frac{2}{3}\bar{u}_{i_L}(x)\gamma^\mu u_{i_L}(x) + \frac{1}{3}\bar{d}_{i_L}(x)\gamma^\mu d_{i_L}(x)\right]\Bigg\} \tag{1.3.34}$$

$$J_{EM}^\mu = \sum_{i=1,2,3}\left[\frac{2}{3}\bar{u}_{i_L}(x)\gamma^\mu u_{i_L}(x) - \frac{1}{3}\bar{d}_{i_L}(x)\gamma^\mu d_{i_L}(x)\right]. \tag{1.3.35}$$

From what is written above, it becomes clear that the basis in family space choice plays a role only in case of the weak charged currents $J_\pm^\mu$,which are responsible for the flavour mixing. These effects are contained in the 3×3 unitary matrix

$$V_{CKM} \equiv V_L^{u\dagger} V_L^d, \tag{1.3.36}$$

which is the famous *Cabibbo-Kobayashi-Maskawa matrix*.
Being a matrix of $U(3)$, it depends on 9 real parameters: $\frac{3(3-1)}{2} = 3$ rotation angles and $\frac{3(3+1)}{2} = 6$ phase factors. Five out of six phases can be reabsorbed by means of phase transformations of the left-handed quarks. Therefore the CKM matrix can be parameterised by three angles θ_{ij} and a phase δ, the latter being responsible for CP-violating phenomena in the flavour changing processes in the SM. With this choice, the CKM matrix has the form

$$\begin{pmatrix} c_{12}c_{13} & s_{12}c_{13} & s_{13}e^{-i\delta} \\ -s_{12}c_{23} - c_{12}s_{23}s_{13}e^{i\delta} & c_{12}c_{23} - s_{12}s_{23}s_{13}e^{i\delta} & s_{23}c_{13} \\ s_{12}s_{23} - c_{12}c_{23}s_{13}e^{i\delta} & -c_{12}s_{23} - s_{12}c_{23}s_{13}e^{i\delta} & c_{23}s_{13} \end{pmatrix}, \tag{1.3.37}$$

where $c_{ij} \equiv \cos\theta_{ij}$, $s_{ij} \equiv \sin\theta_{ij}$ $(i,j = 1,2,3)$ and experimentally $0 < s_{13} \ll s_{23} \ll s_{12} \ll 1$.
This ends the treatment of the GWS model of the electroweak interactions. Strong interactions need now to be introduced.

1.3.2 The Standard Model of the Strong and Electroweak Interactions: open questions

The extension of the GWS model of the electroweak Interactions to the strong interactions is rather straightforward: one has to introduce the gluons vector fields and strength tensors and to modify the covariant derivative of quarks by introducing the term proportional to g_S. In this work one is not interested in formal aspect of strong interactions, therefore nothing more about them will be written.
The lagrangian of the standard model of strong and electroweak interactions, invariant

under $SU(3)_C \times SU(2)_L \times U(1)_Y$ gauge symmetry group is (before SSB)

$$\begin{aligned}\mathcal{L}_{SM} = &-\frac{1}{4}G^A_{\mu\nu}G^{\mu\nu}_A - \frac{1}{4}W^I_{\mu\nu}W^{\mu\nu}_I - \frac{1}{4}B_{\mu\nu}B^{\mu\nu} + \mathcal{D}_\mu\phi^\dagger\mathcal{D}^\mu\phi - V[\phi^\dagger\phi] + \\ &+ \sum_{\ell=e,\mu,\tau}\left[i\bar{L}_\ell \not{\mathcal{D}} L_\ell + \bar{\ell}_R i\not{\mathcal{D}}\ell_R - y_\ell\left(\bar{L}_\ell\cdot\phi\;\ell_R + h.c.\right)\right] + \\ &+ \sum_{colours}\sum_{j=1,2,3}\left[\bar{u}_j i\not{\mathcal{D}}u_j + \bar{d}_j i\not{\mathcal{D}}d_j - \sum_{k=1,2,3}\left(q^-_{j_L}\cdot\phi Y^d_{jk}d_{k_R} + q^-_{j_L}\cdot\tilde{\phi}Y^u_{jk}u_{k_R} + h.c.\right)\right],\end{aligned} \tag{1.3.38}$$

where $G^A_{\mu\nu}$ (A=1,2...8), $W^I_{\mu\nu}$(I=1,2,3), $B_{\mu\nu}$ are, respectively, $SU(3)_C$, $SU(2)_L$, $U(1)_Y$ strength tensor fields, $L_\ell \equiv \begin{pmatrix}\ell_L \\ \nu_{\ell_L}\end{pmatrix}$ and $q_{i_L} \equiv \begin{pmatrix}u_{i_L} \\ d_{i_L}\end{pmatrix}$.
After SSB and after having moved to mass eigenstates basis, one has the broken phase lagrangian

$$\begin{aligned}\mathcal{L}_{SM} = &-\frac{1}{4}G^A_{\mu\nu}G^{\mu\nu}_A - \frac{1}{4}W^I_{\mu\nu}W^{\mu\nu}_I - \frac{1}{4}B_{\mu\nu}B^{\mu\nu} + \\ &+ \frac{\partial_\mu H\partial^\mu H}{2} - \frac{m_H^2}{2}H^2 - \lambda v H^3 - \frac{\lambda}{4}H^4 + \\ &+ \left[m_W^2 W^{+\mu}W^-_\mu - \frac{m_Z^2}{2}Z^{0\mu}Z^0_\mu\right]\left(1 + \frac{H(x)}{v}\right)^2 + \\ &+ \sum_{\ell=e,\mu,\tau}\left[i\bar{L}_\ell\not{\mathcal{D}}L_\ell + \bar{\ell}_R i\not{\mathcal{D}}\ell_R - m_\ell\bar{\ell}\ell\right] + \\ &+ \sum_{colours}\sum_{j=1,2,3}\left[\bar{U}_j i\not{\mathcal{D}}U_j + \bar{D}_j i\not{\mathcal{D}}D_j - \left(m^u_j\bar{U}_jU_j + m^d_j\bar{D}_jD^j\right)\left(1 + \frac{H(x)}{v}\right)^2\right] + \\ &+ A_\mu J^\mu_{EM} + Z^0_\mu J^\mu_0 + W^+_\mu J^\mu_+ + W^-_\mu J^\mu_-,\end{aligned} \tag{1.3.39}$$

where

$$J^\mu_{EM} = -e\sum_{i=1,2,3}\left[\bar{\ell}_i\ell_i + \sum_{colours}\left(\frac{1}{3}\bar{D}_i\gamma^\mu D_i - \frac{2}{3}\bar{U}_i\gamma^\mu U_i\right)\right] \tag{1.3.40}$$

$$J^\mu_+ = \frac{g}{\sqrt{2}}\sum_{i=1,2,3}\left[\bar{\nu}_{\ell_i}\gamma^\mu\ell_{i_L} + \sum_{colours}\bar{U}_{i_L}\gamma^\mu(V_{CKM})_{ij}D_{i_R}\right] = [J^\mu_+]^* \tag{1.3.41}$$

$$\begin{aligned}J^\mu_0 = &\frac{1}{2\cos\theta_W}\sum_{i=1,2,3}\left\{\bar{\nu}_{\ell_i}\gamma^\mu\nu_{\ell_i} - \bar{\ell}_{i_L}\gamma^\mu\ell_{i_R} + 2\sin^2\theta_W\bar{\ell}_i\gamma^\mu\ell_i + \right. \\ &\left. + \bar{U}_{i_L}\gamma^\mu U_{i_L} - \bar{D}_{i_L}\gamma^\mu D_{i_L} + \sin^2\theta_W\left[\frac{2}{3}\bar{D}_i\gamma^\mu D_i - \frac{4}{3}\bar{U}_i\gamma^\mu U_i\right]\right\}.\end{aligned} \tag{1.3.42}$$

This short presentation covers the standard model of classical fields. One should now quantise the theory (through Faddeev-Popov procedure and ξ *gauge*) and show its renormalisability (through BRST symmetry and Taylor-Slavnov identities), but this will not be discussed here. After one has done that, one remains with a renormalised, anomaly-free, quantum field theory which describes three out of four fundamental interactions and explains the physics observed below the electroweak energy scale.
However, one has to test this theory by comparing its predictions with experimental data: history teaches that the agreements between theory and experiments are astonishingly precise. Nevertheless, the standard model of the strong and electroweak interactions is not the ultimate theory. The most obvious reason is that it does not include the gravitational interaction. Another point is that of the neutrino masses: from the observation of neutrino oscillations it is known that at least two out of three neutrino actually have mass, contrasting the standard model picture. The matter-content of the SM constitutes only 5% of the universe: dark matter and dark energy are not foreseen. The SM cannot explain the asymmetry between matter and antimatter in Universe. These are probably the most glaring discrepancies between the SM and data. Other, more technical, questions are the strong CP problem, the Hierarchy problem and the origin of the wide range of particle masses in SM, to quote the most well-known ones. Therefore, the road towards an ultimate theory still has a long way to go.

Over the years, many theories have been proposed to explain physics beyond the standard model have been proposed. However, typically reside a very high scales. The lack of experimental data and the difficulty of realizing experiments which can test such scales directly leave many open questions about their possible realisations and relevance.
A great help in this sense arrives from the Effective Field Theory approach, which enables searches for BSM physics in a model-independent way at low energies and will be the main subject of the next chapter.

Chapter 2

EFT and SMEFT: An Introduction

In this chapter an introduction to Effective Field Theories (EFT) approach and to the Standard Model Effective Field Theory (SMEFT) is proposed. In the first section, the necessity of EFT for finding new physics BSM is highlighted. In the second paragraph, the philosophy behind the EFT is presented together with some examples and explicit calculations. Finally, in the third paragraph, the SMEFT and its main results are described.

2.1 How to get Beyond the Standard Model?

At the end of the previous chapter it was argued that the standard model is not the ultimate theory of nature. This means that there must be new physics BSM and one needs to find it, but how? The discovery of the Higgs boson in 2012 opened a new era in particles physics, both experimentally and theoretically.
Experimentally, we have entered new, unexplored, territory. For the first time in many years, we do not know what exactly to search for and how to look for it: the Higgs boson was the last missing piece of the puzzle and the SM is a unitary and renormalisable field theory and gives no hints of what may lie beyond. One does not know what to search for because there are probably too many theories whose purpose is to go "behind" the SM [11] and one cannot know what to expect from data. One does not know how to look for it because it is not clear whether one should perform experiments giving access to higher energies (and maybe new resonances) or focusing on precision measurements at the current energies looking for deviations from the standard model.
Theoretically, there are several candidates for UV completions of the SM, but what are the principles behind this approach? How can they be tested if one does not have the technology to perform the necessary experiments? Looking at the first question from a different perspective: why, before the Higgs boson discovery in 2012, were people rather optimistic about its existence and about the need for a new particle? A possible answer

can come from so-called *no-lose theorems*.
A "no-lose theorem" is a mathematical argument based on currently established laws of Nature which can guarantee a future discovery under the obligation that experimental conditions become favourable enough. There are many historical examples of "no-lose theorems", but probably the most glaring case of a no-lose theorem in the history of electroweak interactions is the Fermi theory for the weak interaction. Historically this model worked very well in describing the phenomenology of weak interactions. However for theoretical reasons, it became clear that it could not be the fundamental model.
It is well known that those interactions were described by a four fermion operator of dimension $d = 6$ with a coupling constant G_F of mass dimension $d = -2$ in Fermi lagrangian. Whether Fermi's constant (and the theory) is truly a fundamental one or not can be deduced by studying the amplitude in the figure 2.1 below.

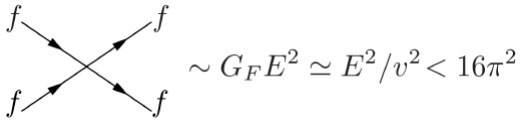

Figure 2.1: [11] High-energy behaviour and unitarity bound for the four fermion scattering amplitude in Fermi theory of the weak interactions.

The four fermion amplitude grows with the square of the center of mass energy (as one could argue from dimensional analysis) and the perturbative treatment of the theory (and the unitarity of the the S-matrix) will eventually break down. Therefore the Fermi theory cannot be used anymore after a certain energy scale, as it ceases to be predictive and becomes internally inconsistent. This implies the necessity for the existence of a new theory and therefore of new physics. This theory will describe physics in the non-perturbative regime or will modify the behaviour of the amplitude with energy before the non-perturbative threshold, keeping the weak interactions perturbative. In any case it will be "more fundamental" and will better explain the origin of Weak Interactions. The Fermi theory is therefore an effective description of weak interactions. Using (a posteriori) $G_F = \frac{1}{\sqrt{2}v^2}$, where $v \simeq 246$ GeV is the electroweak scale, one can deduce that new physics must emerge below the energy scale $\frac{4\pi}{\sqrt{G_F}} \simeq 4\pi v$. Indeed, history teaches us that the theory beyond Fermi's one is the Intermediate Vector Boson (IVB) Theory, which was confirmed experimentally thanks to the discovery of the $W^{\pm}$ bosons with mass $m_W \simeq 80$ GeV, far below the threshold and therefore consistent with the theorem.
Similarly, one can find a theorem that is related to the discovery of the top quark and of the Higgs boson as well as the fact that the SM is not the final theory because of the non renormalisability of gravitational interactions. What is important to underline at the end of this discussion, is that "no-lose theorems" make no assumptions about the nature of the physics beyond the examined theory. They only guarantee that something related to a certain process will happen at a particular energy scale.

no-lose theorems can be an answer to the first question from the theoretical side. The second question (how to test the theory if one does not have the technologies to perform the right experiments) does not have a precise answer, but it may suggest that one should change approach. Some popular theories propose to go beyond the SM and introduce new degrees of freedom in order to do it, but they may be not accessible to current colliders. However, following what written before about "no-lose theorems", there could be some processes, whose bad behaviour with energy is a sign of a new BSM theory. Rephrasing, a theory valid at "high" energies leaves traces at "low" energies. How can such traces (deviations from the SM) be incorporated in a theory which lives at "low" energies, but independently from the model that has to be tested?
This can be achieved using the Effective Field Theory (EFT) approach, which uses the fields of the SM to build operators of (mass) dimension $d > 4$, to find bad-behaving processes and to match with candidate BSM theories. This will be seen in the next two sections: in the first, the philosophy behind EFT is explained, together with the main techniques which are used; in the second, the EFT for the SM, known as the SMEFT, will be presented.

2.2 Effective Field Theories

The description of nature is a matter of scale and energy: varying them, new properties and structures emerge, as well as new kinds of physics. At the human scale, life is governed by electromagnetism (chemistry). However, at larger scales (and lower energies) new structures form like planets, galaxies and, at the very end, the Universe where we live. Here, gravity (general relativity) rules. Conversely, going down at smaller scales (and higher energies), one finds out that everything is made of molecules and atoms, and deeper nuclei, quarks and electron: one has entered the kingdom of quantum mechanics (relativistic field theory), where almost anything can happen, and new forces, like the strong and weak nuclear interactions arise.
For now, let's come back to the human scale and consider two friends, who meet one evening for a pool game. While playing, they can safely ignore the gravitational attraction between the balls and the quantum fluctuations of their quark structure when they scatter. The pool game is reduced to a (non simple) problem of classical mechanics in this way, being other interactions and structures negligible.
This example serves to illustrate that at every scale, one can find a theory which describes reality with sufficient precision, even if one ignores the existence of substructures or superstructures at other inaccessible scales. However, it is important to remark what follows: at each scale there is a suitable theory for describing what happens, but its range of validity (in terms of predictivity, consistency and approximation) is strictly limited to that scale. Rephrasing: one theory can fail in describing reality up to a certain scale (and then one must find a new theory which can do it) or can become "redundant" in

doing it (i.e. it complicates the description of reality which could be done with a theory less precise but easier to use and more effective).
Looking at the history of the exploration of the microscopic world, one can see how a tower of theories has formed as we accessed new scales through experiments. Using a physics dictionary: passing from lower/larger energies/scales (IR) to higher/smaller energies/scales (UV) has led to the discovery of new physics that the IR theory cannot describe and a new (testable) UV theory, which reduces to the IR one in low energies limit, had to be found. However, the concept of high and low is purely relative: a UV theory at a certain scale will play the role of the IR one at higher energies and vice-versa. This mechanism will go on until somebody will find (is it even possible?) the ultimate UV theory which can describe every aspect of reality and incorporates all the IR theories. Until that moment, one has to be content with the Effective (Field) Theory one can build at every scale. The main aspects of EFTs will be discussed in the following in a more rigorous way.

2.2.1 Dimensional Analysis

An effective field theory is just a quantum field theory like any other, characterised by an energy scale Λ, before which new physics arise. The difference from a common quantum field theory is that the lagrangian of an EFT is an expansion in powers of $\frac{1}{\Lambda}$. This means that it has an infinite number of terms and operators of arbitrarily high mass dimension and it is not renormalisable strictly speaking. However, one can truncate the expansion to a given order and use it to calculate physical observables at the precision desired.
To see and explain better what has been written above, it is necessary to do some dimensional analysis and introduce some power counting rules. Working in natural units ($\hbar = c = 1$) and in d space-time dimensions, it is well known that the action, i.e. the integral of a local lagrangian

$$S = \int d^d x \mathcal{L}(x), \qquad [S] = 1 = [M]^0 \tag{2.2.1}$$

is a pure number. Therefore the lagrangian must have mass dimension d

$$[\mathcal{L}(x)] = [M]^d \equiv d, \qquad \mathcal{L}(x) = \sum_i c_i \mathcal{O}_i \tag{2.2.2}$$

and to be a sum of local, gauge invariant and Lorentz invariant operators $\mathcal{O}_i$ with dimension $[\mathcal{O}] = D$ times coefficients c_i with dimension $[c_i] = d - D$.
The fields in the lagrangian are the usual scalar, fermion and vector fields. The mass dimensions of the scalar and fermion fields are easily inferred from their kinetic terms

$$S \supset \int d^d x \; \bar{\psi} i \not{\partial} \psi, \qquad S \supset \int d^d x \; \frac{1}{2} \partial^\mu \phi \partial_\mu \phi \tag{2.2.3}$$

and are

$$[\psi] = \frac{d-1}{2}, \qquad [\phi] = \frac{d-2}{2}. \tag{2.2.4}$$

Passing to vector fields and gauge couplings, knowing that the covariant derivative $\mathcal{D}_\mu = \partial_\mu - igA_\mu$ and the gauge field strength $X_{\mu\nu} \propto [\mathcal{D}_\mu, \mathcal{D}_\nu]$ have mass dimensions $[\mathcal{D}_\mu] = 1$ and $[X_{\mu\nu}] = 2$, one has

$$[A_\mu] = \frac{d-2}{2}, \qquad [g] = \frac{4-d}{2}. \tag{2.2.5}$$

When one considers renormalisable field theories, one knows that the lagrangian must not have operators with negative mass dimension coefficients. This automatically limits the sum in the lagrangian to operators with mass dimensions $D \leq d$

$$\mathcal{L} = \sum_{D=0}^{d} c_i^{(d-D)} \mathcal{O}_i^{(D)}. \tag{2.2.6}$$

For example, in the usual $d = 4$ spacetime, one has

$$[\phi] = 1 = [A_\mu], \qquad [\psi] = \frac{3}{2}, \qquad [g] = 0. \tag{2.2.7}$$

As a consequence, the only $D \leq d = 4$ gauge and Lorentz invariant operators which can appear in a renormalisable lagrangian are

$$\begin{aligned} &D = 0 \to 1 \\ &D = 1 \to \phi \\ &D = 2 \to \phi^2 \\ &D = 3 \to \phi^3,\ \bar{\psi}\psi \end{aligned} \tag{2.2.8}$$

$$D = 4 \to \phi^4,\ \phi\bar{\psi}\psi,\ \mathcal{D}^\mu\phi\mathcal{D}_\mu\phi,\ \bar{\psi}i\not{\mathcal{D}}\psi,\ X_{\mu\nu}X^{\mu\nu}. \tag{2.2.9}$$

However, here one is interested in EFT: there is no restriction of power counting renormalisability and it is possible to go further by building higher dimensional operators (even though some issues will emerge, e.g. finding a complete basis of operator to a given dimension and others, as it will be seen in the following).
Introducing an energy scale Λ in order to have dimensionless coefficients (of order unity so one can works in perturbative regime), one can write the effective lagrangian

$$\mathcal{L}_{EFT} = \sum_{i,D\geq 0} \frac{c_i^{(D)}\mathcal{O}_i^{(D)}}{\Lambda^{D-d}} = \mathcal{L}_{D<d} + \sum_{D>d} \frac{\mathcal{L}_D}{\Lambda^{D-d}}. \tag{2.2.10}$$

In the case $d = 4$ it becomes

$$\mathcal{L}_{EFT} = \mathcal{L}_{D<4} + \frac{\mathcal{L}_5}{\Lambda} + \frac{\mathcal{L}_6}{\Lambda^2} + ... \tag{2.2.11}$$

One thing is remarkable: renormalisable theories are recovered in the limit $\Lambda \to +\infty$ and are a particular case of EFT.

Now one has the general structure for the lagrangian of an EFT and can discuss how to work with it. Most of the concepts and techniques used for renormalisable field theories apply as well to EFTs. However an EFT alone is not enough to explain new physics: it can be used to find deviations from a renormalisable (IR) theory and to understand in which processes new physics can be found, but it does not foresee what the new physics will be like or at which scales it will emerge. This is because no new degrees of freedom are introduced in the EFT with respect to the IR theory and the (energy) scale at which the EFT will break down is not specified. Therefore the EFT description of physics is independent from any UV theory which should replace the IR one. But how to connect an EFT with a UV (Full) theory, if the former does not depend on the latter? One uses a procedure called "matching" which takes advantage of the fact that the two theories must have the same IR behaviour (because they must reduce to the same IR theory) and matches the couplings parameters of the two theories. This procedure involves a complex machinery like renormalisation and Renormalisation Group Equations (RGE) and some of its aspects will be discussed in the next section with some examples.
Another problem, which one has not treated here, is how to find a complete basis of operators at a given dimension D. This will be seen after the next section.

2.2.2 Power Counting, Loops and Matching

Before doing an example of tree-level matching, it is interesting to see how an operator contributes to physical observables, like amplitudes. Let one consider a dimensionless amplitude $\mathcal{M}$ in d dimensions at a certain momentum scale p. It follows by dimensional analysis that the contribution of an operator of dimension D to the amplitude is of order

$$\mathcal{M} \sim \left(\frac{p}{\Lambda}\right)^{D-d}.$$

The power of the energy scale at the denominator is due to the mass dimension coefficient of the operator, while the momentum power derives from kinematic factors (e.g. external momenta). From what has been found above, it is easy to understand that the insertion of a collection of higher dimensional operators in a tree graph gives rise to an amplitude

$$\mathcal{M} \sim \left(\frac{p}{\Lambda}\right)^{n}, \qquad n = \sum_i \left(D_i - d\right). \tag{2.2.12}$$

The relation(2.2.12) takes the name of *EFT power counting formula* and gives information on the suppression of a given graph.
What is remarkable is that (2.2.12) is still valid for any graph, even in presence of loops.

(This is interesting because the integration over the loop momenta includes regions where the EFT expansion breaks down.) Moreover, it helps when one has to do calculations, because it makes it clear that the leading order of the amplitude is given by the renormalisable lagrangian $\mathcal{L}_{D<d}$. Another important difference between renormalisable theories and EFTs is revealed by (2.2.12), observing that in d=4 dimension the insertion of two dimension five operators in a graph gives the same order contribution to the amplitude as the insertion of a single dimension six operator. Generally, this translates to the fact that multiple insertion of operators of dimension $D > d$ cannot be absorbed by counterterms of dimension D in the renormalised lagrangian. In this way an infinite number of higher dimensional counterterms operator are generated and the effective theory is therefore non-renormalisable. Despite that, it is useful to repeat that if one is interested in corrections with a maximum value of n in (2.2.12) and truncates the expansion, only a finite number of operators contributes and the non-renormalisable theory is as good as a renormalisable one.

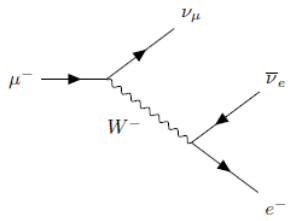

Figure 2.2: Tree-level diagram for muon decay.

Let one see now a practical example of EFT and a tree-level matching. For historical reasons, the Fermi theory for the weak interaction is chosen, whose full (UV) theory is the standard model (actually IVBM). The matching takes place passing from the full theory to one valid at small momenta compared to $M_{W/Z}$. The studied process is the classical muon decay (Fig.2.2).
In the SM the W boson interacts with leptons through the weak charged current

$$J^\mu_W = \frac{g_W}{\sqrt{2}} \bar{\nu}_\ell \gamma^\mu \left(\frac{1-\gamma_5}{2} \right) \ell \tag{2.2.13}$$

and the tree-level amplitude for the process is consequently (for simplicity's sake the spin states are labelled with the corresponding particle letters and one works in Feynman-'t Hooft gauge)

$$\mathcal{M} = \left(\frac{-ig_W}{\sqrt{2}} \right)^2 (\bar{\nu}_{\mu^-} \gamma^\mu P_L \mu) \left(\frac{-ig_{\mu\nu}}{p^2 - M_W^2} \right) (\bar{e} \gamma^\nu P_L \nu_{e^-}) \,. \tag{2.2.14}$$

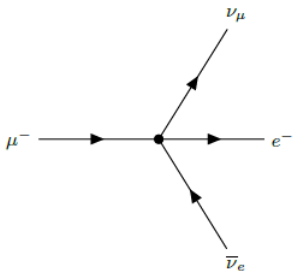

Figure 2.3: Muon decay vertex in the Fermi theory.

If the transferred momentum is low, i.e. $p^2 << M_W^2$ one can expand the W propagator in powers of $\frac{p^2}{M_W^2}$ as follows:

$$\frac{-ig_{\mu\nu}}{p^2 - M_W^2} = -\frac{-ig_{\mu\nu}}{M_W^2} \sum_{n=0}^{\infty} \left(\frac{p^2}{M_W^2} \right)^n . \tag{2.2.15}$$

At the first order the tree level amplitude becomes then

$$\mathcal{M} = \frac{i}{M_W^2} \left(\frac{-ig_W}{\sqrt{2}} \right)^2 (\bar{\nu}_{\mu^-} \gamma^\mu P_L \mu) (\bar{e} \gamma^\nu P_L \nu_{e^-}) + O\left(\frac{1}{M_W^4} \right). \tag{2.2.16}$$

However, the very same amplitude can be written starting from the lagrangian

$$\mathcal{L}_{EFT} = -\frac{g_W^2}{2M_W^2} (\bar{\nu}_{\mu^-} \gamma^\mu P_L \mu) (\bar{e} \gamma^\nu P_L \nu_{e^-}) , \tag{2.2.17}$$

which is the lowest order lagrangian for the muon decay in the EFT and gives rise to the vertex in Fig. 2.3. If one now considers the Fermi theory lagrangian

$$\mathcal{L}_{Fermi} = -\frac{4G_F}{\sqrt{2}} (\bar{\nu}_{\mu^-} \gamma^\mu P_L \mu) (\bar{e} \gamma^\nu P_L \nu_{e^-}) , \tag{2.2.18}$$

one can easily identify it with the EFT lagrangian imposing

$$\frac{G_F}{\sqrt{2}} \equiv \frac{g_W^2}{8M_W^2} = \frac{1}{2v^2}, \tag{2.2.19}$$

with $v \simeq 246$ GeV the scale of the electroweak symmetry breaking.
After this, it becomes clear that the EFT lagrangian is the low-energy limit of the standard model: the W is no longer a dynamical degree of freedom, having been integrated out; the W exchange effect has been absorbed in a dimension six four-fermion operator.

If one calculates the decay rate (here the formula in the massless electron approximation is presented)

$$\Gamma(\mu \to e\nu_\mu \bar{\nu_e}) = \frac{G_F^2 m_\mu^5}{192\pi^3}, \tag{2.2.20}$$

one can clearly see that it contains complete dependence on the low energy scale m_μ, but drops terms proportional to $\frac{m_\mu}{M_W}$, simplifying the calculation.
Moreover, using experimental values of the Fermi constant G_F and the power counting rule $G_F \sim \frac{1}{\Lambda^2}$ one gets an estimate $\Lambda \sim 300$ GeV, which is the upper energy bound to the breaking scale of the EFT.
Again, using power counting arguments for amplitudes, it is glaring that leading terms in decay amplitudes are given by single insertions of dimension six operators, whereas the next leading terms from a double insertion or by a dimension eight operator insertion, and so on. What is important to notice again, is that the value of Λ has never entered in this discussion. Historically, when the SM was developed, G_F was known, not M_W and M_Z: their values were not necessary to apply Fermi theory to low-energy weak interactions and were measured experimentally, determining the scale at which the EFT breaks and has to be replaced by the SM.

Loops

One has seen before that EFT simplifies tree-level calculation to some extent. Despite that, the true power of EFT is brought to life when one has to work with loops. When one works with loops, subtleties arises and the choice of the right regularisation procedure is one of them.
Let one consider an EFT lagrangian for a massive real scalar field ϕ:

$$\mathcal{L} = \mathcal{L}_{D<4} - \frac{c_6}{\Lambda^2}\frac{1}{6!}\phi^6 - \frac{c_8}{\Lambda^4}\frac{1}{8!}\phi^4(\partial_\mu\phi)^2. \tag{2.2.21}$$

The dimension six operator contributes to the $\phi - \phi$ scattering processes through the diagram in Fig.2.4

$$\mathcal{M}_6 = \frac{c_6}{\Lambda^2}\int \frac{d^4k}{(2\pi)^4}\frac{1}{k^2 - m_\phi^2}. \tag{2.2.22}$$

Since the EFT works for momenta $k < \Lambda$, the use of a cutoff regulator $\Lambda_C < \Lambda$ to regularise the integral would seem natural and one gets ($m_\phi << \Lambda_C$)

$$\mathcal{M}_6 \simeq \frac{c_6}{\Lambda^2}\frac{\Lambda_C^2}{16\pi^2}, \tag{2.2.23}$$

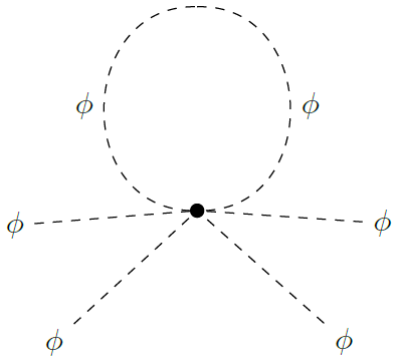

Figure 2.4: ϕ^6 operator contribution to the $\phi\phi \to \phi\phi$ scattering.

which divergences with the cut-off scale squared. Similarly, the dimension eight operator will contribute as

$$\mathcal{M}_8 = \frac{c_8}{\Lambda^4} \int \frac{d^4k}{(2\pi)^4} \frac{k^2}{k^2 - m_\phi^2} \simeq \frac{c_8}{\Lambda^4} \frac{\Lambda_C^4}{16\pi^2}, \tag{2.2.24}$$

which is quartically divergent.
When $\Lambda_C \simeq \Lambda$, both contributes are of order $O(1)$, the theory loses its predictivity [14] and the power counting formula of EFTs is lost. Therefore the cutoff regulator is not a good one, being Λ_C an artificial scale introduced without any relation to any physical scale. Moreover, the cutoff regulator violates gauge invariance.
One must therefore find another regularisation procedure suitable for EFTs. One is interested in the (non analytical) IR behaviour of such integrals, since the UV behaviour connects to the full theory through the matching procedure, and wants to maintain the EFT power counting. The best way (up to now) to do this is the use of *dimensional regularisation*, which also has the advantage of respecting gauge invariance.

Before giving an example with explicit calculation, it is useful to point out some important features of dimensional regularisation. The key identity is ($d = 4 - 2\epsilon$, $0 \leq \epsilon < 1$)

$$\mu^{2\epsilon} \int \frac{dk^d}{(2\pi)^d} \frac{(k^2)^a}{(k^2 - M^2)^b} = (-1)^{a-b} \frac{i(M^2)^{a-b+2}}{16\pi^2} \left(\frac{4\pi\mu^2}{M^2}\right)^\epsilon \frac{\Gamma\left(2 + a - \epsilon\right) \Gamma\left(b - a - 2 + \epsilon\right)}{\Gamma(2-\epsilon)\Gamma(b)}, \tag{2.2.25}$$

which can be demonstrated to hold using first Wick's rotation to switch to Euclidean coordinates and then performing a Mellin transformation or passing to d-dimensional spherical coordinates. At that point, one expands in powers of ϵ, using at the first order

the relations ($n \in \mathbb{N}$)

$$\Gamma(-n+\epsilon) = \frac{(-1)^n}{n!}\left[\frac{1}{\epsilon} + \psi(n+1) + O(\epsilon)\right]$$
$$\psi(n+1) = \left(\sum_{k=1}^{n}\frac{1}{k}\right) - \gamma_E, \qquad \psi(1) = -\gamma_E, \tag{2.2.26}$$

where γ_E is the Eulero-Mascheroni constant, and

$$\left(\frac{4\pi\mu^2}{M^2}\right)^{\epsilon} = 1 + \log\left(\frac{4\pi\mu^2}{M^2}\right)\epsilon + O(\epsilon^2). \tag{2.2.27}$$

As example, let one consider again the quadratically and quartically divergent integrals of the previously presented lagrangian ($\bar{\mu}^2 \equiv 4\pi e^{-\gamma_E}\mu^2$), which become

$$\mu^{2\epsilon}\int\frac{d^dk}{(2\pi)^d}\frac{1}{k^2-m_\phi^2} = \frac{im_\phi^2}{16\pi^2}\left[\frac{1}{\epsilon} + \log\left(\frac{\bar{\mu}^2}{m_\phi^2}\right) + 1 + O(\epsilon)\right] \tag{2.2.28}$$

$$\mu^{2\epsilon}\int\frac{d^dk}{(2\pi)^d}\frac{k^2}{k^2-m_\phi^2} = \frac{im_\phi^4}{16\pi^2}\left[\frac{1}{\epsilon} + \left(\frac{\bar{\mu}^2}{m_\phi^2}\right) + 1 + O(\epsilon)\right]. \tag{2.2.29}$$

Now, the integrals depend only on powers of the IR scale m_ϕ: there are no power divergences nor any (unphysical) dependence on any UV scale and $\bar{\mu}$ power. Moreover, scaleless integrals (i.e. $M = 0$) vanish (when one takes the limit $M \to 0$, one must assume $\frac{d}{2} + a - b > 0$ or do an analytical continuation for $\frac{d}{2} + a - b \leq 0$).
Using dimensional regularisation, one is also able to extend the validity of the power counting formula (2.2.12) to loops. Inserting EFT vertices of order $\frac{1}{\Lambda^a}$, $\frac{1}{\Lambda^b}$ and so on in a loop graph, one gets the Λ dependence

$$\frac{1}{\Lambda^a}\frac{1}{\Lambda^b}\ldots = \frac{1}{\Lambda^{a+b+\ldots}}, \tag{2.2.30}$$

with no compensations in the numerator (excluding IR scales much smaller than Λ).

It is now useful to do an explicit example of matching through a toy model, which is in this case is a two-scale integral generated by the diagram in Fig.2.5.
Let one suppose to have from the full theory

$$I_F = \mu^{2\epsilon}\int\frac{d^dk}{(2\pi)^d}\frac{1}{(k^2-m^2)(k^2-M^2)}, \tag{2.2.31}$$

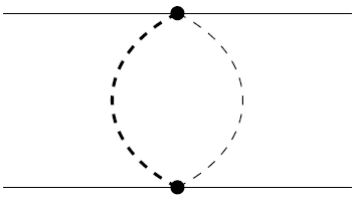

Figure 2.5: Feynman diagram generating 2.2.31: the external solid lines are the light external fields, whereas the thin and the thick dashed lines are the light and heavy particles of mass m and M respectively. The heavy particle will be integrated out and will not be present in the EFT.

with $m << M$ the IR and UV scales, respectively. Making use of Feynman parameterisation and of the general formula (2.2.25), one can proceed with the calculation:

$$\begin{aligned} I_F &= \mu^{2\epsilon} \int \frac{d^d k}{(2\pi)^d} \int_0^1 dx \frac{1}{\left[k^2 - x(m^2 - M^2)\right]^2} = \frac{i\Gamma(\epsilon)}{16\pi^2 \Gamma(2)} \int_0^1 dx \left(\frac{4\pi\mu^2}{x(m^2 - M^2) + M^2} \right)^\epsilon \\ &= \frac{i}{16\pi^2} \int_0^1 dx \left\{ \frac{1}{\epsilon} + \log \bar{\mu}^2 - \log \left[x(m^2 - M^2) + M^2 \right] + O(\epsilon) \right\} = \\ &= \frac{i}{16\pi^2} \left[\frac{1}{\epsilon} + \log \bar{\mu}^2 - \log m^2 + \int_0^1 dx \frac{x(m^2 - M^2)}{x(m^2 - M^2) + M^2} \right] = \\ &= \frac{i}{16\pi^2} \left[\frac{1}{\epsilon} - \log \frac{M^2}{\bar{\mu}^2} + \frac{m^2}{M^2 - m^2} \log \frac{m^2}{M^2} + 1 \right]. \end{aligned} \tag{2.2.32}$$

Else, if one integrates out the heavy particle M expanding the propagator, one gets a series of contribution in the EFT:

$$I_{EFT} = -\frac{\mu^{2\epsilon}}{M^2} \int \frac{d^d k}{(2\pi)^d} \frac{1}{k^2 - m^2} \sum_{n=0}^{\infty} \left(\frac{k^2}{M^2} \right)^n = \frac{i m^2}{16\pi^2 M^2} \left(-\frac{1}{\epsilon} + \log \frac{m^2}{\bar{\mu}^2} - 1 \right) \sum_{n=0}^{\infty} \left(\frac{m^2}{M^2} \right)^n , \tag{2.2.33}$$

which one has to compare with I_F.
The two results are different evidently: the order of integration and expansion has to be taken in account. The divergent terms are not the same: they require different counterterms which give rise to different anomalous dimensions. The two theories are therefore independent, but tuned to give the same S-matrix. The non-analytical, IR terms $\log m^2$ are the same in both theory: the UV theory must have the same IR behaviour of the EFT. The difference between I_F and I_{EFT} arises from the UV part, but it is analytical in the IR scale m: $I_F - I_{EFT}$ is called the *matching contribution* to the lagrangian. In I_F there are terms involving the ratio of the two scales, such as $\log \frac{M^2}{m^2}$: these can be summed through RGE in EFT.

The matching integral can be computed after having eliminated the divergences through counterterms and reads

$$I_M = \frac{i}{16\pi^2}\left(\log\frac{\bar{\mu}^2}{M^2}+1\right)\sum_{n=0}^{\infty}\left(\frac{m^2}{M^2}\right)^n, \tag{2.2.34}$$

which brings corrections to operators $\frac{1}{M^{2n}}$ that are clearly analytic in the IR scale m. One can read what has been done as I_F being separated in two pieces: I_M and I_{EFT}. The two scales problem has been reduced in two one-scale calculations using $\bar{\mu}$, which can assume different values when computing the twos:

$$\log\frac{m^2}{M^2} = -\log\frac{M^2}{\bar{\mu}^2}+\log\frac{m^2}{\bar{\mu}^2}. \tag{2.2.35}$$

What is interesting, is that there is a much quicker way to proceed, which avoids the calculation of the two-scales integral I_F. One can directly get I_M using $I_M = I_F^{exp} - I_{EFT}^{exp}$, where I_F and I_{EFT} have both been expanded in power of $\frac{m^2}{k^2}$ before being calculated and the non-analytical IR parts of the two cancel each other mutually. However, what one actually sees, is that it is enough to calculate I_F^{exp} this way, because of the many vanishing scaleless integrals which appear. Very briefly:

$$I_F^{exp}(m) = \sum_r m^r I_F^{(r)} = \sum_r m^r\left(\frac{A^{(r)}}{\epsilon_{UV}}+\frac{B^{(r)}}{\epsilon_{IR}}+C^{(r)}\right) \tag{2.2.36}$$

$$I_{EFT}^{exp}(m) = \sum_r m^r I_{EFT}^{(r)} = \sum_r m^r\left(-\frac{B^{(r)}}{\epsilon_{UV}}+\frac{B^{(r)}}{\epsilon_{IR}}\right), \tag{2.2.37}$$

Where A and B are UV and IR divergences, respectively, while C is the finite part. Renormalizing the two theories, one gets

$$I_F^{(r)} + I_{F,ct}^{(r)} = \frac{B^{(r)}}{\epsilon_{IR}} + C^{(r)} \tag{2.2.38}$$

$$I_{EFT}^{(r)} + I_{EFT,ct}^{(r)} = \frac{B^{(r)}}{\epsilon_{IR}} \tag{2.2.39}$$

$$I_M^{(r)} = \left[I_F^{(r)} + I_{F,ct}^{(r)}\right] - \left[I_{EFT}^{(r)} + I_{EFT,ct}^{(r)}\right] = C^{(r)} \tag{2.2.40}$$

and the IR divergences have canceled out.
At the end, the prescription for the matching condition is simply expanding I_F in the IR scale and keeping the finite part only. What is remarkable, is that the full theory has an anomalous dimension proportional to the UV counterterm -A, whereas the EFT has its own proportional to the IR counterterm B. However, B was the infrared divergence of the full theory: thanks to the use of EFT, one has converted the IR divergences of the

full theory into UV divergences of the EFT. This also means converting IR logarithms to UV ones and resumming them by means of RGE.
Summarizing the steps: the full theory graphs have to be computed expanding all IR scales in order to get the matching contribution to match with the appropriate EFT; through RGE of the EFT one evolves its coupling parameters from a high scale $\mu \simeq M$ to a low scale $\mu \simeq m$ (this means "resumming the logarithms"), one studies the EFT at scale $\mu \simeq m$ and sees what are the results.

It has been shown that EFTs allows to break up the calculation in to many simpler ones, involving only a single scale at time.

2.2.3 Field Redefinitions and Equations of Motion

What an EFT is and its utilities, as well as some guidelines for calculation, have been presented in the previous sections. However, one does not know yet, how to build the lagrangians $\mathcal{L}_{D>d}$ with the degrees of freedom (i.e. the fields) of the theory. The same d.o.f. of $\mathcal{L}_{D<d}$ will be necessary to build higher dimensional operators. At a given dimension subtleties arise: not all of the local, Lorentz and gauge invariant operators are independent and one must find a complete basis. This can be done by means of field redefinitions or using Equation of Motion. These two approaches are equivalent at lowest order.
Using field redefinitions, $\phi(x) \to \phi'(x) = F[\phi(x)]$ (where ϕ is a field of the theory), one changes the correlation functions of the theory, but the observable quantities, and therefore the S-matrix, must be unaffected. This is true as long as $\langle p_1 | F[\phi] | 0 \rangle \neq 0$, with $|p_1\rangle$ the one-particle state created by the field ϕ. If this holds, the LSZ formula [16], which links correlation functions to S-matrix elements, also holds and picks out the poles corresponding to physical external states in the scattering amplitude.
The use of EOMs is a special case of field redefinition and an operator proportional to the EOMs

$$\theta[\phi] = F[\phi]E[\phi] \equiv F[\phi]\frac{\delta S[\phi]}{\delta \phi} \tag{2.2.41}$$

can be eliminated by means of the field redefinition ($\epsilon << 1$)

$$\phi(x) = \phi'(x) + \epsilon F[\phi'(x)] \tag{2.2.42}$$

and produces a change in the lagrangian

$$\mathcal{L}[\phi] = \mathcal{L}[\phi'] + \epsilon F[\phi']\frac{\delta S \phi'}{\delta \phi'} + O(\epsilon^2) = \mathcal{L}[\phi'] + \epsilon\theta[\phi'] + O(\epsilon^2), \tag{2.2.43}$$

which leaves the S-matrix untouched. This can be demonstrated in the path integral formulation. EOMs are primarily used to eliminate operators with derivatives in the

EFT lagrangian.

Now, an example is presented in order to show that finding a complete basis and the use of EOMs is not so trivial as one could think at first. Let one consider a theory for a massless scalar field, invariant under Z_2 transformations. The lagrangian at dimension four is therefore

$$\mathcal{L}_{D\leq 4} = \frac{1}{2}\partial_\mu\phi\partial^\mu\phi - \frac{\lambda}{4!}\phi^4 \tag{2.2.44}$$

with EOMs

$$\Box\phi + \frac{\lambda}{3!}\phi^3 = 0. \tag{2.2.45}$$

One wants to build the dimension six lagrangian. Owing to Lorentz invariance and dimensional analysis, one finds at dimension six the following operators: ϕ^6, $\phi^2\partial_\mu\phi\partial^\mu\phi$ and $(\Box\phi)^2$. One shows now, that only one of them is actually independent. When EOMs hold one has namely

$$(\Box\phi)^2 \sim \lambda^2\phi^6, \tag{2.2.46}$$

where the symbol $\sim$ denotes here equivalence. Concerning $\phi^2\partial_\mu\phi\partial^\mu\phi$, integrating by parts and discarding total derivatives, one has

$$\begin{aligned}&\phi^2\partial_\mu\phi\partial^\mu\phi \doteq -\phi\partial_\mu\left(\phi^2\partial^\mu\phi\right) = -\phi^3\Box\phi - 2\phi^2\partial_\mu\phi\partial^\mu\phi \Rightarrow \\ &\Rightarrow \phi^2\partial_\mu\phi\partial^\mu\phi = -\frac{1}{3}\phi^3\Box\phi \sim \lambda\phi^6.\end{aligned} \tag{2.2.47}$$

Suppose now to stop before the last equivalence. At this point one has two operator left: ϕ^6 and $\phi^3\Box\phi$. Then the lagrangian is

$$\mathcal{L} = \frac{1}{2}\partial_\mu\phi\partial^\mu\phi - \frac{\lambda}{4!}\phi^4 - \frac{c_\Box}{\Lambda^2}\phi^3\Box\phi - \frac{c_6}{\Lambda^2}\phi^6 + O(\frac{1}{\Lambda^4}). \tag{2.2.48}$$

The use of EOMs in the last equivalence is equivalent to the field redefinition

$$\phi \to \phi - \frac{c_\Box}{\Lambda^2}\phi^3 \tag{2.2.49}$$

and the lagrangian becomes

$$\begin{aligned}\mathcal{L} &= \frac{1}{2}\partial_\mu\phi\partial^\mu\phi - 3\frac{c_\Box}{\Lambda^2}\phi^2\partial_\mu\phi\partial^\mu\phi - \frac{\lambda}{4!}\phi^4 + \frac{\lambda}{3!}\frac{c_\Box}{\Lambda^2}\phi^6 - \frac{c_\Box}{\Lambda^2}\phi^3\Box\phi - \frac{c_6}{\Lambda^2}\phi^6 + O(\frac{1}{\Lambda^4}) \\ &= \frac{1}{2}\partial_\mu\phi\partial^\mu\phi - \frac{\lambda}{4!}\phi^4 - \frac{\left(c_6 - \frac{\lambda}{3!}c_\Box\right)}{\Lambda^2}\phi^6 + O(\frac{1}{\Lambda^4}),\end{aligned} \tag{2.2.50}$$

where in the last passage one has used

$$\phi^2\partial_\mu\phi\partial^\mu\phi \doteq -\frac{1}{3}\phi^3\Box\phi \tag{2.2.51}$$

One has eliminated again the field $\phi^3\Box\phi$ using a field redefinition getting the same result of EOMs. This all at the price of redefining the coefficients of the ϕ^6 operator (if ϕ had been massive, also the coefficient of ϕ^4 would have been modified).
Concluding, generally one has many operators which can be eliminated by using EOM or field redefinitions E_i at a given dimension. Those operators mix among themselves when one renormalises the theory

$$\mu\frac{d}{d\mu}E_i = \Gamma_{ij}E_j, \tag{2.2.52}$$

with Γ_{ij} that can be gauge dependent, but one need not worry about this because the E_i are not observable quantities. Taking this into account, the most general anomalous dimension of an operator $\mathcal{O}_i$ takes the form

$$\mu\frac{d}{d\mu}\mathcal{O}_i = \gamma_{ij}\mathcal{O}_j + \Gamma_{ik}E_k. \tag{2.2.53}$$

Operators $\mathcal{O}_i$ can mix with equation-of-motion operators E_i, but the latter do not contribute to S-matrix elements. On the other hand, $\mathcal{O}_i$ do contribute to S-matrix elements and therefore γ_{ij} must be gauge independent.

2.3 An Effective Field Theory for the Standard Model: the SMEFT

As discussed in the previous sections, the SM cannot be the ultimate physical theory. Moreover, it is not clear at all at which scale new physics could emerge. The use of EFTs is a good way to parameterise our ignorance and it is also a model independent way to include effects of new unknown physics accessible at the present energy-scales of experiments.
In this section, the Standard Model Effective Field Theory (SMEFT) is presented with a brief look at its main features and results.

2.3.1 The SMEFT Lagrangian

Being an EFT, one can write the SMEFT lagrangian schematically as follows:

$$\mathcal{L}_{SMEFT} = \mathcal{L}_{SM} + \frac{\mathcal{L}_5}{\Lambda} + \frac{\mathcal{L}_6}{\Lambda^2} + ... \quad , \tag{2.3.1}$$

where $\mathcal{L}_{SM}$ is the usual renormalisable $D \leq 4$ SM lagrangian and the $D > 4$ lagrangians are the corrections to the SM due to BSM Physics effects. Λ is the (unknown) energy scale before which new physics emerges and the SMEFT breaks down.

The first step is to build the $D > 4$ lagrangian, understanding the d.o.f. involved and constructing the operators. Following the spirit of EFTs, it appears clear that the d.o.f. involved are the SM fields before the electroweak symmetry breaking and one can build the operators using naive dimensional analysis together with Lorentz and gauge invariance as a first approach.

X^3		ϕ^6 and $\phi^4\mathcal{D}^4$		$\psi^2\phi^3$	
$\mathcal{O}_G$	$f^{ABC}G^{\nu}_{A_\mu}G^{\rho}_{B_\nu}G^{\mu}_{C_\rho}$	$\mathcal{O}_\phi$	$\left(\phi^\dagger\phi\right)^3$	$\mathcal{O}_{e\phi}$	$\left(\phi^\dagger\phi\right)\left(\bar{\ell}\phi e_r\right)$
$\mathcal{O}_{\tilde{G}}$	$f^{ABC}\tilde{G}^{\nu}_{A_\mu}G^{\rho}_{B_\nu}G^{\mu}_{C_\rho}$	$\mathcal{O}_{\phi\Box}$	$\left(\phi^\dagger\phi\right)\Box\left(\phi^\dagger\phi\right)$	$\mathcal{O}_{u\phi}$	$\left(\phi^\dagger\phi\right)\left(\bar{q}\phi u_r\right)$
$\mathcal{O}_W$	$\epsilon^{IJK}W^{\nu}_{I\mu}W^{\rho}_{J\nu}W^{\mu}_{K\rho}$	$\mathcal{O}_{\phi\mathcal{D}}$	$\left(\phi^\dagger\mathcal{D}_\mu\phi\right)^*\left(\phi^\dagger\mathcal{D}^\mu\phi\right)$	$\mathcal{O}_{d\phi}$	$\left(\phi^\dagger\phi\right)\left(\bar{q}\phi d_r\right)$
$\mathcal{O}_{\tilde{W}}$	$\epsilon^{IJK}\tilde{W}^{\nu}_{I\mu}W^{\rho}_{J\nu}W^{\mu}_{K\rho}$				
$X^2\phi^2$		$\psi^2X\phi$		$\psi^2\phi^2\mathcal{D}$	
$\mathcal{O}_{\phi G}$	$\phi^\dagger\phi G^A_{\mu\nu}G^{\mu\nu}_A$	$\mathcal{O}_{eW}$	$\left(\bar{\ell}\sigma^{\mu\nu}e_r\right)\tau^I\phi W_{I\mu\nu}$	$\mathcal{O}^{(1)}_{\phi\ell}$	$\left(\phi^\dagger i\overleftrightarrow{\mathcal{D}}_\mu\phi\right)\left(\bar{\ell}\gamma^\mu\ell\right)$
$\mathcal{O}_{\phi\tilde{G}}$	$\phi^\dagger\phi\tilde{G}^A_{\mu\nu}G^{\mu\nu}_A$	$\mathcal{O}_{eB}$	$\left(\bar{\ell}\sigma^{\mu\nu}e_r\right)\phi B_{I\mu\nu}$	$\mathcal{O}^{(3)}_{\phi\ell}$	$\left(\phi^\dagger i\overleftrightarrow{\mathcal{D}}^I_\mu\phi\right)\left(\bar{\ell}\tau^I\gamma^\mu\ell\right)$
$\mathcal{O}_{\phi W}$	$\phi^\dagger\phi W^I_{\mu\nu}W^{\mu\nu}_I$	$\mathcal{O}_{uG}$	$\left(\bar{q}\sigma^{\mu\nu}T^Au\right)\tilde{\phi}G^A_{\mu\nu}$	$\mathcal{O}_{\phi e}$	$\left(\phi^\dagger i\overleftrightarrow{\mathcal{D}}_\mu\phi\right)\left(\bar{e}\gamma^\mu e\right)$
$\mathcal{O}_{\phi\tilde{W}}$	$\phi^\dagger\phi\tilde{W}^I_{\mu\nu}W^{\mu\nu}_I$	$\mathcal{O}_{uW}$	$\left(\bar{q}\sigma^{\mu\nu}u\right)\tau^I\tilde{\phi}W^I_{\mu\nu}$	$\mathcal{O}^{(1)}_{\phi q}$	$\left(\phi^\dagger i\overleftrightarrow{\mathcal{D}}_\mu\phi\right)\left(\bar{q}\gamma^\mu q\right)$
$\mathcal{O}_{\phi B}$	$\phi^\dagger\phi B_{\mu\nu}B^{\mu\nu}$	$\mathcal{O}_{uB}$	$\left(\bar{q}\sigma^{\mu\nu}u\right)\tilde{\phi}B_{\mu\nu}$	$\mathcal{O}^{(3)}_{\phi q}$	$\left(\phi^\dagger i\overleftrightarrow{\mathcal{D}}^I_\mu\phi\right)\left(\bar{q}\tau^I\gamma^\mu q\right)$
$\mathcal{O}_{\phi\tilde{B}}$	$\phi^\dagger\phi\tilde{B}_{\mu\nu}B^{\mu\nu}$	$\mathcal{O}_{dG}$	$\left(\bar{q}\sigma^{\mu\nu}T^Ad\right)\phi G^A_{\mu\nu}$	$\mathcal{O}_{\phi u}$	$\left(\phi^\dagger i\overleftrightarrow{\mathcal{D}}_\mu\phi\right)\left(\bar{u}\gamma^\mu u\right)$
$\mathcal{O}_{\phi WB}$	$\phi^\dagger\tau^I\phi W_{I\mu\nu}B^{\mu\nu}$	$\mathcal{O}_{dW}$	$\left(\bar{q}\sigma^{\mu\nu}d\right)\tau^I\phi W^I_{\mu\nu}$	$\mathcal{O}_{\phi d}$	$\left(\phi^\dagger i\overleftrightarrow{\mathcal{D}}_\mu\phi\right)\left(\bar{d}\gamma^\mu d\right)$
$\mathcal{O}_{\phi\tilde{W}B}$	$\phi^\dagger\tau^I\phi\tilde{W}_{I\mu\nu}B^{\mu\nu}$	$\mathcal{O}_{dB}$	$\left(\bar{q}\sigma^{\mu\nu}d\right)\phi B_{\mu\nu}$	$\mathcal{O}_{\phi ud}$	$\left(\tilde{\phi}^\dagger i\overleftrightarrow{\mathcal{D}}_\mu\phi\right)\left(\bar{u}\gamma^\mu d\right)$

Table 2.1: Dimension six not four-fermion operators.[12]

These alone allow to completely determine $\mathcal{L}_5$, which contains "one and only one" operator (here and only here all the indices are present) and had already been found by Weinberg [17] in 1979:

$$\mathcal{L}_5 = c_5^{rs}\epsilon^{ij}\epsilon^{kl}\left(\ell^T_{ir}C\ell_{ks}\right)\phi_j\phi_l + h.c., \tag{2.3.2}$$

where r, s are the generation indices and i, j, k, l the SU(2) gauge indices and C is the charge conjugation matrix. It is interesting to notice that $\mathcal{L}_5$ contains a $\Delta L = 2$ interaction, which violates the lepton numbers conservation and gives a Majorana mass term to the neutrinos after the EWSSB. The breaking of lepton (and baryon) number conservation could seem a coincidence, but it has been demonstrated [21] that every operator built from SM fields satisfy

$$\frac{\Delta B - \Delta L}{2} \equiv D \qquad mod\ 2. \tag{2.3.3}$$

This makes it clear that a $D = 5$ operator cannot conserve both lepton and baryon number. However, here one is interested in $D = 6$ operators and the $D = 5$ one will be ignored in what follows.

$(\bar{L}L)(\bar{L}L)$		$(\bar{R}R)(\bar{R}R)$		$(\bar{L}L)(\bar{R}R)$	
$\mathcal{O}_{\ell\ell}$	$(\ell\gamma_\mu\ell)(\ell\gamma^\mu\ell)$	$\mathcal{O}_{ee}$	$(\bar{e}\gamma_\mu e)(\bar{e}\gamma^\mu e)$	$\mathcal{O}_{\ell e}$	$(\bar{\ell}\gamma_\mu\ell)(\bar{e}\gamma_\mu e)$
$\mathcal{O}_{qq}^{(1)}$	$(\bar{q}\gamma_\mu q)(\bar{q}\gamma^\mu q)$	$\mathcal{O}_{uu}$	$(\bar{u}\gamma_\mu u)(\bar{u}\gamma^\mu u)$	$\mathcal{O}_{\ell u}$	$(\bar{\ell}\gamma_\mu\ell)(\bar{u}\gamma_\mu u)$
$\mathcal{O}_{qq}^{(3)}$	$(\bar{q}\gamma_\mu\tau^I q)(\bar{q}\gamma^\mu\tau_I q)$	$\mathcal{O}_{dd}$	$(\bar{d}\gamma_\mu d)(\bar{d}\gamma^\mu d)$	$\mathcal{O}_{\ell d}$	$(\bar{\ell}\gamma_\mu\ell)(\bar{d}\gamma_\mu d)$
$\mathcal{O}_{\ell q}^{(1)}$	$(\bar{\ell}\gamma_\mu\ell)(\bar{q}\gamma^\mu q)$	$\mathcal{O}_{eu}$	$(\bar{e}\gamma_\mu e)(\bar{u}\gamma^\mu u)$	$\mathcal{O}_{qe}$	$(\bar{q}\gamma_\mu q)(\bar{e}\gamma^\mu e)$
$\mathcal{O}_{\ell q}^{(3)}$	$(\bar{\ell}\gamma_\mu\tau^I\ell)(\bar{q}\gamma^\mu\tau_I q)$	$\mathcal{O}_{ed}$	$(\bar{e}\gamma_\mu e)(\bar{d}\gamma^\mu d)$	$\mathcal{O}_{qu}^{(1)}$	$(\bar{q}\gamma_\mu q)(\bar{u}\gamma^\mu u)$
		$\mathcal{O}_{ud}^{(1)}$	$(\bar{u}\gamma_\mu u)(\bar{d}\gamma^\mu d)$	$\mathcal{O}_{qu}^{(8)}$	$(\bar{q}\gamma_\mu T^A q)(\bar{u}\gamma^\mu T_A u)$
		$\mathcal{O}_{ud}^{(8)}$	$(\bar{u}\gamma_\mu T^A u)(\bar{d}\gamma^\mu T_A d)$	$\mathcal{O}_{qd}^{(1)}$	$(\bar{q}\gamma_\mu q)(\bar{d}\gamma^\mu d)$
				$\mathcal{O}_{qd}^{(8)}$	$(\bar{q}\gamma_\mu T^A q)(\bar{d}\gamma^\mu T_A d)$
$(\bar{L}R)(\bar{R}L)$ and $(\bar{L}R)(\bar{L}R)$		B-violating			
$\mathcal{O}_{\ell edq}$	$(\bar{\ell}^j e)(\bar{d}q^j)$	$\mathcal{O}_{duq}$	$\epsilon_{\alpha\beta\gamma}\epsilon_{ij}\left[(d^\alpha)^T C u^\beta\right]\left[(q^{\gamma j})^T C e\right]$		
$\mathcal{O}_{quqd}^{(1)}$	$(\bar{q}^j u_r)\,\epsilon_{jk}\,(\bar{q}^k d)$	$\mathcal{O}_{qqu}$	$\epsilon^{\alpha\beta\gamma}\epsilon_{jk}\left[(q_j^\alpha)^T C q_k^\beta\right]\left[(u^\gamma)^T C e\right]$		
$\mathcal{O}_{quqd}^{(8)}$	$(\bar{q}^j T^A u_r)\,\epsilon_{jk}\,(\bar{q}^k T_A d)$	$\mathcal{O}_{qqq}$	$\epsilon^{\alpha\beta\gamma}\epsilon_{jk}\epsilon_{km}\left[(q_j^\alpha)^T C q_k^\beta\right]\left[(q^\gamma)^T C \ell^n\right]$		
$\mathcal{O}_{\ell equ}^{(1)}$	$(\bar{\ell}^j e)\,\epsilon_{jk}\,(\bar{q}^k u)$	$\mathcal{O}_{duu}$	$\epsilon_{\alpha\beta\gamma}\left[(d^\alpha)^T C u^\beta\right]\left[(u^\gamma)^T C e\right]$		
$\mathcal{O}_{\ell equ}^{(3)}$	$(\bar{\ell}^j\sigma_{\mu\nu}e)\,\epsilon_{jk}\,(\bar{q}^k\sigma^{\mu\nu}u)$				

Table 2.2: Dimension six four-fermion operators.[12]

Passing to $\mathcal{L}_6$ makes things much more complicated than one might imagine, judging by $\mathcal{L}_5$. A complete basis for the dimension six lagrangian was found by [12] in 2010, refining the work made by [22] twenty-five years before. This basis is usually called the "Warsaw basis" and one can see the operators in Tables 2.1 and 2.2 divided in the eight classes $X^3, H^6, H^4\mathcal{D}^2, X^2H^2, \psi^2H^3, \psi^2XH, \psi^2H^2\mathcal{D}, \psi^4$. The complete basis of operators in the $D = 6$ case will not be derived here, but some details and ideas about how to proceed are given in Appendix A.

What is interesting is that there are different ways of counting the species of operators in literature. According to the "Warsaw basis" table (and a number of generation $n_g = 1$) one has 4 $\Delta B = \Delta L = 1$ operators and 59 $\Delta B = \Delta L = 0$ operators. However in [13] one has (Table 2.3) 76 hermitian $\Delta B = \Delta L = 0$ operators. This is due to the fact that some of the operator types are not hermitian and therefore have to be counted as two hermitian operators. If one extends all to $n_g = 3$ generations, in the dimension $D = 6$ case one has 273 $\Delta B = \Delta L = 1$ operators (plus their hermitian conjugated ones) and 2499 $\Delta B = \Delta L = 0$ hermitian operators.

DIM		$n_g = 1$			$n_g = 3$		
		CP-even	CP-odd	Total	CP-even	CP-odd	Total
5	$\Delta L = 2$			1			6
5	$\Delta L = -2$			1			6
6	$\Delta B = \Delta L = 1$			4			273
6	$\Delta B = \Delta L = 1$			4			273
6	X^3	2	2	4	2	2	4
6	ϕ^6	1	0	1	1	0	1
6	$\phi^4\mathcal{D}^2$	2	0	2	2	0	2
6	$X^2\phi^2$	4	4	8	4	4	8
6	$\psi^2\phi^3$	3	3	6	27	27	54
6	$\psi^2 X\phi$	8	8	16	72	72	144
6	$\psi^2\phi^2\mathcal{D}$	8	1	9	51	30	81
6	$(\bar{L}L(\bar{L}L))$	5	0	5	171	126	297
6	$(\bar{R}R(\bar{R}R))$	7	0	7	255	195	450
6	$(\bar{L}R(\bar{R}L)) + h.c.$	1	1	2	81	81	162
6	$(\bar{L}R(\bar{L}R)) + h.c.$	4	4	8	324	324	648
	Total $\Delta B = \Delta L = 0$	53	23	76	1350	1149	2499

Table 2.3: Operators number $D = 5, 6$ in SMEFT.

2.3.2 Some results

Once one has built the $D = 6$ SMEFT lagrangian, one can start looking at the effects induced by some operators with respect to the SM.
In some cases those effects translate in a simple shift of some SM parameters already at tree level, in other cases they have a deeper meaning.
Since second order contributions of $D = 6$ operators contribute as the first order ones of the $D = 8$ operators, one needs only to consider those at the first order of the former.
The derivation present in [20] is followed.

Higgs lagrangian

Let one consider the Higgs lagrangian and the correction it receives.
The potential gets a ϕ^6 term by means of the operator $\mathcal{O}_\phi$

$$V[\phi] = \lambda\left(\phi^\dagger\phi - \frac{v^2}{2}\right)^2 - c_\phi\left(\phi^\dagger\phi\right)^3 : \tag{2.3.4}$$

this translates into a shift of the vev equal to (first order in c_ϕ)

$$\left\langle\phi^\dagger\phi\right\rangle = \frac{v^2}{2}\left(1 + \frac{3c_\phi v^2}{4\lambda}\right) \equiv \frac{v_T^2}{2}. \tag{2.3.5}$$

Also the kinetic term gets a correction because of the operators $\mathcal{O}_{\phi\Box}$ and $\mathcal{O}_{\phi\mathcal{D}}$

$$\mathcal{L}_{kin,\phi} = (\mathcal{D}_\mu\phi)^\dagger(\mathcal{D}^\mu\phi) + c_{\phi\Box}(\phi^\dagger\phi^\dagger)\Box(\phi^\dagger\phi^\dagger) + c_{\phi\mathcal{D}}(\phi^\dagger\mathcal{D}_\mu\phi)^*(\phi^\dagger\mathcal{D}_\mu\phi). \tag{2.3.6}$$

In order to normalise it correctly, one gets (in unitary gauge)

$$\phi = \frac{1}{\sqrt{2}} \begin{pmatrix} 0 \\ (1 + c_{H,kin})H + v_T \end{pmatrix}, \tag{2.3.7}$$

where again, at the first order in operators coefficients

$$c_{H,kin} \equiv \left(c_{\phi\Box} - \frac{c_{\phi\mathcal{D}}}{4} \right) v^2, \qquad v_T \equiv \left(1 + \frac{3c_\phi v^2}{8\lambda} \right) v. \tag{2.3.8}$$

Expanding new Higgs lagrangian, one can find

$$\begin{aligned} \mathcal{L} = & \frac{1}{2}\partial_\mu H \partial^\mu H - \frac{c_{H,kin}}{v_T^2} \left(H^2 + 2vH \right) \left(\partial_\mu H \partial^\mu H \right) - \lambda v_t^2 \left(1 - \frac{3c_\phi v^2}{2\lambda} + 2c_{H,kin} \right) H^2 \\ & - \lambda v_T \left(1 - \frac{5c_\phi v^2}{2\lambda} + 3c_{H,kin} \right) H^3 - \frac{\lambda}{4} \left(1 - \frac{15c_\phi v^2}{2\lambda} + 4c_{H,kin} \right) H^4 + \frac{3}{4} c_H v H^5 + \frac{c_\phi}{8} H^6 \end{aligned} \tag{2.3.9}$$

and redefine the Higgs mass as

$$m_H^2 = 2\lambda v_T^2 \left(1 - \frac{3c_\phi v^2}{2\lambda} + 2c_{H,kin} \right). \tag{2.3.10}$$

Fermion masses and Fermi constant

Interesting modifications take place in the Yukawa sector, where fermions and the Higgs boson interact. Before SSB, the lagrangian for a fermion ψ takes the following form:

$$\begin{aligned} \mathcal{L}_{yuk} = & - \left[\phi^{\dagger j} \bar{d}_r \left[Y_d \right]_{rs} q_{js} + \tilde{\phi}^{\dagger j} \bar{u}_r \left[Y_u \right]_{rs} q_{js} \phi^{\dagger j} \bar{e}_r \left[Y_e \right]_{rs} \ell_{js} + h.c. \right] \\ & + \left[c^*_{\substack{d\phi \\ sr}} \left(\phi^\dagger \phi \right) \phi^{\dagger j} \bar{d}_r q_{js} + c^*_{\substack{u\phi \\ sr}} \left(\phi^\dagger \phi \right) \tilde{\phi}^{\dagger j} \bar{u}_r q_{js} + c^*_{\substack{e\phi \\ sr}} \left(\phi^\dagger \phi \right) \phi^{\dagger j} \bar{e}_r q_{js} + h.c. \right] \end{aligned} \tag{2.3.11}$$

Expanding about the vev after the SSB, one gets the fermion ψ mass matrix

$$\left[M_\psi \right]_{rs} = \frac{v_T}{\sqrt{2}} \left(\left[Y_\psi \right]_{rs} - \frac{v^2 (c^*_{\psi\phi})_{sr}}{2} \right), \tag{2.3.12}$$

and the following interaction matrix between the Higgs and a fermion ψ

$$\left[\Upsilon_\psi \right]_{rs} = \frac{\left[M_\psi \right]_{rs}}{v_T} \left(1 + c_{H,kin} \right) - \frac{v^2}{\sqrt{2}} (c^*_{\phi\phi})_{sr}. \tag{2.3.13}$$

What is noticeable is that the interaction matrix it not simply proportional to the mass matrix of the fermions: the coupling of the Higgs boson to the fermion will not be therefore diagonal in flavour.

Also the Fermi's constant is affected by the dimension six operators: the four fermion operators and the one from the W exchange. Remembering that this parameter is obtained by studying the muon lifetime, one has:

$$\frac{4G_F}{\sqrt{2}} = \frac{2}{v_T^2} - ((c_{ll})_{\mu ee\mu} + (c_{ll})_{e\mu\mu e}) + 2\left((c_{Hl}^{(3)})_{ee} + (c_{Hl}^{(3)})_{\mu\mu}\right). \tag{2.3.14}$$

Gauge bosons masses and couplings

Some dimension six terms also affect the definition of gauge fields and their couplings and they are encoded in the following lagrangian:

$$\begin{aligned}\mathcal{L}_{gauge}^{(6)} = {} & c_{\phi G}\phi^\dagger\phi G^A_{\mu\nu}G_A^{\mu\nu} + c_{\phi W}\phi^\dagger\phi W^I_{\mu\nu}W_I^{\mu\nu} + c_{HB}\phi^\dagger\phi B_{\mu\nu}B^{\mu\nu} + c_{\phi WB}\phi^\dagger\tau^I\phi W^I_{\mu\nu}B^{\mu\nu} \\ & + c_G f^{ABC}G^{A\nu}_\mu G^{B\rho}_\nu G^{C\mu}_\rho + c_W\epsilon^{IJK}W^\nu_{I\mu}W^\rho_{J\nu}W^\mu_{K\rho}.\end{aligned} \tag{2.3.15}$$

Moreover, after SSB, the gauge kinetic term receives contributions by the $X\phi^2$ operators as follows:

$$\begin{aligned}\mathcal{L}_{gauge,kin}^{SM} + \mathcal{L}^{(6)} = {} & -\frac{1}{2}W^+_{\mu\nu}W_-^{\mu\nu} - \frac{1}{4}W^3_{\mu\nu}W_3^{\mu\nu} - \frac{1}{4}B^{\mu\nu}B_{\mu\nu} - \frac{1}{4}G^A_{\mu\nu}G_A^{\mu\nu} + \frac{v_T^2}{2}c_{\phi G}G^A_{\mu\nu}G_A^{\mu\nu} \\ & + \frac{v_T^2}{2}c_{\phi W}W^I_{\mu\nu}W_I^{\mu\nu} + \frac{v_T^2}{2}c_{\phi B}B^{\mu\nu}B_{\mu\nu}\frac{v_T^2}{2}c_{\phi W}c_{\phi WB}W^3_{\mu\nu}B^{\mu\nu}.\end{aligned} \tag{2.3.16}$$

As one can notice, this implies a non canonical normalisation of the gauge fields. In addition to that, the last term in the above lagrangian leads to a kinetic mixing between W^3 and B. Even the gauge boson mass term gets some corrections,

$$\mathcal{L}_{gauge,mass} = \frac{g^2v_T^2}{4}W^+_\mu W_-^\mu + \frac{v_T^2}{8}\left(gW^3_\mu - g'B_\mu\right)^2\frac{v_T^4}{16}c_{\phi D}\left(gW^3_\mu - g'B_\mu\right)^2. \tag{2.3.17}$$

As one can guess, it is necessary to redefine the gauge fields and the coupling constants as follows:

$$G^A_\mu = \mathcal{G}^A_\mu\left(1 + c_{\phi G}v_T^2\right), \quad W^I_\mu = \mathcal{W}^I_\mu\left(1 + c_{\phi W}v_T^2\right), \quad B_\mu = \mathcal{B}_\mu\left(1 + c_{\phi B}v_T^2\right) \tag{2.3.18}$$

$$\bar{g}_s = g_s\left(1 + c_{\phi G}v_T^2\right), \quad \bar{g} = g\left(1 + c_{\phi W}v_T^2\right), \quad \bar{g}' = g'\left(1 + c_{\phi B}v_T^2\right), \tag{2.3.19}$$

leaving $gW^I_\mu = \bar{g}\mathcal{W}^I_\mu$ unchanged.
However, this is not the end of the story. One has to find the mass eigenstates for W^3_μ and B_μ after the above redefinitions.
Let one consider once again the lagrangian for the electroweak bosons:

$$\begin{aligned}\mathcal{L}_{EW,gauge} = {} & -\frac{1}{2}\mathcal{W}^+_{\mu\nu}\mathcal{W}_-^{\mu\nu} - \frac{1}{4}\mathcal{W}^3_{\mu\nu}\mathcal{W}_3^{\mu\nu} - \frac{1}{4}\mathcal{B}_\mu\nu\mathcal{B}^{\mu\nu} - \frac{1}{2}v_T^2c_{\phi WB}\mathcal{W}^3_{\mu\nu}\mathcal{B}^{\mu\nu} + \\ & + \frac{1}{4}\bar{g}^2v_T^2\mathcal{W}^3_{\mu\nu}\mathcal{B}^{\mu\nu} + \frac{v_T^2}{8}\left(\bar{g}\mathcal{W}^3_\mu - \bar{g}'\mathcal{B}\right)^2 + \frac{v_T^4}{16}c_{\phi\mathcal{D}}\left(\bar{g}\mathcal{W}^3_\mu - \bar{g}'\mathcal{B}_\mu\right)^2.\end{aligned} \tag{2.3.20}$$

It turns out, that in order obtain canonical kinetic terms and diagonalise simultaneously the mass matrix one has to do the following transformation [23]

$$\begin{pmatrix}\mathcal{W}_\mu^3\\ \mathcal{B}_\mu\end{pmatrix}=\begin{pmatrix}1 & -\frac{v_T^2}{2}c_{\phi WB}\\ -\frac{v_T^2}{2}c_{\phi WB} & 1\end{pmatrix}\begin{pmatrix}\cos\bar\theta & \sin\bar\theta\\ -\sin\bar\theta & \cos\bar\theta\end{pmatrix}\begin{pmatrix}\mathcal{Z}_\mu\\ \mathcal{A}_\mu\end{pmatrix}, \tag{2.3.21}$$

and in this way

$$\tan\bar\theta=\frac{\bar g'^2}{\bar g^2}+\frac{v_T^2}{2}c_{\phi WB}\left(1-\frac{\bar g'^2}{\bar g^2}\right) \tag{2.3.22}$$

$$\sin\bar\theta=\frac{\bar g'}{\sqrt{\bar g'^2+\bar g^2}}\left[1+\frac{v_T^2}{2}\frac{\bar g}{\bar g'}\frac{\bar g^2-\bar g'^2}{\bar g^2+\bar g'^2}c_{\phi WB}\right] \tag{2.3.23}$$

$$\cos\bar\theta=\frac{\bar g}{\sqrt{\bar g'^2+\bar g^2}}\left[1-\frac{v_T^2}{2}\frac{\bar g'}{\bar g}\frac{\bar g^2-\bar g'^2}{\bar g^2+\bar g'^2}c_{\phi WB}\right]. \tag{2.3.24}$$

After this transformation, one finally obtains the mass eigenstates. As expected, the photon is massless due to $U(1)_{EM}$ invariance, while the W and Z masses become

$$\begin{aligned}m_W^2&=\frac{\bar g^2 v_T^2}{4}\\ m_Z^2&=\frac{v_T^2}{4}\left(\bar g'^2+\bar g^2\right)+\frac{v_T^4}{8}c_{\phi\mathcal{D}}\left(\bar g'^2+\bar g^2\right)+\frac{v_T^4}{2}\bar g'\bar g c_{\phi WB}.\end{aligned} \tag{2.3.25}$$

To conclude, one presents the new covariant derivative structure and some effective couplings.
The covariat derivative takes the form

$$\mathcal{D}_\mu=\partial_\mu+i\frac{\bar g}{\sqrt{2}}\left(\mathcal{W}_\mu^+T_++\mathcal{W}^-T_-\right)+i\bar g_Z\left(T_3-\bar s^2Q\right)\mathcal{Z}_\mu+i\bar e\mathcal{A}_\mu \tag{2.3.26}$$

and the effective couplings are

$$\begin{aligned}\bar e&=\frac{\bar g'\bar g}{\sqrt{\bar g'^2+\bar g^2}}\left(1-\frac{\bar g'\bar g}{\bar g'^2+\bar g^2}v_T^2c_{\phi WB}\right)=\bar g\sin\bar\theta-\frac{1}{2}\cos\bar\theta\bar g v_T^2c_{\phi WB},\\ \bar g_Z&=\sqrt{\bar g'^2+\bar g^2}+\frac{\bar g'\bar g}{\bar g'^2+\bar g^2}v_T^2c_{\phi WB}=\frac{\bar e}{\sin\bar\theta\cos\bar\theta}\left(1+\frac{\bar g'^2+\bar g^2}{2\bar g'\bar g}v_T^2c_{\phi WB}\right),\\ \bar s^2&\equiv\sin^2\bar\theta=\frac{\bar g'^2}{\bar g'^2+\bar g^2}+\frac{\bar g'\bar g\left(\bar g^2-\bar g'^2\right)}{\left(\bar g'^2+\bar g^2\right)^2}v_T^2c_{\phi WB}.\end{aligned} \tag{2.3.27}$$

Another important quantity which is redefined is the ρ parameter:

$$\rho\equiv\frac{\bar g^2m_Z^2}{\bar g_Z^2m_W^2}=1+\frac{v_T^2}{2}c_{\phi D}. \tag{2.3.28}$$

The introduced $\bar g,\bar g',v_T,c_{\phi WB}$, $c_{\phi\mathcal{D}}$ can be fixed by measuring, for example, the W and Z masses and couplings, and the photon coupling.

RGE

In the previous paragraphs the SMEFT and its 2499 operators have been introduced. One has seen after that many important consequences appear already at the tree-level. However, one needs to go to one loop level and study the renormalisation rroup equations in order to get more precise predictions. The results of this monumental work by E. E. Jenkins, A. V. Manohar and M. Trott are illustrated in [18], [19] and [20], where the one loop anomalous 2499 x 2499 anomalous dimension matrix for the dimension six operators in SMEFT is given.

Chapter 3

Unitarity cancellations and the Goldstone Equivalence Theorem

In this chapter some useful concepts for what comes next are introduced.
In the first section, some hints about how to get in to the ξ gauge through the Faddeev-Popov trick are briefly given. In this gauge, even unphysical particles can give contributions to process diagrams and their presence is fundamental for the unitarity of the theory.
Next, in the second section, one will focus on the Goldstone bosons and introduce the Goldstone Equivalence Theorem (GET), which helps in simplifying calculations at high-energy.
In the third and last section, the case of the $W_L^- W_L^+ \to W_L^- W_L^+$ will be considered as application of the concepts introduced in the two preceding sections.

3.1 R_ξ gauge and unitarity cancellations

In Chapter 1 the SSB Mechanism and the Higgs mechanism were studied and applied in order to get the standard model lagrangian. During that procedure, one got rid of the unphysical Goldstone bosons by choosing a particular gauge, i.e. the *unitary gauge*, which allowed one to keep only the physical degrees of freedom.
However, it is not clear in this gauge what the rules of perturbation theory are and how such a gauge constraint is preserved when computing Feynman diagrams.
The solution to this is to perform a formal *gauge fixing procedure* by means of the Faddeev-Popov trick in the path integral approach. This will lead to a one parameter gauge family, called R_ξ *gauge*, where R stands for "renormalisability". One will see that the Goldstone bosons are kept, together with other unphysical fields (i.e. ghost fields), and play a major role entering in computations and in the intricate cancellations that happen in order to maintain the unitarity of the theory.

Since it is far beyond the goal of this work, one will only show the main points of the gauge fixing procedure in the simple case of an Abelian gauge theory.
Let one consider again the scalar QED-like lagrangian for a complex scalar field ϕ (of charge $q = -e$) with U(1) gauge symmetry $\delta\phi = -ie\alpha(x)\phi$, $\delta A_\mu(x) = \partial_\mu\alpha(x)$

$$\mathcal{L} = -\frac{1}{4}F^{\mu\nu}F_{\mu\nu} - (\mathcal{D}_\mu\phi)^* (\mathcal{D}^\mu\phi) - V[\phi], \tag{3.1.1}$$

where $\mathcal{D}_\mu\phi \equiv (\partial_\mu + ieA_\mu)\,\phi$.
Differently from what it was done in Chapter 1, here one will work explicitly with the real components of the scalar field

$$\phi_1 = \frac{\phi + \phi^*}{\sqrt{2}}, \qquad \phi_2 = \frac{\phi - \phi^*}{\sqrt{2}i}. \tag{3.1.2}$$

This implies that the lagrangian is symmetric under the infinitesimal local transformations:

$$\delta\phi_1 = e\alpha(x)\phi_2, \qquad \delta\phi_2 = -e\alpha(x)\phi_1, \qquad \delta A_\mu = \partial_\mu\alpha(x). \tag{3.1.3}$$

Like in Chapter 1, the potential is such that the scalar field acquires a vacuum expectation value $\langle\phi_1\rangle = v$ and $\langle\phi_2\rangle = 0$, and one expands the lagrangian around the vev

$$\phi_1(x) = v + H(x), \qquad \phi_2(x) = \varphi(x) : \tag{3.1.4}$$

$$\begin{aligned}\mathcal{L}(A, H, \varphi) = &-\frac{1}{4}F_{\mu\nu}F^{\mu\nu} + \frac{(\partial_\mu H - eA_\mu\varphi)\,(\partial^\mu H - eA^\mu\varphi)}{2} \\ &+ \frac{[\partial_\mu\varphi - eA_\mu\,(v + H(x))]\,[\partial^\mu\varphi - eA^\mu\,(v + H(x))]}{2} - V[\phi],\end{aligned} \tag{3.1.5}$$

preserving the symmetry of Eq. (3.1.3).
Passing to the path integral formulation, one has

$$Z = \int DA\; DH\; D\varphi\; e^{i\int \mathcal{L}[A,H,\varphi]}, \tag{3.1.6}$$

which is ill-defined because of the infinite number of points (corresponding to equivalent physical configurations) for every gauge orbit. In order to choose only one point for each orbit, one introduces a gauge fixing condition using the Fadeev-Popov trick and ends with:

$$Z = N\int DA\; DH\; D\varphi\; e^{i\int \mathcal{L}[A,H,\varphi]}\delta[\Phi(A, H, \varphi)]det\left[\frac{\delta\Phi}{\delta\alpha}\right], \tag{3.1.7}$$

with N proportional to the gauge volume. By choosing $\Phi = G(A, H, \varphi) - \omega$ (with ω some scalar function) and integrating over ω using a gaussian weight centered in $\omega = 0$, one gets:

$$Z = N'\int DA\; DH\; D\varphi\; e^{i\int\left[\mathcal{L}[A,H,\varphi] - \frac{G^2}{2}\right]}det\left[\frac{\delta G}{\delta\alpha}\right] \tag{3.1.8}$$

The R_ξ gauge class corresponds to the choice

$$G(A,H,\varphi) = -\frac{(\partial_\mu A^\mu - \xi ev\varphi)}{\sqrt{\xi}} \tag{3.1.9}$$

and (after having expanded the potential) keeping only the quadratic terms, one gets:

$$\begin{aligned}\left(\mathcal{L} - \frac{G^2}{2}\right)_{quadratic} =& -\frac{1}{2}A_\mu\left[-g^{\mu\nu}\Box + \left(1-\frac{1}{\xi}\right)\partial^\mu\partial^\nu - (ev)^2 g^{\mu\nu}\right]A_\nu \\ &+ \frac{\partial_\mu H\partial^\mu H}{2} + \frac{\partial_\mu\varphi\partial^\mu\varphi}{2} - \frac{m_H^2}{2}H^2 - \frac{\xi(ev)^2}{2}\varphi^2,\end{aligned} \tag{3.1.10}$$

where m_H is the one found in Chapter 1. Defining $ev \equiv m_A$, one observes that the Goldstone Boson gets a mass, $m_{GB} = \sqrt{\xi}m_A$; its dependence on the gauge parameter is a clear footprint of the unphysical nature of this field.
From this lagrangian, one can deduce the general propagator form for the fields. Before doing so, one completes the Fadeev-Popov procedure, introducing the anticommuting ghost fields. They arise from the functional determinant

$$det\left[\frac{\delta G}{\delta\alpha}\right] = det\left[-\frac{\Box + \xi m_A^2\left(1+\frac{H}{v}\right)}{\sqrt{\xi}}\right], \tag{3.1.11}$$

which corresponds to the ghost lagrangian

$$\mathcal{L}_{ghost} = -\bar{c}\left[\Box + \xi m_A^2\left(1+\frac{H}{v}\right)\right]c. \tag{3.1.12}$$

It is noticeable that also the unphysical ghost fields acquire the same gauge dependent mass as the Goldstone boson, i. e. $m_{ghost} = \sqrt{\xi}m_A$.
Passing to momentum space, it is straightforward to get the propagators

$$\tilde{D}_F^{\mu\nu}(k) = \frac{i}{k^2 - m_A^2 + i\epsilon}\left[-g^{\mu\nu} + (1-\xi)\frac{k^\mu k^\nu}{k^2 - \xi m_A^2 + i\epsilon'}\right] \tag{3.1.13}$$

$$\tilde{D}_F^{H}(k) = \frac{i}{k^2 - m_H^2 + i\epsilon} \tag{3.1.14}$$

$$\tilde{D}_F^{GB}(k) = \frac{i}{k^2 - \xi m_A^2 + i\epsilon} \tag{3.1.15}$$

$$\tilde{D}_F^{Gh}(p) = \frac{i}{k^2 - \xi m_A^2 + i\epsilon} \tag{3.1.16}$$

(here, one has preferred to separate the Goldstone and the ghost propagators, because they are different in the non-Abelian case). One clearly sees that the unitary gauge is

recovered in the limit $\xi \to \infty$.
If one analyses the non-Abelian case, the steps are the same as for the Abelian case (albeit slightly more complicated because of the richer non-Abelian structure).
Before looking at a practical example of cancellations, some comments.
Firstly, such cancellations are expected to take place because no term depending on the gauge fixing parameter must appear in S-matrix elements. Even in non-Aabelian case, the cancellations have been proved to happen at all orders in perturbation theory thanks to the BRST symmetry of the gauge fixing lagrangian ([24, 25]).
Secondly, consider the massive vector boson propagator, which one expects to have three degrees of freedom (two transverse and one longitudinal). This is not so clear in the unitary gauge. Consider instead the propagator in the ξ gauge and rewrite it as (add and subtract $\frac{k^\mu k^\nu}{m_A^2}$ and split the expression in gauge dependent and independent parts)

$$D_F^{\mu\nu}(k) = \frac{-i}{k^2 - m_A^2}\left(g^{\mu\nu} - \frac{k^\mu k^\nu}{m_A^2}\right) + \frac{-i}{k^2 - \xi m_A^2}\left(\frac{k^\mu k^\nu}{m_A^2}\right). \tag{3.1.17}$$

The second (gauge dependent) term is exactly the opposite of the Goldstone boson propagator: that term will be the cancelled in processes which admit a diagram with a vector boson exchange and another in which the Goldstone boson is exchanged. Consider now the numerator of the first term: the tensor structure is the one of a vector boson polarisation sum. Moreover, if the vector is on shell and a boost in the rest frame is performed, the numerator becomes a projector onto three purely spatial directions. If only the on-shell contribution is required, the numerator is the the projector onto physical states. The gauge dependent, time-like part, is exactly cancelled by the Goldstone boson contribution.
That cancellation takes place in a more or less intricate way, depending on the process. As an example at tree level, consider the coupling of a fermion to the spontaneously broken gauge lagrangian through a chiral interaction

$$\mathcal{L}_f = \bar{\psi}_L(i\not{\mathcal{D}})\psi_L + \bar{\psi}_R(i\not{\mathcal{D}})\psi_R - \lambda_f\left(\bar{\psi}_L\phi\psi_R + h.c.\right). \tag{3.1.18}$$

The fermion mass is given by $m_f = \lambda_f \frac{v}{\sqrt{2}}$ from the SSB. For a fermion-fermion scattering process, one has in Fig.3.1 three diagrams which contribute: the scalar H exchange one, the Goldstone exchange one and the vector boson exchange one. As mentioned before, one expects that the Goldstone boson contribution will be cancelled in some way. Looking at the Goldstone boson and the vector boson contributions to the amplitude, one has

$$i\mathcal{M}_\varphi = \frac{\lambda_f^2}{2}\bar{u}(p')\gamma^5 u(p)\tilde{D}_F^\varphi(p'-p;\xi)\bar{u}(k')\gamma^5 u(k) \tag{3.1.19}$$

$$i\mathcal{M}_A = -e^2\bar{u}(p')\gamma^\mu\frac{1-\gamma^5}{2}u(p)\tilde{D}_{F\mu\nu}(p'-p;\xi)\bar{u}(k')\gamma^\nu\frac{1-\gamma^5}{2}u(k). \tag{3.1.20}$$

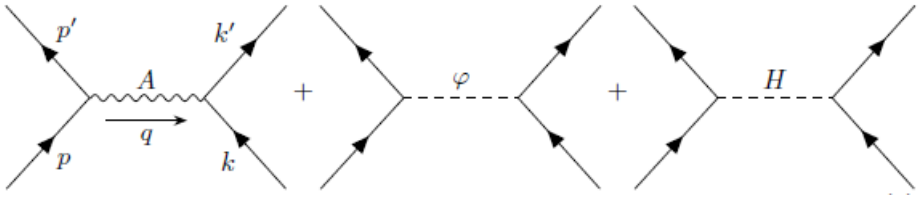

Figure 3.1: Diagrams involved in the fermion-fermion scattering from the lagrangian in Eq. (3.1.18).

It is easy to check that writing the vector boson propagator as in Eq. (3.1.17), and using

$$(p'-p)^\mu \bar{u}(p')\gamma^\mu \frac{1-\gamma^5}{2}u(p) = m_f \bar{u}(p')\gamma^5 u(p), \tag{3.1.21}$$

one gets

$$\begin{aligned} i\mathcal{M}_A = &-e^2 \bar{u}(p')\gamma^\mu \frac{1-\gamma^5}{2}u(p)\frac{i}{q^2-m_A^2}\left(g_{\mu\nu}-\frac{q^\mu q^\nu}{m_A^2}\right)\bar{u}(k')\gamma^\nu \frac{1-\gamma^5}{2}u(k) \\ &+\frac{\lambda_f^2}{2}\bar{u}(p')\gamma^5 u(p)\frac{-i}{q^2-\xi m_A^2}\bar{u}(k')\gamma^5 u(k), \end{aligned} \tag{3.1.22}$$

and clearly the unphysical gauge dependent part is identically cancelled by the Goldstone boson contribution to the process, whose amplitude is therefore gauge independent, as expected.

3.1.1 Unitarity and tree-level unitarity

In this chapter (see Section 3.3) and in chapter 2, unitarity violating behaviour in amplitudes has been mentioned several times but the criterion used to identify this has never been explained for a general scattering process.
How can it be understood whether or not the behaviour of an an amplitude breaks the unitarity of the S-matrix, and therefore of the theory? In the 2 to 2 process the answer is simple: if an amplitude grows like E^n, where E is an energy scale and $n > 0$, then unitarity will be violated at some scale. Why can one say this, and what is the answer for a 2 to N process?
This can be seen from a simple dimensional analysis argument. It is well known that for a 2 to N process the differential cross section at high energy is roughly the following:

$$d\sigma_{(2\to N)} \sim \frac{|\mathcal{M}_{(2\to N)}|^2}{s}\left(\prod_{i=1}^{N}\frac{d^3p_i}{(2\pi)^3\,2E_{p_i}}\right)(2\pi)^4\,\delta^{(4)}\left(P_I-\sum_{i=1}^{N}p_i\right) \equiv \frac{|\mathcal{M}_{(2\to N)}|^2}{s}d\Phi. \tag{3.1.23}$$

The natural energy dimension of the cross section $[d\sigma] = [E]^{-2}$ is already given by the $\frac{1}{s}$ term and therefore the product of the squared amplitude and the phase space element must be a pure number. From dimensional analysis it is rather easy to see that $[d\Phi] = E^{2N-4}$ and therefore $[|\mathcal{M}|^2] = E^{4-2N}$ or $[\mathcal{M}] = E^{2-N}$.
One notices that in the 2 to 2 case the amplitude has energy dimension $\mathcal{M}_{2\to 2} = E^0$ and it is a pure number. Moreover the energy dimension coincides with the maximal energy growth the amplitude is allowed to undergo in order to respect unitarity, i.e. E^0. Is it also true for a generic 2 to N process, that its energy dimension $[\mathcal{M}] = E^{2-N}$ corresponds to maximal energy behaviour $\mathcal{M} = E^{2-N}$ it can have in a unitary theory? If yes, why?
The answer is positive and it is encoded in the *tree-unitarity criterion*. One can summarise it as follows: a theory is called tree-unitary iff all the amplitudes with N' particles incoming and N particles outgoing at high energies grow at most as $\mathcal{M} \sim E^{4-N-N'}$ in the tree-approximation. This can be shown starting from the unitarity condition on the S-matrix and has been done in [30]. Moreover, tree-level unitarity is a necessary condition for the renormalisability of a theory. Applying this criterion a 2 to N process, the scattering amplitude cannot grow more than $\mathcal{M}_{2\to N} \sim E^{2-N}$.

3.2 The Goldstone Boson Equivalence Theorem

As shown in the previous section, computations in the R_ξ gauge involve cancellations among unphysical particles. Nevertheless, there are cases where even unphysical particles leave their mark in physical observables.
One of the most iconic cases is perhaps that of the Goldstone bosons eaten by a massive vector boson, which in the high-energy limit still have control over amplitudes where the gauge boson is emitted or absorbed in longitudinal polarisation state.
This point is encoded in the so-called *Goldstone Boson Equivalence Theorem* which was first proved by Cornwall, Levin, Tiktopoulos and Vayonakis in [26] and [27]. The main idea is the following: by eating a Goldstone Boson and becoming massive, a gauge boson passes from having two transverse polarisation states to three polarisation states, one of which is longitudinal. At low energy (at rest) the three polarisation states seem to be equivalent: however, in the relativistic regime, the longitudinal one clearly distinguishes from the transverse two, showing its origin as Goldstone Boson.
As a consequence, at high-energies an amplitude where longitudinal gauge bosons are emitted/absorbed becomes equivalent to the one where, instead of longitudinal gauge bosons, Goldstone Bosons are emitted/absorbed (see Fig. 3.2).

The demonstration of this theorem is strongly based on the use of Ward's identities and was shown in [28]. A simple case where one can give an idea of the procedure is the one of a single emission/absorption of a gauge boson and requires the use of the Ward identity satisfied by a current between on-shell states.
Before doing it, it can be useful to better study the structure of the longitudinal po-

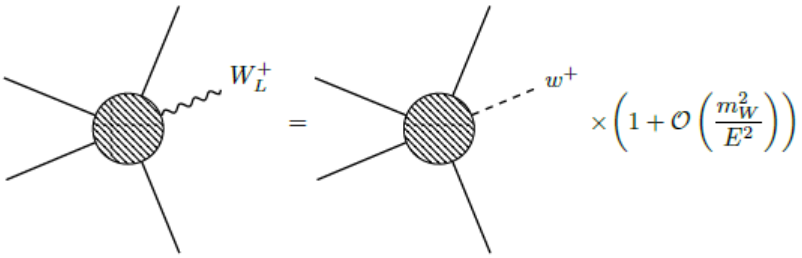

Figure 3.2: The Goldstone Boson Equivalence Theorem.

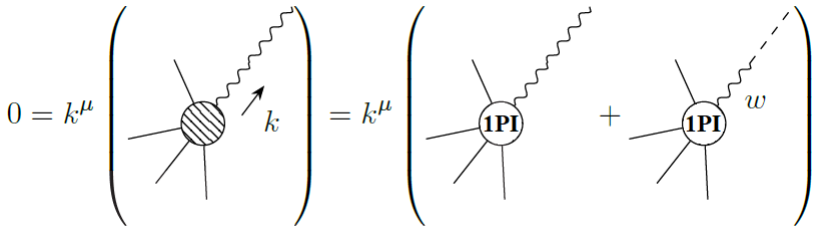

Figure 3.3: Goldstone equivalence Theorem for a single longitudinal $W_L^\pm$ absorption/emission.

larisation vector. Given a vector boson longitudinally polarised along the z-axis with a momentum $k^\mu = (E_k, 0, 0, k)$, a corresponding longitudinal polarisation vector is

$$\begin{aligned}\epsilon_L^\mu(k) = \left(\frac{k}{m_W}, 0, 0, \frac{E_k}{m_W}\right) = \frac{k^\mu}{m_W} + \frac{1}{m_W}\left(-E_k + k, 0, 0, E_k - k\right) \overset{E_k >> m_W}{\sim} \\ \overset{E_k >> m_W}{\sim} \frac{k^\mu}{m_W} + \frac{1}{m_W}\left(-E_k\frac{m_W^2}{2E_k^2}, 0, 0, E_k\frac{m_W^2}{E-k^2}\right) + \frac{E_k}{m_W}\mathcal{O}\left(\frac{m_W^4}{2E_k^4}\right) = \\ = \frac{k^\mu}{m_W} + \mathcal{O}\left(\frac{m_W}{E_k}\right) \qquad (3.2.1)\end{aligned}$$

As one can observe, the polarisation vector becomes increasingly parallel to k^μ as k increases: this is an important feature.
A brief sketch of the proof for the single emission/absorption is given in the following. Working in the generalised Lorentz gauge $\xi = 0$ (in this way Goldstone bosons are not involved in the gauge fixing term), one considers the Ward identity in Fig.3.3, which translates in terms of 1PI graphs as follows:

$$k_\mu\Gamma^\mu(k) - m\Gamma(k) = 0 \overset{E_k >> m}{\Rightarrow} \left[\epsilon_{L\mu}(k) - \mathcal{O}\left(\frac{m_W}{E_k}\right)\right]\Gamma^\mu(k) = \Gamma(k). \qquad (3.2.2)$$

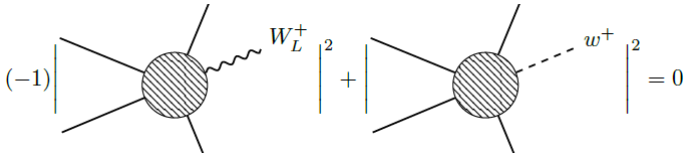

Figure 3.4: Cutkosky cut.

An alternative approach is based on the counting of physical degrees of freedom and the unitarity of S-matrix. In the Feynman-'t Hooft gauge ($\xi = 1$), where the gauge boson propagator numerator is proportional to the metric tensor. Remembering the polarisation sum rules in this gauge, one has

$$-g^{\mu\nu} = \sum_{A=1,2,L} \epsilon_A^m u(k) \epsilon_A^{*\nu}(k) - \frac{k^\mu k^\nu}{m^2}. \tag{3.2.3}$$

Using the Cutkoski rules (see [29]) and the unitarity of S-matrix, it is necessary that when a Cutkoski cut through a diagram puts a vector boson on-shell, this contribution must be cancelled by a Cutkoski cut through a Goldstone boson line (Fig.3.4). In this way, one again has

$$-\left|\frac{k_\mu}{m}\Gamma^\mu(k)\right|^2 + |\Gamma(k)|^2 = 0 \overset{E_k >> m}{\Rightarrow} \left[\epsilon_{L\mu}(k) - \mathcal{O}\left(\frac{m_W}{E_k}\right)\right]\Gamma^\mu(k) = \Gamma(k). \tag{3.2.4}$$

These two different approaches show that the Goldstone boson equivalence theorem holds at least at the tree-level.
In the next paragraph, an application of this theorem (and of unitarity cancellations as well) will be shown.

3.3 An example: longitudinal W boson scattering

Usually the academical examples given as application of the Goldstone Equivalence Theorem are top quark decay $t \to W^+ b$ and $e^- e^+ \to W^- W^+$ annihilation (see [1]). In the first process the theorem is useful to find where the amplitude enhancement comes from, while in the second case the unitarity cancellations are highlighted.
However, in this section one considers the following process: $W_L^- + W_L^+ \to W_L^- + W_L^+$. This choice is due to the kind of cancellations which take place in this process and the fact that, from the perspective of the No-Lose Theorems, the Higgs boson (or something else) must exist in order to guarantee the right behaviour of the amplitude.
The calculation will be structured in two parts: in the first part, one will perform the full calculation, showing how intricate cancellations take place and studying the behaviour

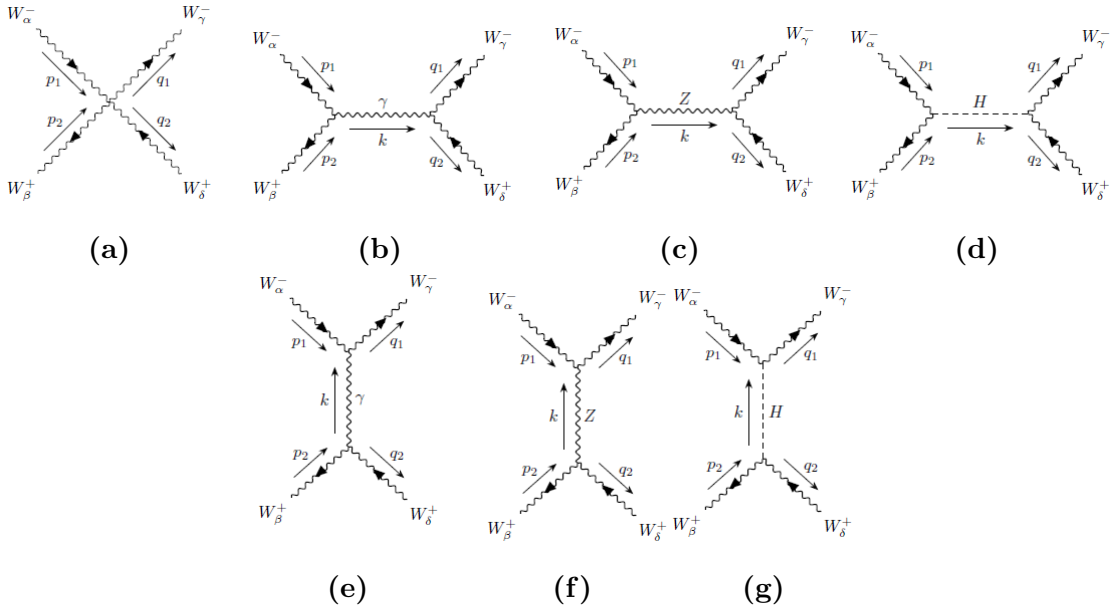

Figure 3.5: Feynman diagrams contributing to the process at three level with the used notation included.

of the amplitude at high energies; in the second part, one will assume the high-energy regime and will use the Goldstone Boson Equivalence theorem to perform the computation, reaching the same result. The set of Feynman rules used is derived in [31].

3.3.1 Full calculation

In this process seven Feynman diagrams (see Fig. 3.5) are involved: the four W self-interaction contact terms, the s and t channels with Z/γ exchange and the s and t channel with the Higgs boson exchange. Before starting the computation, some important points will be anticipated here. Firstly, it will become clear that if one ignores the gauge structure and uses only the gauge self-interaction contact term, one will get a matrix element unacceptably growing like E^4, where E is an energy scale. Secondly, even if one includes the diagrams with the exchange of the γ and Z gauge bosons, the self interaction term proportional to E^4 will be killed. Nevertheless, the amplitude will be still grow like E^2, which is still an unacceptable behaviour concerning the unitarity of the S-matrix. Thirdly and lastly, it will be shown that only the introduction of the Higgs boson exchange diagrams will eliminate this freak behaviour and recover an acceptable constant behaviour with the energy of the scattering amplitude. All the cancellations

that take place are connected with the gauge nature of the theory and with unitarity. During the whole duration of the computation, one will work in the Feynman-'t Hooft gauge $\xi = 1$ and will use as reference frame the center of mass frame of the system. Since the four particles involved in the scattering process have all the same mass, one can parameterise the four momenta and the polarisation vectors as follows:

$$\begin{aligned} p_1^\mu &= \frac{\sqrt{s}}{2}(1,\vec{\beta}), \qquad & \epsilon_L^\mu(p_1) &= \frac{\sqrt{s}}{2m_W}(|\vec{\beta}|,\hat{\beta}) \\ p_2^\mu &= \frac{\sqrt{s}}{2}(1,-\vec{\beta}), \qquad & \epsilon_L^\mu(p_2) &= \frac{\sqrt{s}}{2m_W}(|\vec{\beta}|,-\hat{\beta}) \\ q_1^\mu &= \frac{\sqrt{s}}{2}(1,\vec{\beta}'), \qquad & \epsilon_L^\mu(q1) &= \frac{\sqrt{s}}{2m_W}(|\vec{\beta}'|,\hat{\beta}') \\ q_2^\mu &= \frac{\sqrt{s}}{2}(1,-\vec{\beta}'), \qquad & \epsilon_L^\mu(q2) &= \frac{\sqrt{s}}{2m_W}(|\vec{\beta}'|,-\hat{\beta}'), \end{aligned} \tag{3.3.1}$$

where

$$\vec{\beta} = \left(\sqrt{1-\frac{4m_W^2}{s}}\right)\hat{\beta}, \qquad \vec{\beta}' = \left(\sqrt{1-\frac{4m_W^2}{s}}\right)\hat{\beta}', \tag{3.3.2}$$

$$\vec{\beta}\cdot\vec{\beta}' = \left(1-\frac{4m_W^2}{s}\right)\cos\theta_{CM} \equiv \beta^2\cos\theta_{CM}, \qquad \cos\theta_{CM} = \frac{2t}{s\beta^2}+1, \tag{3.3.3}$$

with s and t the Mandelstam variables which will be used to parametrise the whole amplitude.
From the Feynman rules one can build the following matrix elements:

$$\mathcal{M}_{4W} = g^2\epsilon_L^\alpha(p1)\epsilon^\beta(p2)\epsilon^\gamma(q1)\epsilon^\delta(q2)\left[2g_{\alpha\delta}g_{\beta\gamma} - g_{\alpha\beta}g_{\delta\gamma} - g_{\alpha\gamma}g_{\beta\delta}\right] \tag{3.3.4}$$

$$\mathcal{M}_\gamma^s = \frac{g^2\sin^2\theta_W g^{\mu\nu}}{s}\epsilon_L^\alpha(p1)\epsilon^\beta(p2)\epsilon^\gamma(q1)\epsilon^\delta(q2)\Gamma_{\alpha\beta\mu}\left(p1,p2,-p1-p2\right)\Gamma_{\delta\gamma\nu}\left(-q2,q1,p1+p2\right) \tag{3.3.5}$$

$$\mathcal{M}_Z^s = \frac{g^2\cos^2\theta_W g^{\mu\nu}}{\left(s-\frac{m_W^2}{\cos^2\theta_W}\right)}\epsilon_L^\alpha(p1)\epsilon^\beta(p2)\epsilon^\gamma(q1)\epsilon^\delta(q2)\Gamma_{\alpha\beta\mu}\left(p1,p2,-p1-p2\right)\Gamma_{\delta\gamma\nu}\left(-q2,q1,p1+p2\right) \tag{3.3.6}$$

$$\mathcal{M}_\gamma^t = \frac{g^2\sin^2\theta_W g^{\mu\nu}}{t}\epsilon_L^\alpha(p1)\epsilon^\beta(p2)\epsilon^\gamma(q1)\epsilon^\delta(q2)\Gamma_{\alpha\gamma\mu}\left(p1,-q1,q1-p1\right)\Gamma_{\delta\beta\nu}\left(-q2,p2,q2-p2\right) \tag{3.3.7}$$

$$\mathcal{M}_Z^t = \frac{g^2\cos^2\theta_W g^{\mu\nu}}{\left(t-\frac{m_W^2}{\cos^2\theta_W}\right)}\epsilon_L^\alpha(p1)\epsilon^\beta(p2)\epsilon^\gamma(q1)\epsilon^\delta(q2)\Gamma_{\alpha\gamma\mu}\left(p1,-q1,q1-p1\right)\Gamma_{\delta\beta\nu}\left(-q2,p2,q2-p2\right) \tag{3.3.8}$$

$$\mathcal{M}_H^s = -\frac{g^2m_W^2}{s-m_H^2}g_{\alpha\beta}g_{\gamma\delta}\epsilon_L^\alpha(p1)\epsilon^\beta(p2)\epsilon^\gamma(q1)\epsilon^\delta(q2) \tag{3.3.9}$$

$$\mathcal{M}_H^t = -\frac{g^2m_W^2}{t-m_H^2}g_{\alpha\gamma}g_{\beta\delta}\epsilon_L^\alpha(p1)\epsilon^\beta(p2)\epsilon^\gamma(q1)\epsilon^\delta(q2), \tag{3.3.10}$$

where

$$\Gamma_{\alpha\beta\mu}(p,q,k) = g_{\alpha\beta}\left(p-q\right)_\mu + g_{\beta\mu}\left(q-k\right)_\alpha + g_{\mu\alpha}\left(k-p\right)_\beta. \tag{3.3.11}$$

Before proceeding further with the computation, it is worth observing that, by using dimensional analysis, it is already possible to foresee the energy behaviours of the amplitudes: the contact term and the γ/Z exchange diagrams will be dominated by a E^4 term, while the Higgs exchange diagrams will singularly grow at most as E^2.
Making an explicit use of the four momenta and parameterisation of the polarisation vectors (3.3.1), after some effort with calculations, one can expand the amplitudes at high energies and get:

$$\mathcal{M}_{4W} = \frac{g^2 s}{4m_W^4(s-4m_W^2)}\left[-64m_W^6 + 48m_W^4(s+t) - 4m_W^2 s(3s+7t) + s(s^2+4st+t^2)\right] \overset{HE}{\sim}$$
$$\overset{HE}{\sim} \frac{g^2\left(s^2+4st+t^2\right)}{4m_W^4} - \frac{g^2\left(s^2-st-2t^2\right)}{m_W^2 s} + \frac{4g^2\left(st+3t^2\right)}{s^2} \tag{3.3.12}$$

$$\mathcal{M}_\gamma^s = \frac{g^2\sin^2\theta_W}{4m_W^2 s}\left(2m_W^2+s\right)^2\left(4m_W^2-s-2t\right) \overset{HE}{\sim}$$
$$\overset{HE}{\sim} -\frac{g^2 s(s+2t)\sin^2\theta_W}{4m_W^4} - \frac{2\left(g^2 t\sin^2\theta_W\right)}{m_W^2} + \frac{g^2(3s-2t)\sin^2\theta_W}{s} \tag{3.3.13}$$

$$\mathcal{M}_Z^s = -\frac{\cos^4\theta_W g^2\left(2m_W^2+s\right)^2\left(4m_W^2-s-2t\right)}{4m_W^4\left(m_W^2-\cos^2\theta_W s\right)} \overset{HE}{\sim}$$
$$\overset{HE}{\sim} -\frac{g^2 s(s+2t)\cos^2\theta_W}{4m_W^4} - \frac{g^2\left(s+8t\cos^2\theta_W+2t\right)}{4m_W^2} + \frac{g^2\left(4(3s-2t)\cos^4\theta_W - s - 8t\cos^2\theta_W - 2t\right)}{4s\cos^2\theta_W} \tag{3.3.14}$$

$$\mathcal{M}_\gamma^t = \frac{g^2\sin^2\theta_W}{4m_W^4 t\left(s-4m_W^2\right)^2}\times$$
$$\times\left[256m_W^{10} - 64m_W^8(4s+t) + 16m_W^6 s(5s+14t) - 4m_W^4 s\left(2s^2+21st+20t^2\right) + 8m_W^2 s^2 t(s+3t) - s^2t^2(2s+t)\right] \overset{HE}{\sim}$$
$$\overset{HE}{\sim} -\frac{g^2 t(2s+t)\sin^2\theta_W}{4m_W^4} + \frac{2g^2\left(s^2+st-t^2\right)\sin^2\theta_W}{sm_W^2} - \frac{g^2\left(2s^3+5s^2t-4st^2+12t^3\right)\sin^2\theta_W}{s^2 t} \tag{3.3.15}$$

$$\mathcal{M}_Z^t = -\frac{\cos^4\theta_W g^2}{4m_W^4\left(s-4m_W^2\right)^2\left(m_W^2-\cos^2\theta_W t\right)}\times$$
$$\times\left[256m_W^{10} - 64m_W^8(4s+t) + 16m_W^6 s(5s+14t) - 4m_W^4 s\left(2s^2+21st+20t^2\right) + 8m_W^2 s^2 t(s+3t) - s^2t^2(2s+t)\right] \overset{HE}{\sim}$$
$$\overset{HE}{\sim} -\frac{g^2 t(2s+t)\cos^2\theta_W}{4m_W^4} + \frac{g^2\left[8\left(s^2+st-t^2\right)\cos^2\theta_W - s(2s+t)\right]}{(4s)m_W^2} -$$
$$-\frac{g^2\left[-8s\left(s^2+st-t^2\right)\cos^2\theta_W + s^2(2s+t) + 4\left(2s^3+5s^2t-4st^2+12t^3\right)\right]\cos^4\theta_W}{4s^2 t\cos^2\theta_W} \tag{3.3.16}$$

$$\mathcal{M}_H^s = \frac{g^2\left(s-2m_W^2\right)^2}{4m_W^2\left(m_H^2-s\right)} \overset{HE}{\sim} -\frac{g^2 s}{4m_W^2} + \left(g^2 - \frac{g^2 m_H^2}{4m_W^2}\right) \tag{3.3.17}$$

$$\mathcal{M}_H^t = \frac{g^2\left(-8m_W^4+2m_W^2 s+st\right)^2}{4\left(m_H^2-t\right)\left(m_W s-4m_W^3\right)^2} \overset{HE}{\sim} \frac{1}{4}g^2\left(-\frac{m_H^2}{m_W^2} - \frac{8t}{s} - 4\right) - \frac{g^2 t}{4m_W^2} \tag{3.3.18}$$

As anticipated before, one can see that every amplitude has the expected behaviour as the energy grows. If one considers the amplitudes individually, they seem to violate unitarity.
However, by summing the first five amplitudes, one gets an improvement (passing from E^4 to E^2), even if it is not sufficient to guarantee unitarity:

$$\mathcal{M}_{4W} + \mathcal{M}^s_\gamma + \mathcal{M}^t_\gamma + \mathcal{M}^s_Z \mathcal{M}^t_Z = \frac{g^2(s+t)}{4m_W^2} - \frac{g^2\left(s^2 + st - 4t^2\cos^2\theta_W + t^2\right)}{2\left(st\cos^2\theta_W\right)}. \quad (3.3.19)$$

It is thanks to the existence of the Higgs exchange diagrams that it is possible to recover a well behaved amplitude. Adding the last two amplitudes to what has been found above, one gets at the end:

$$\mathcal{M}_{(W_L^- W_L^+ \to W_L^- W_L^+)} = \frac{g^2}{2}\left(-\frac{m_H^2}{m_W^2} - \frac{s^2 + st + t^2}{st\cos^2\theta_W}\right), \quad (3.3.20)$$

which is a constant with the energy and restores unitarity, as expected.

3.3.2 Applying the Goldstone Equivalence Theorem

In the previous paragraph one has seen how important the gauge structure of the theory is in order to prevent unitarity violating behaviours and how the existence of the Higgs Boson is fundamental in this process, guaranteeing that cancellations take place.
However, in order to have such cancellations, one had to struggle with a rather long computation. Since one is interested in the high-energy behaviour, it would be pleasant to find a shortcut which allows to skip the study of the process at low energies.
Fortunately, this shortcut exists when one has to deal with longitudinally polarised gauge vector bosons and it is encoded in the GET, introduced in the previous section.
Here, one will study the same process of the previous paragraph, but applying the theorem (see Fig.3.6) and show that one gets the same result. In order to do that, it is sufficient to replace the longitudinal $W^\pm$ bosons with their corresponding Goldstone bosons $w^\pm$ and use the corresponding Feynman rules (see again [31]). The involved diagrams in this version of the process are the very same seven diagrams of the full case, where the substitution mentioned above has been made. One works again in the center of mass frame in the Feynman-t' Hooft gauge $\xi = 1$. Since this choice ($m_{w^\pm} = \sqrt{\xi} m_W = m_W$) permits to adopt the same parameterisation for the four momenta used in the full calculation (even though one could directly work in the massless limit, since one is studying the process in the high-energy regime).
From the Feynman's rules, it is straightforward to find the matrix elements

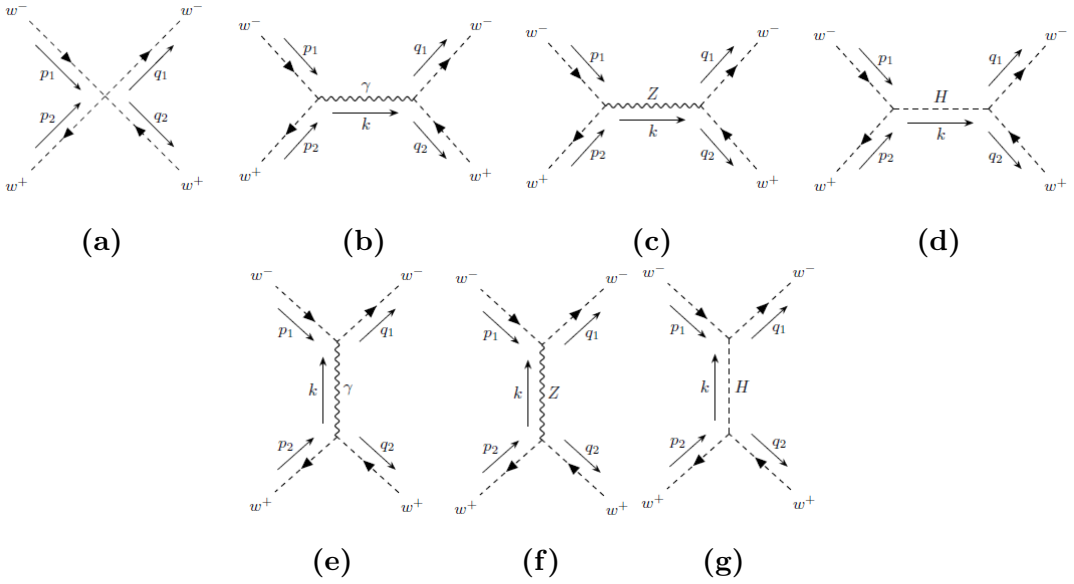

Figure 3.6: Feynman diagrams of the process at tree level using GET.

$$\mathcal{M}_{4W} = -4\lambda \tag{3.3.21}$$

$$\mathcal{M}^s_\gamma = -\frac{e^2(p_1^\mu - p_2^\mu)(q_{1\mu} - q_{2\mu})}{s} \tag{3.3.22}$$

$$\mathcal{M}^s_Z = -\frac{g^2\cos^2(2\theta_W)}{4\cos^2\theta_W(s - m_Z^2)}(p_1^\mu - p_2^\mu)(q_{1\mu} - q_{2\mu}) \tag{3.3.23}$$

$$\mathcal{M}^t_\gamma = -\frac{e^2}{t}(p_1^\mu + q_1^\mu)(p_{2\mu} + q_{2\mu}) \tag{3.3.24}$$

$$\mathcal{M}^t_Z = -\frac{g^2\cos^2(2\theta_W)}{4\cos^2\theta_W(t - m_Z^2)}(p_1^\mu + q_1^\mu)(p_{2\mu} + q_{2\mu}) \tag{3.3.25}$$

$$\mathcal{M}^s_H = -\frac{4\lambda^2 v^2}{s - m_H^2} \tag{3.3.26}$$

$$\mathcal{M}^t_H = -\frac{4\lambda^2 v^2}{t - m_H^2}, \tag{3.3.27}$$

Using the following kinematic relationships

$$
\begin{aligned}
p_1^\mu p_{2\mu} &= \frac{s}{2} - m_W^2 = q_1^\mu q_{2\mu} \\
p_1^\mu q_{1\mu} &= -\frac{t}{2} + m_W^2 = p_2^\mu q_{2\mu} \\
p_1^\mu q_{2\mu} &= \frac{s+t-2m_W^2}{s} = p_2^\mu q_{1\mu} \\
(p_1^\mu - p_2^\mu)\,(q_{1\mu} - q_{2\mu}) &= -\left(2t + s - 4m_W^2\right) \qquad (3.3.28) \\
(p_1^\mu + q_1^\mu)\,(p_{2\mu} + q_{2\mu}) &= 2s + t - 4m_W^2, \qquad (3.3.29)
\end{aligned}
$$

and working a little bit on the amplitudes, one obtains ($\lambda = \frac{m_H^2}{2v^2}$,$e = g\sin\theta_W$):

$$
\begin{aligned}
\mathcal{M}_{4W} + \mathcal{M}_H^s + \mathcal{M}_H^t &= -\frac{m_H^2}{v^2}\left[2 + \frac{m_H^2}{s-m_H^2} + \frac{m_H^2}{t-m_H^2}\right] \qquad (3.3.30) \\
\mathcal{M}_\gamma^s &= -\frac{g^2\sin^2\theta_W}{s}(2t + s - 4m_W^2) \qquad (3.3.31) \\
\mathcal{M}_Z^s &= -\frac{g^2\cos^2(2\theta_W)}{4\cos^2\theta_W\,(s-m_Z^2)}(2t + s - 4m_W^2) \qquad (3.3.32) \\
\mathcal{M}_\gamma^t &= -\frac{g^2\sin^2\theta_W}{t}\left(2s + t - 4m_W^2\right) \qquad (3.3.33) \\
\mathcal{M}_Z^t &= -\frac{g^2\cos^2(2\theta_W)}{4\cos^2\theta_W}\frac{(2s + t - 4m_W^2)}{s-m_Z^2} \qquad (3.3.34)
\end{aligned}
$$

Summing them up and taking the high-energy limit, it is easy to see that one gets ($v = \frac{2m_W}{g}$):

$$
\mathcal{M}_{(w^-w^+\to w^-w^+)} \approx -\frac{g^2}{2}\left(\frac{m_H^2}{m_W^2} + \frac{s^2+st+t^2}{st\cos^2\theta_W}\right), \qquad (3.3.35)
$$

which is exactly the same result obtained in the full case with a lot of hard work. However, it noticeable that in applying the Goldstone equivalence theorem, one loses track of the cancellations that happened at low energies.

In this chapter we have seen that non-trivial cancellations between different contributions happen in SM amplitudes in order to keep the unitary of the theory at tree level. So the question is now: what happens passing to SMEFT? What is the effect of new operators and contact interactions? This will be the topic of the next chapter.

Chapter 4

High-energy behaviour of scattering amplitudes in SMEFT

In this chapter the original part of the thesis is presented.
The main question of this project is whether it is possible to get a better sensitivity to new physics from 2 to N scattering amplitudes with respect to the 2 to 2 processes involving the heaviest states of the SM (the weak gauge bosons and the top quark.)
The starting point is to extend what was done in the 2 to 2 case in (see [32]) to the 2 to 3 scattering amplitudes. The main difference with the work previously done is that one here focuses on the Vector Boson Scattering (VBS) processes involving the gauge bosons $W^{\pm}$ and Z, the Higgs boson H and the (anti)top quark. The rationale behind this exploration is that 2 to 2 amplitudes display a very limited number topologies, up to to four point interactions, which are not, per se, unitarity violating. On the other hand, five-point interactions are intrinsically higher dimensional and can appear in 2 to 3 scattering amplitudes at the tree level.
The study is based on the analysis of scattering amplitudes in the SMEFT framework which is a consistent framework where to study effects of Beyond Standard Model (BSM) physics on the interactions among SM particles.
The main reason underlying the choice to work with the heavy bosons and fermions of the SM is rather simple: they are the only particle of the SM which reside at the electroweak scale and therefore might shed light on the origin of this scale. In addition, interactions among the vector bosons, the Higgs and the top quark are the least known ones, in fact the least constrained by precision measurements at LEP, and therefore allowing for the largest deviations.
The choice for VBS processes is motivated by the fact that they can be embedded in Vector Boson Fusion (VBF) processes that will be the most studied ones in a future lepton collider, like CLIC ([46, 47]) or a muon collider ([48]), which can also be thought as WW or WZ or ZZ colliders. Especially VBF involving Higgs particles in the final state will be very useful to better measure its properties.

As it will be shown in the following, 2 to 3 processes can reveal many aspects of the intricate pattern of cancellations leading to unitarity cancellations (or violations thereof). They are much richer than the 2 to 2 case: the increase in the number of degrees of freedom increases the complexity of the process, with more topologies contributing at tree level in the SM. Needless to say, the complementary consequence of the increase in richness is that 2 to 3 amplitudes are more much challenging from a computational point of view.

4.1 Unitarity and energy growth in the SMEFT

In the SMEFT, unitarity violation behaviours are expected. However, this breakdown actually can have two distinct origins, both connected to the introduction of new operators. The most glaring one is the appearance of new contact terms, which generate anomalous high-energy behaviour in the Feynman diagrams contributing to a given process. Another reason lies in the shift of some couplings or fields of the SM due to new operators, even in absence of contact terms. The induced shifts may spoil the cancellations among the SM amplitudes and result in a growth with the energy.
According to the argument used in 3.1.1, in a general 2 to N process an amplitude can violate unitarity even if it does not grow with the energy. Take the 2 to 3 and the 2 to 4 processes as example: by dimensional analysis $[\mathcal{M}_{2\to3}] = E^{-1}$ and $[\mathcal{M}_{2\to4}] = E^{-2}$ and therefore the two can "grow" at most as E^{-1} and E^{-2}. Therefore a E^0 behaviour in the 2 to 3 case and a E^{-1} behaviour in the 2 to 4 case would be a sign of unitarity violation, even if the two amplitudes do not increase with the energy, per se.
Another important point to clarify for what follows is the maximal energy growth that an amplitude can have by introducing dimension D operators. A naive approach based again on dimensional analysis gives a simple answer to this question. As shown in 3.1.1, a 2 to N amplitude must have energy dimension $[\mathcal{M}_{2\to N}] = E^{2-N}$. The insertion of a dimension D operator will imply the appearance of the energy scale of the EFT Λ^{4-D} that must be compensated by an opposite energy dependence at the numerator, leading to

$$\mathcal{M}_{(2\to N)} \propto \frac{E^{2-N+D-4}}{\Lambda^{D-4}} = \frac{E^{D-N-2}}{\Lambda^{D-4}}. \tag{4.1.1}$$

However, one has also to consider the possibility that vector bosons longitudinally polarised and vev insertions appear in the process. As it was seen in the previous chapter, a longitudinal polarised vector boson contributes to the amplitude with a term $\frac{E}{m_V}$, where m_V is the mass of the vector boson. Moreover, one must also consider vev insertions which reduce energy growth, since they can take place, especially in SMEFT, when contact interactions appear after SSB. Keeping this in mind, the final naive formula for the maximal energy growth of an amplitude becomes (m is the number of external

longitudinally polarised vector bosons, while n is the number of vev insertions):

$$\mathcal{M}_{(2\to N)} \propto \frac{v^n}{\Lambda^{D-4}} \frac{E^{D-N-2+m-n}}{m_V^m}. \tag{4.1.2}$$

From this formula it seems that the maximal energy growth can be reached by contact terms, that means by minimising the number of vev insertions. However, as seen in the fully longitudinal WW scattering, if more amplitudes contribute to the same process, it is not guaranteed that the highest behaviour of the contact term will be the dominant one due to possible cancellations.
Considering instead a process amplitude in SMEFT, eventually unitarity violating behaviours will always come from the dimension six terms, since they can "grow" as (D=6 in Eq. (4.1.1)) E^{4-N}, i.e. two more powers than what allowed by unitarity. However, when a process is studied, one is interested in the computation of its cross-section and therefore what has to be taken in account is the square of the scattering amplitude (suppose, for simplicity, that only one dimension six operator with Wilson coefficient c_i contributes):

$$|\mathcal{M}_{2\to N}|^2 = |\mathcal{M}_{SM} + \frac{c_i}{\Lambda^2}\mathcal{M}_{D=6}|^2 = |\mathcal{M}_{SM}|^2 + \frac{c_i}{\Lambda^2} 2\mathrm{Re}\left[\mathcal{M}_{SM}\mathcal{M}_{D=6}^*\right] + \frac{c_i^2}{\Lambda^4}|\mathcal{M}_{D=6}|^2. \tag{4.1.3}$$

As can be observed, the squared dimension six term is higher order in the Λ expansion of the EFT. It arises at the same order as possible interference contributions of dimension 8 operators and one could be tempted to ignore it and keep the dimension 6 interference term only. However, the interference term is not guaranteed to be unitarity violating in general, even if the pure dimension dimension six contribution to the amplitude is. This term may be suppressed due to symmetries or selection rules [43] or even completely absent. Moreover, it is not positive definite, meaning that cancellations may happen such that its contribution to the process is less important of the squared dimension-six one, even if the latter belongs to the next order in the Λ expansion.
Since this behaviour changes from process to process, in this work the quadratic dimension six term is kept in the calculations, knowing that, once the constraints on the operators sufficiently improved, they will naturally become subdominant.

4.2 Choice of operators

In order to study the processes in Table 4.1 and parameterise the dimension-6 SMEFT effects, the Warsaw basis truncated at dimension six is employed.
One here is interested in the EW sector and top quark interactions and, in order to single out the last ones, a flavour symmetry $U(3)_\ell \times U(3)_e \times U(3)_d \times U(2)_q \times U(2)_u$ is imposed and CP conservation assumed. These choices limit the number of operators entering in

Bosonic	Top quark
$W^+W^- \to HHH$	$W^+W^- \to t\bar{t}H$
$W^+W^- \to HHZ$	$W^+W^- \to t\bar{t}Z$
$W^+W^- \to W^+W^-H$	$ZZ \to t\bar{t}H$
$W^+W^- \to W^+W^-Z$	$ZZ \to t\bar{t}Z$
$W^+W- \to ZZH$	
$W^+W^- \to ZZZ$	
$ZZ \to HHH$	

Table 4.1: The set of the studied processes. They are grouped in two classes: the purely bosonic processes and the processes involving the top quark.

$\mathcal{O}_\phi = \left(\phi^\dagger\phi\right)^3$	$\mathcal{O}^{(1)}_{\phi Q} = i\left(\phi^\dagger \overleftrightarrow{\mathcal{D}_\mu}\, \phi\right)\left(\bar{Q}\gamma^\mu Q\right)$
$\mathcal{O}_{\phi d} = \left(\phi^\dagger\phi\right)\Box\left(\phi^\dagger\phi\right)$	$\mathcal{O}^{(3)}_{\phi Q} = i\left(\phi^\dagger \overleftrightarrow{\mathcal{D}_\mu}\, \tau_I\phi\right)\left(\bar{Q}\gamma^\mu\tau^I Q\right)$
$\mathcal{O}_{\phi\mathcal{D}} = \left(\phi^\dagger\mathcal{D}_\mu\phi\right)^\dagger\left(\phi^\dagger\mathcal{D}^\mu\phi\right)$	$\mathcal{O}_{\phi t} = i\left(\phi^\dagger \overleftrightarrow{\mathcal{D}_\mu}\, \phi\right)\left(\bar{t}\gamma^\mu t\right)$
$\mathcal{O}_{\phi W} = \left(\phi^\dagger\phi - \frac{v^2}{2}\right) W_I^{\mu\nu}W^I_{\mu\nu}$	$\mathcal{O}_{t\phi} = \left(\phi^\dagger\phi - \frac{v^2}{2}\right)\bar{Q}t\phi + h.c.$
$\mathcal{O}_{\phi WB} = \left(\phi^\dagger\tau_I\phi\right)B^{\mu\nu}W^I_{\mu\nu}$	$\mathcal{O}_{tW} = i\left(\bar{Q}\sigma^{\mu\nu}\tau_I t\right)\tilde{\phi}W^I_{\mu\nu} + h.c.$
$\mathcal{O}_{\phi B} = \left(\phi^\dagger\phi - \frac{v^2}{2}\right)B^{\mu\nu}B_{\mu\nu}$	$\mathcal{O}_{tB} = i\left(\bar{Q}\sigma^{\mu\nu}t\right)\tilde{\phi}B_{\mu\nu} + h.c.$
$\mathcal{O}_W = \epsilon_{IJK}W^I_{\mu\nu}W^{J\nu\rho}W^{K\mu}_{\rho}$	

Table 4.2: SMEFT operators describing new interactions involving the EW and top quark sectors, consistent with a $U(3)^3 \times U(2)^2$ flavour symmetry. Q and t denote the third generation components of q and u.

the processes to those in Table 4.2, while in Table 4.3 the current constraints on these operators are reported.
From Table 4.3, it is possible to observe a clear difference in the magnitude of the constraints on the Wilson's coefficients in the Warsaw basis between the operators where the top quark appears and those where it is absent. This means that the VBS processes with the top quark appearing in the final state will provide more information in order to better constrain the top operators.
Some of the operators induce non-canonical kinetic terms for the gauge vector bosons and the Higgs boson after SSB. As shown in 2.3.2,these effects can be absorbed by redefining properly some fields and appear in physical quantities by making use of the m_W, G_F, m_Z input scheme. The Universal FeynRules output (UFO) which has been employed is available at [33].

Operators	Limit on c_i TeV^{-2}		Operators	Limit on c_i TeV^{-2}	
	Individual	Marginalised		Individual	Marginalised
$\mathcal{O}_{\phi D}$	[-0.021,0.0055] [34]	[-0.45,0.50] [34]	$\mathcal{O}_{t\phi}$	[-5.3,1.6] [35]	[-60,10] [35]
$\mathcal{O}_{\phi d}$	[-0.78,1.44] [34]	[-1.24,16.2] [34]	$\mathcal{O}_{tB}$	[-7.09,4.68] [36]	–
$\mathcal{O}_{\phi B}$	[-0.0033,0.0031] [34]	[-0.13,0.21] [34]	$\mathcal{O}_{tW}$	[-0.4,0.2] [35]	[-1.8,0.9] [35]
$\mathcal{O}_{\phi W}$	[-0.0093,0.011] [34]	[-0.50,0.40] [34]	$\mathcal{O}_{\phi Q}^{(1)}$	[-3.10,3.10] [36]	–
$\mathcal{O}_{\phi WB}$	[-0.0051,0.0020] [34]	[-0.17,0.33] [34]	$\mathcal{O}_{\phi Q}^{(3)}$	[-0.9,0.6] [35]	[-5.5,5.8] [35]
$\mathcal{O}_W$	[-0.18,0.18] [37]	–	$\mathcal{O}_{\phi t}$	[-6.4,7.3] [35]	[-13,18] [35]
$\mathcal{O}_\phi$	–	–			

Table 4.3: Operators studied and constraints over their Wilson's coefficients at 95% confidence level. The individual limits come from studying a single operator at a time, while the marginalised ones come from global fits, allowing many coefficients to vary simultaneously.

The set of operators modifies interactions between the top quark and the massive gauge vector bosons. For what concerns the bosonic side, one has shifts in triple and quartic gauge coupling and the interactions between Higgs and gauge bosons as well as the appearance of new Lorentz structures. An interesting feature of SMEFT is that single operators can contain more than than one interaction vertex.
In the 2 to 3 processes study, it emerges that different operators contribute to multiple interaction vertices relative to a specific scattering amplitude. This can also happen by means of 5-point contact interactions, which are often the origin of maximal energy growth (cfr. Eq. (4.1.2)).
Thanks to these properties, one is able to connect, as example, modifications of vertices in the SM with higher point interactions that would contribute in new processes, in some cases even with a new energy growth that one can look for at colliders.

4.3 Helicity amplitudes and selection rules

For each process considered in this work, the first step is the study of the helicity amplitudes. As it is well known, helicity amplitudes for the same process do not interfere each other and allow to use an explicit parametrisation of polarisation states, which is sometimes helpful in order to simplify calculations. In addition, it is possible to understand which helicity configuration contributes most to the high energy behaviour of an amplitude and therefore where eventual unitary violating behaviours come from.
The study of the helicity amplitudes has been performed both numerically, using MadGraph5_aMC@NLO ([38], [39]) and the SMEFT UFO model mentioned above, and analytically using the FeynArts ([40]) SMEFT model and FeynCalc ([41]), together with some Mathematica libraries developed for the 2 to 2 case generalised to the 2 to 3 one.

The results obtained with the two different procedures have been found to agree.
Concretely, the helicity amplitudes in SM were studied first. Next, the SMEFT effects the same process were determined by turning on one operator at time. In this way, it was possible to isolate the contribution of each operator to every process and understand in which helicity configurations unitarity violating behaviour was induced. The summary of these operations has been collected in a "Helicity Table" (see Appendix B) for each process. These also give an idea of the behaviour of the interference term between SM and SMEFT operator, just by multiplying the two energy behaviours. This allowed in some cases to determine that interference term does not violate unitarity even though the single operator term does. However, one will see that the situation is not so clean when one embeds core processes in a collider process (summing the squared helicity amplitudes can cause cancellations due to the possible non positive sign of the interference terms, for example).
The analytical computation of 2 to 3 process has turned out to be much more complex than the 2 to 2 case, especially in finding explicitly a general parameterisation of the amplitudes as function of kinematic invariants. Actually, one can easily parameterise all the possible four momenta Lorentz products combinations as a function of five kinematic invariants (five is the number of degree of freedom necessary to describe the three particle final state kinematics, see [42]). This would allow the study of a 2 to 3 process involving only scalar particles, since in this case the scattering amplitude can be expressed as a function of products of the four momenta only. However, if the external particles have spin, this implies the appearance of spin and polarisation states from the external legs in the amplitudes. This would not be a problem if one was studying matrix elements, where one can sum (and average) over these states, but in the helicity amplitude case one needs explicit expressions for them in terms of the four momenta components. This necessitates a parameterisation of the four momenta components as a function of the five kinematics invariants and it is highly non-trivial in the general case. However, since the target of this study was the high-energy behaviour of the amplitudes, it was sufficient to restrict oneself to a simpler kinematic configuration, rather than focusing on obtaining a general solution to the 3 body-phase space kinematics.
The chosen configuration was the so called "Mercedez" where the three particles in the final state share the same modulus of linear momentum and (therefore) are disposed such that the relative angles between them are $\frac{2}{3}\pi$. More information about this can be found in the first section of the Appendix B.
Although this enabled a verification of the consistency between the numerical (where one has to fix the phase space point) and analytical computations, it is possible that some energy behaviours are spoilt by this explicit phase space point choice. This is an important point for testing the selection rules found for the SM helicity amplitudes presented hereafter.

Selection rules

While studying the helicity amplitudes, some recurrent patterns were noticed and the possibility of finding some rule to obtain the high-energy dependence of a given amplitude without doing any kind of computation was considered, at least for the SM.
It is useful to start by looking at the 2 to 2 helicity tables of the processes studied in [32] involving two fermions and two vector bosons and also some processes involving only gauge bosons. The helicity amplitudes can be expanded at high energies as follows:

$$\mathcal{M}_{(2\to 2,SM)} = \sum_{n=0}^{n=\infty} a_n E^{-n}, \tag{4.3.1}$$

where E is an energy variable of the process (e.g. the center of mass energy).
The first thing that one notices is the fact that there is a jump of two units in the power of energy (given a term $a_n E^{-n}$ the next non zero term of the series is $a_{n+2}E^{-(n+2)}$) between the non-zero terms of the series. This aspect allows one to classify the amplitudes into *even amplitudes* and *odd amplitudes* according to the fact they have only n-even or n-odd terms in the high-energy series expansion. This makes one wonder whether some kind of "parity" rule could be responsible for this.
Another occurrence which has been noticed is that violation of helicity conservation plays a major role in determining the dominant energy behaviour (the highest power in the energy) of a helicity amplitude. Let one indicate the helicity of a state with h and the difference between the initial and final state helicity as $\Delta h \equiv h_i - h_f$. What has been found is that the dominant behaviour at high energies for a helicity amplitude which violates helicity conservation by $|\Delta h|$ is given by $E^{-|\Delta h|}$. One can easily see that Δh is always integer for a SM process.
However, this is not all of it: it appears to be possible to also attribute a mass dependence at high energy to the helicity amplitudes. Every longitudinal vector boson V gives an overall factor m_V^{-1} to the amplitude: nevertheless, this factor may not appear in the final expression due to simplifications with the numerator (as happens in the $W^+W^- \to W^+W^-$ case in Table 4.4; for the details, one can consider the fully longitudinal amplitude in 3.3). An overall mass factor m_ψ can also come from a fermion ψ present both in the initial and in the final state, if it undergoes a helicity flip. In general, it is difficult to find other overall mass factors and one should study the Feynman diagrams for every process in order to foresee what could happen.
Moreover, even the rules about the energy behaviour do not always work: they give only the minimal suppression law with the energy of an helicity amplitude. Therefore, in some cases it is possible to have amplitudes more suppressed than what has been predicted: this is due to physical reasons which do not allow some diagrams normally involved in the process.
As an application of these rules, consider the following two scattering processes: $W^+W^- \to W^+W^-$ (Tab. 4.4) and $tZ \to tZ$ (Tab. 4.5).

$W^{out}_+, W^{out}_- = ++$			$W^{out}_+, W^{out}_- = 00$			$W^{out}_+, W^{out}_- = +,-$			$W^{out}_+, W^{out}_- = 0+$		
W^{in}_+	W^{in}_-	Scaling	W^{in}_+	W^{in}_-	Scaling	W^{in}_+	W^{in}_-	Scaling	W^{in}_+	W^{in}_-	Scaling
$+$	$+$	ε^0	$+$	$+$	ε^2	$+$	$+$	ε^2	$+$	$+$	ε
0	$+$	ε	0	$+$	ε	0	$+$	ε	0	$+$	ε^0
$-$	$+$	ε^2	$-$	$+$	ε^0	$-$	$+$	ε^0	$-$	$+$	ε
$+$	0	ε	$+$	0	ε	$+$	0	ε	$+$	0	ε^2
0	0	ε^2	0	0	ε^0	0	0	ε^0	0	0	ε
$-$	0	ε^3	$-$	0	ε	$-$	0	ε	$-$	0	ε^2
$+$	$-$	ε^2	$+$	$-$	ε^0	$+$	$-$	ε^0	$+$	$-$	ε
0	$-$	ε^3	0	$-$	ε	0	$-$	ε	0	$-$	ε^2
$-$	$-$	ε^4	$-$	$-$	ε^2	$-$	$-$	ε^2	$-$	$-$	ε^3

Table 4.4: The high-energy behaviour of the helicity amplitudes for $W^+W^- \to W^+W^-$ scattering, $\varepsilon \equiv m_W/E$. The missing combinations can be obtained by exploiting the C and P symmetry of the W lagrangian. The table was found in [45] and agrees with our calculations.

t_{in}, Z_{in}, t_{out}, Z_{out}	$----$	$---0$	$---+$	$--+-$	$--+0$	$--++$
scaling	E^0	$(m_Z E)^{-1}$	E^{-2}	$m_t E^{-1}$	$\frac{m_t}{m_Z}E^{-2}$	$m_t E^{-3}$
t_{in}, Z_{in}, t_{out}, Z_{out}	$-0--$	$-0-0$	$-0-+$	$-0+-$	$-0+0$	$-0++$
scaling	$(m_Z E)^{-1}$	$m_Z^{-2}E^0$	$(m_Z E)^{-1}$	$\frac{m_t}{m_Z}E^0$	$\frac{m_t}{m_Z^2}E^{-1}$	$\frac{m_t}{m_Z}E^{-2}$
t_{in}, Z_{in}, t_{out}, Z_{out}	$-+--$	$-+-0$	$-+-+$	$-++-$	$-++0$	$-+++$
scaling	E^{-2}	$(m_Z E)^{-1}$	E^0	$m_t E^{-1}$	$\frac{m_t}{m_Z}$	$m_t E^{-1}$

Table 4.5: The table shows the high-energy behaviour of the helicity amplitudes for the $tZ \to tZ$ scattering. The remaining 18 amplitude can be deduced by flipping all the signs in every amplitude.

As one can see, the 81 helicity amplitudes of $W^+W^- \to W^+W^-$ scattering respect the energy behaviour rules, with the only exception of the $(0\ \pm\ \pm\ 0)$ and $(\pm\ 0\ 0\ \pm)$ amplitudes, which are more suppressed than what is foreseen. In these helicity amplitudes the s-channel where the Higgs boson is exchanged does not contribute.
In the $tZ \to tZ$ case instead, the behaviours agree fully with the rules. If one had instead considered the $tW \to tW$, a lot of helicity amplitudes would have been more suppressed than what the rules foresee because of chiral nature of the W boson. For example, the amplitude $++++$, which is expected to have a high-energy behaviour like E^0, behaves like E^{-2}. Since the W boson interacts with left-handed fermions, the Feynman diagram where the right-handed bottom quark is exchanged is zero.
Apparently, these rules work well for the 2 to 2 case when one has to estimate the minimal energy suppression of a given helicity amplitude. Why do they hold? The jumps of two power of the energy in the series expansion suggest that there may be some parity-like symmetry of the lagrangian. It happens that in the purely gauge vector scattering, such a symmetry actually exists (a deeper discussion on selection rules in vector boson scattering can be found in [44], both in the massive and the massless case).
The SM lagrangian for the Goldstone and gauge fields (with or without the Higgs) in

the ξ gauge turns out to be invariant under the following transformation:

$$W_\mu \to W_\mu, \qquad w \to -w, \qquad m \to -m,$$

where W_μ stands for a gauge boson and w for a Goldstone boson. This means that the sign of the mass is not a physical observable. However, since the probability $\mathcal{M}^*\mathcal{M}$ is an observable, this means that an amplitudes $\mathcal{M}$ must be even or odd under $m \to -m$. The key point is to observe that the longitudinal polarisation vector for a massive vector boson changes sign under this operation. This allows one to define unambiguously *even* and *odd helicity amplitudes* under this transformation according to the number of longitudinally polarised vectors that are involved in vector boson scattering $VV \to VV$. (Notice, however, that here *even* and *odd* refers to how the amplitude transforms under the lagrangian symmetry and not at the even or odd power of the energy of the high-energy behaviour. In the purely bosonic case, the parity of the amplitude sign is the same as the parity of the energy power.)
In summary, the rules which have been found for the 2 to 2 scattering of massive particles in the SM are:

(i) : If helicity conservation between the initial and final state is violated by $\Delta h \in \mathbb{Z}$ units, then the corresponding helicity amplitude will be suppressed at high-energies at least as $E^{-|\Delta h|}$;

(ii) : If vector bosons are involved in the scattering process, for every longitudinally polarised gauge vector boson V, an overall factor m_V^{-1} appears in the helicity amplitude (modulo simplifications with the numerator).

(iii) : If a fermion ψ is present both in the initial and final state and if the fermion undergoes a helicity flip, then an overall factor m_ψ appears in the helicity amplitude.

Processes of the type $FF \to FF$ have not been considered, but one can guess that similar rules hold even for this kind of process.
Based on observations of the many 2 to 3 amplitudes computed in this work, a straightforward generalisation of these rules is proposed. 2 to N processes follow the above rules with the additional requirement that they obey tree-unitarity, which is that at high-energies $\mathcal{M}_{2\to N} \sim E^{2-N}$ at most. This truncates the series expansion of the amplitude at high energies and implies that the dominant amplitudes will not be the ones where helicity is conserved in general, as it is the case for 2 to 3 scattering processes. As example, consider the $W^+W^- \to W^+W^-H$ processes and its helicity table Tab.B.4 in Appendix B. The fully longitudinal amplitude (or any amplitude where helicity is conserved) is expected to behave as a constant E^0 at high-energy, if only the above rules are used without employing tree-unitarity. When the latter is included, it is clear that the constant behaviour at high-energies is not allowed and those amplitude must behave like E^{-2}. In this way, the dominant helicity amplitudes are those which violate helicity

conservation by one unit and behave as E^{-1} at high-energies.
For what concerns the SMEFT helicity amplitudes in the 2 to 2 case, similar rules to the 2 to 2 case were searched for, but the only recurrence which holds is the even and odd nature of the amplitudes. Given an arbitrary operator appearing in a process, it seems there is no a priori way to know the behaviour of its helicity amplitudes at high energy, since new diagrams arise and they should be studied in detail for every operator and every process. What is possible to affirm in this case, is only that an even helicity amplitude in the dimension-6 SMEFT will grow at most as E^2, while an odd one like E^1 in a 2 to 2 scattering process. (Actually, contact terms can grow with even higher power of the energy, but they are usually cancelled when the diagrams contributing to a process are summed. Some examples in 2 to 2 scattering processes are reported in [32].)Examples of these kind of behaviour in 2 to 2 amplitudes are discussed in [43].

4.4 Embedding processes in a lepton collider

It is well known that VBS processes are not directly accessible (i.e. it is not possible to have the gauge vector bosons in the initial state and the particle produced like the Higgs and the top quark in the final state in reality) and that they can be studied only when embedded in a VBF collider process. Moreover, if working at helicity amplitudes level can be useful in order to understand where new physics might be found, what one measures are actually cross-sections. In the computation one has to sum and average over the helicity amplitudes: by doing so one loses information about them and at interference level between the SM amplitudes and the SMEFT ones it may happen that unitarity violating behaviour disappears. When one analyses the situation in a collider process, one will be more interested in looking for deviation from the SM at the cross-section level. In this perspective, considering that here one is doing a naive sensitivity study, one will switch on an operator at time and will evaluate its impact on the process by considering ratios between the cross-section from the SMEFT term and the SM one at interference and quadratic level.
However, when embedding VBS processes into a collider one, one has to deal with diagrams/processes which contribute and may hide the original one. The most natural choice in order to minimise the number of background processes is to study VBF in the context of a future lepton collider.

Future Lepton colliders

As mentioned several times in previous chapters, one of the main goals of high energy physics is to study the interactions in the electroweak sector between the Higgs and the gauge boson as well as the Higgs self-coupling. Another very important field of research is top-quark physics: the top quark is the heaviest particle of the SM and its strong cou-

pling with the Higgs can give important information about the latter. The best processes to use to analyse this kind of interactions, especially in the electroweak sector, are the VBFs. However, in the meantime, one would also like to look for new physics, exploring higher energy regions or by means of precision measurements. A lepton collider would be the best way to do all this, hitting two birds with one stone.
The LHC will continue working for many years, but a hadron collider is not necessarily the most suited one to study the electroweak sector at high energies. Two major drawbacks play a role against it: the first one is the strong QCD background given by the proton anti-proton collisions; the second one is the low fraction of the center of mass energy which is available for electroweak processes due to the proton's partonic structure. A lepton collider surpasses these technical problems: since, to our knowledge, a lepton has no internal structure, all of the center of mass energy will be at our disposition; moreover, a lepton does not interact strongly and the QCD background will be extremely reduced. However, a high energy lepton collider constitutes an amazing technological challenge for the future and one will have to wait several decades before one is properly realised. Another issue is whether to build circular or a linear collider. Two projects that seem to have caught more the attention of the scientific community are the Compact Linear Collider (CLIC) ([46, 47]) and the muon collider ([48, 49]) and their main aspects will be discussed below briefly.

The Compact Linear Collider is a TeV-scale high-luminosity e^-e^+ collider under development at CERN. It is foreseen to operate in three stages, with center of mass energies of 380 GeV, 1.5 TeV and 3 TeV and it will have a length ranging from 11 km to 50 km. The building of the first CLIC stage could start by 2026, while the first beams should be available by 2035, starting the CLIC physics programme spanning 25-30 years.
The first stage at 380 GeV will give access to model independent measurements of the Higgs couplings and width, e.g. through Higgstrahlung and WW-fusion. Moreover also precision top-quark physics will be available as it will be possible to study top-quark pair production. The second stage at 1.5 TeV enters in the energy range where new physics phenomena may be discovered and more Higgs production channels like the double Higgsstrahlung $e^-e^+ \to HHZ$ can be observed and rare Higgs branching ratios tested. The third and final stage at 3 TeV may provide the discovery of new electroweak particles or dark matter candidates and improve the sensitivity to new physics processes at higher energy scales through indirect searches.
All these possibilities offered by a electron-positron collider seem to be very exciting, however there are some limits: the CLIC is thought to be a linear collider, since a circular collider would have problem of high synchrotron radiation at those energies, and should be built from scratch. A future high energy circular lepton collider could however be realised, if instead of electrons one uses muons. The larger muon mass reduces the problem of the synchrotron radiation significantly and the muon collider could potentially re-use the LHC tunnel.

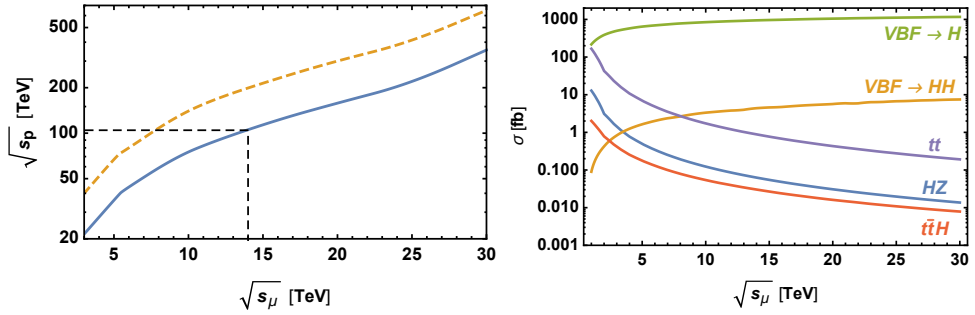

Figure 4.1: In the left figure the energy at which the muon collider cross section is equal to the proton collider one, with comparable Feynman amplitudes for the production processes (dashed line) and the proton squared amplitude enhanced by a factor ten (continuous line). In the right figure there are some cross-sections for Higgs and top-quark production at a lepton collider [48].

In this sense, a muon collider has great potential for high-energy physics, offering collisions of point like particles at very high energies. However, the drawback of the finite muon lifetime and the actual difficulty in producing muon beams present great technological challenges. The comparisons with a proton-proton collider seem to suggest that a 14 TeV muon collider would provide an effective energy reach similar to that of a 100 TeV one [50]: as mentioned, this comes from the advantage of having the entire center of mass energy available for hard scattering processes. Therefore a muon collider would be ideal in order to look for and eventually study new physics, resolving resonances both as a precision facility and or an exploratory machine. An example of this could be the search for new particles coupled with the Higgs boson by exploiting the "large" cross-sections of VBF (see Fig. 4.1). Also the possibility to indirectly probe the existence new physics would be a highly coveted feature of a muon collider. Thanks to the high-energies in play, indirect new physics, such as the SMEFT effects discussed previously, would be enhanced and could show up even in relatively inaccurate measurements. Moreover, exploiting again the VBF cross-sections, a muon collider could be an Higgs factory (e.g. with an integrated luminosity of 10 ab^{-1}, a 10 TeV muon collider would produce $8 \cdot 10^6$ Higgs bosons) and might allow for a programme of Higgs coupling determination.
Concluding, it is clear why a lepton-anti-lepton collider would be a wonderful machine for future studies in Particle Physics. both CLIC and a muon collider could provide important contributions in this sense, even if both have strengths and weaknesses and constitute a tough technological challenge.

4.5 Processes and results

In this section what has been done is explained, the main and most significant plots for every process are presented and discussed.

Blueprint for the analysis

A total of 11 VBF processes (8 W^+W^- and 3 ZZ fusions, see Table 4.1) have been systematically studied and analysed. As already mentioned in 4.2, one has evaluated the impact of the 13 SMEFT operators in Table 4.2 qualitatively.
For every process, one has first studied the behaviour of the helicity amplitudes at high energies as a function of the center of mass energy in the so called "Mercedez" configuration. This study has been done both for the SM and SMEFT contributions to the process, switching on one operator at a time. This has been done both numerically with MadGraph and analytically with Mathematica and the results agree. A data summary has been reported in the helicity tables present in Appendix B and some more details are given.
In the helicity amplitudes study, no explicit sensitivity to the Wilson coefficients has been determined. In order to do a naive sensitivity study in the context of a future muon collider, one has embedded every process in a collider one and performed some cuts in some kinematic quantities in order to access the high-energy regime. The study has been conducted at 3, 14 and 30 TeV center of mass energies with corresponding integrated benchmark luminosities of 6, 20 and 100 ab^{-1} respectively. Since every VBF process has five particles in the final state when embedded in a muon collider, many diagrams other than the ones in the original process arise. In this way, not only may the contribution of the original process be hidden, but also the numerical simulations are extremely computationally demanding. Because of this and the fact that this is a naive sensitivity study at very high-energies, instead of using the s-channel $\mu^-\mu^+ \to final\ state$, $e^-\mu^+ \to final\ state$ has been employed in order to reduce the number of diagrams. In some cases it has been possible reduce the number of diagrams to the ones of the original process.
One has computed the cross-section for the SM process, for the interference term between the SM and the SMEFT and for the SMEFT only. Next, the ratios $r_{INT} \equiv \frac{\sigma_{INT}}{\sigma_{SM}}$ and $r_{SQ} \equiv \frac{\sigma_{SQ}}{\sigma_{SM}}$ have been studied and organised in different kind of plots for each operator in every process in order to highlight the sensitivity of the process to it in several ways. Moreover, a substantial growth of an operator's relative impact in the high-energy phase space region can indicate the presence of unitarity violating behaviour due to the effective operator insertion. However, the interference term is often difficult to interpret, since the matrix elements can change sign over the phase space: this can lead to cancellations upon integration and to relatively small contributions which hide the high-energy behaviour of the EFT to the amplitude.

Three main kinds of plot have been realised: the "parabola plot", where the ratio between the relative impact of each operator on the cross section is plotted as a function of the operator Wilson coefficient (i.e. one plots the function $R(c_i) \equiv 1 + c_i r_{INT} + c_i^2 r_{SQ}$); the "radar plot", where a summary of r_{INT} and r_{SQ} for each operator in a process and their limits given the actual constraints on the operators Wilson coefficients is illustrated at given center of mass energy; a "shape plot" where r_{INT} and r_{SQ} are presented for a fixed c_i as a function of the invariant mass of the particles of the final state.
In the next paragraphs, a selection of such plots for every process for the most interesting operators is presented. For each purely bosonic process, the "parabola plot" and the "shape plot" of the operator, which the process can give more information on, are presented. This choice is due to the fact that the Wilson's coefficients of the bosonic operators are rather strongly constrained and the constraints can be improved only for a restricted class of processes. For each top-quark process instead, a radar plot with the sensitivity ratios for interference and square contributions of all the top-quark operators at the intermediate center of mass energy of 14 TeV are presented, since every top-quark process can improve the constraints over the Wilson's coefficients of every top-quark operator.
Finally, plots with a summary of the contribution of some operators in every process appear at the end of this section.

4.5.1 Bosonic processes

$W^+W^- \to HHH$

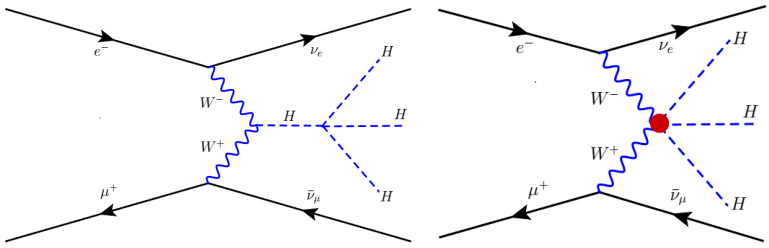

(a) **(b)**

Figure 4.2: Examples of Feynman diagrams from the SM (left) and from SMEFT (right) for the collider process embedding $W^+W^- \to HHH$. The blue subdiagrams contribute to the core process, while the red dot indicates a new (contact) interaction from SMEFT.

At the tree-level, four operators contributes to this process: $\mathcal{O}_\phi$, $\mathcal{O}_{\phi W}$, $\mathcal{O}_{\phi d}$ and $\mathcal{O}_{\phi D}$. The triple Higgs in the final state allows the presence of diagrams where the triple and quartic Higgs self-interaction are involved. This makes this process suitable to better study the Higgs boson self-interaction and to constrain the operator $\mathcal{O}_\phi$, as it is confirmed by the summary plot 4.25.
Focusing on this operator, from Table B.1 it appears that only the fully longitudinal amplitude undergoes a tree-level unitarity violation from its contribution. The contribution of this operator are likely due to a five point contact term with two Goldstone bosons, three Higgs and a vev insertion.
The tree-level process has been embedded in the lepton collider process $e^-\mu^+ \to HHH\nu_e\bar{\nu}_\mu$ and the sensitivity to the operator $\mathcal{O}_\phi$ has been studied. From Figure 4.3 one observes that this operator has a major impact to the process in the low-energy region of the phase space. This could have been argued looking at the structure of this operator, which does not involve any derivative: consequently, the Feynman rules in the momentum space do not depend on the momenta of the particles. This observation is here made since other operators have derivatives and their Feynman rules depend on the particles momenta and one may expect that their contribution to a process increases with the energy.
The major drawback of this process is that it is rather rare, as one can see from the number of events reported in the parabola plot and an interesting event number may be accessible starting from 14 TeV center of mass energy. However, constraints on this operator can be derived also from other bosonic processes with a bigger cross-section (as the 2 to 2 processes like the VBF into double Higgs).

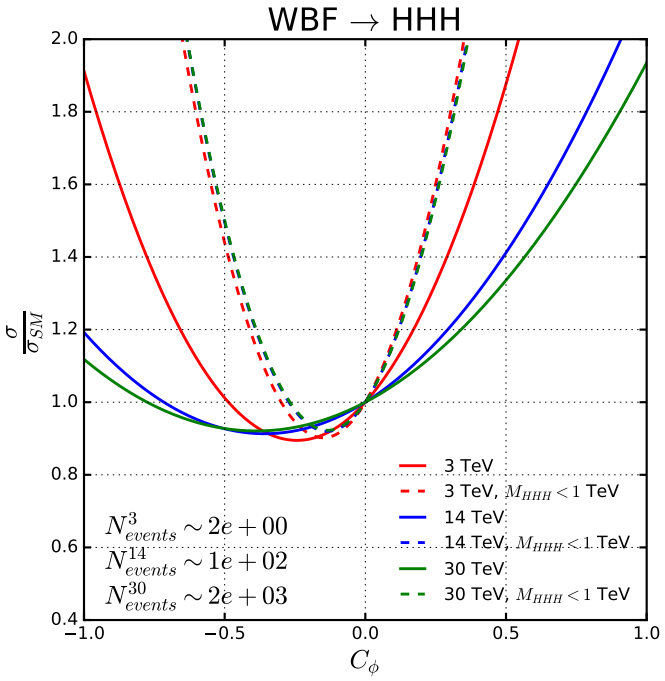

(a)

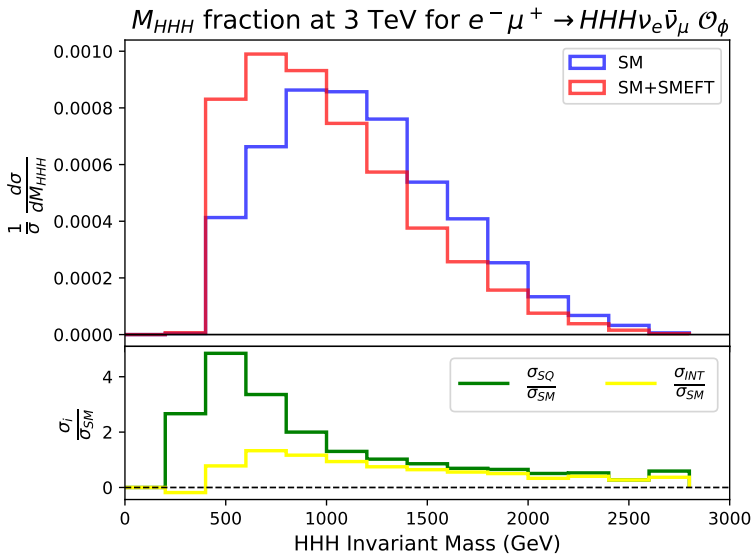

(b)

Figure 4.3: Fig. a: WBF to triple Higgs sensitivity to the $\mathcal{O}_\phi$ operator with and without invariant mass cut at 3, 14, 30 TeV. Fig. b upper: Differential cross section as a function of M_{HHH} normalised to one to show the impact of the dimension six term. Fig. b lower: Sensitivity ratios r_{INT} and r_{SQ} as M_{HHH} function for $c_\phi = 1\ TeV^{-2}$.

$ZZ \to HHH$

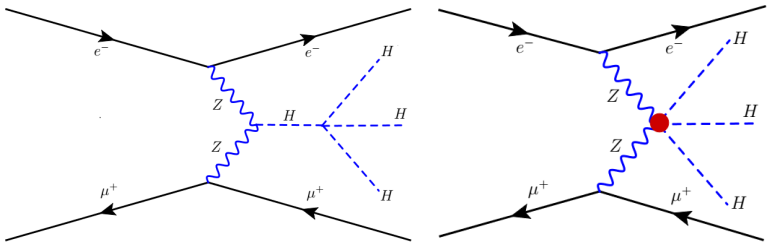

(a) **(b)**

Figure 4.4: The same as in Fig. 4.2 for $ZZ \to HHH$.

This process is very similar to the WW to triple Higgs one, but two more operators, $\mathcal{O}_{\phi WB}$ and $\mathcal{O}_B$, are involved thanks to the presence of the Z instead of the W. Again, this process allows to better study the Higgs self-interaction and it is the most sensitive one to the operator $\mathcal{O}_{\phi WB}$ among the studied processes. At the helicity amplitudes level (Table B.2), the behaviour is exactly the same as $W^+W^- \to HHH$ and for operators different from $\mathcal{O}_\phi$ tree-level unitarity violation takes place in every helicity amplitude.
The process has been embedded in the lepton collider process $e^-\mu^+ \to HHHe^-\mu^+$ and in the Figure 4.5 the sensitivity plots for the operator $\mathcal{O}_{\phi WB}$ are shown. As one had anticipated in the previous paragraph, this operator involves derivatives and contributes more at high energies. From the parabola plot one observes that the collider process sensitivity to this operator is extremely enhanced by the mass invariants cut on the three final state particles of the not embedded process, especially for 14 TeV and 30 TeV center of mass energies.
Unfortunately, the cross section of this process is extremely small and even using the benchmark luminosities introduced in Sec. 4.5 it is not possible to get even a single event in the SM. That makes this process not very useful for a future lepton collider study: even if it is more sensitive than other bosonic processes to many operators, it is not accessible.

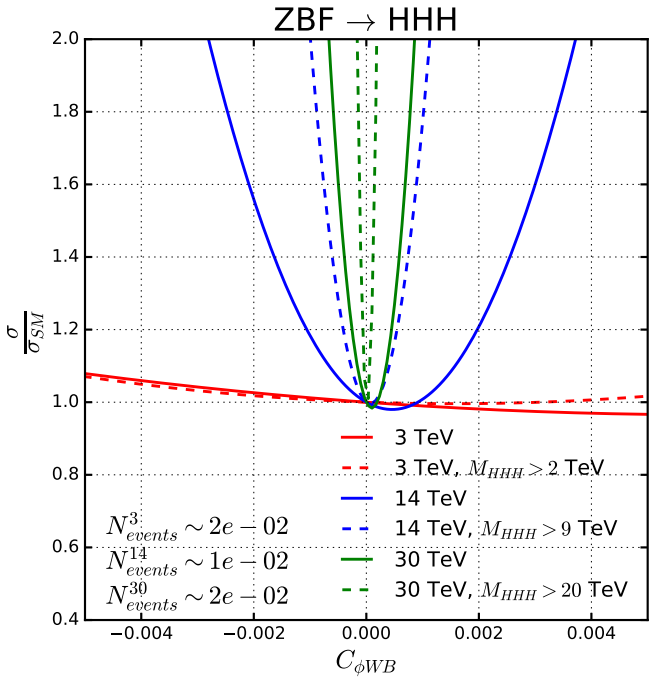

(a)

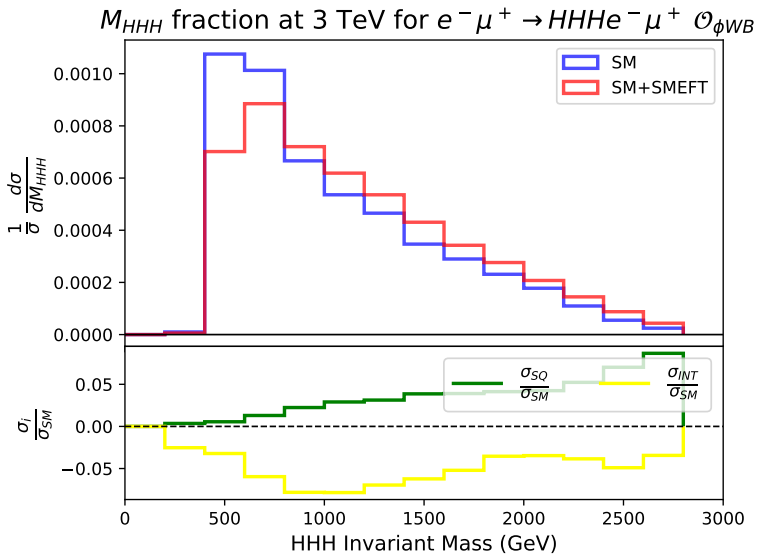

(b)

Figure 4.5: Fig. a: ZBF to triple Higgs sensitivity to the $\mathcal{O}_{\phi WB}$ operator with and without invariant mass cut at 3, 14, 30 TeV. Fig. b upper: Differential cross section as a function of M_{HHH} normalised to one to show the impact of the dimension six term. Fig. b lower: Sensitivity ratios r_{INT} and r_{SQ} as M_{HHH} function for $c_{\phi WB} = 0.005\ TeV^{-2}$.

$W^+W^- \to HHZ$

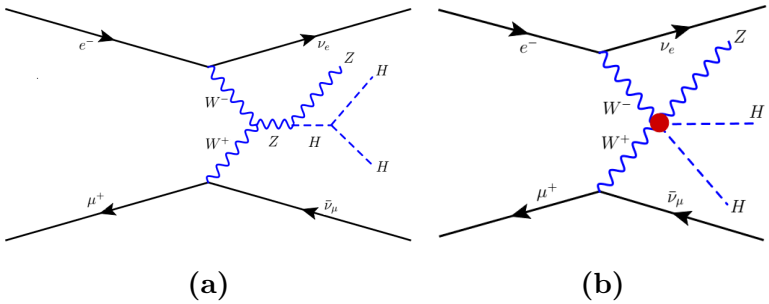

Figure 4.6: The same as in Fig. 4.2 for $W^+W^- \to HHZ$.

At the tree-level, this process involves the six out of seven bosonic operators studied, but not $\mathcal{O}_\phi$. Moreover, it involves all the bosons of the electroweak sector and it is very interesting in order to improve the knowledge about how they interact among each other. The much higher number of helicity amplitudes allows to find a lot of cases where tree-level unitarity is violated, especially for $\mathcal{O}_{\phi WB}$, $\mathcal{O}_{\phi B}$ and $\mathcal{O}_W$.
The process was embedded in the lepton collider $e^-\mu^+ \to HHZ\nu_e\bar{\nu}_\mu$. It turned out that this process is the most sensitive one to the $\mathcal{O}_{\phi W}$ operator. This operator is strongly constrained, but it may be possible to get additional information at energies of 30 TeV, especially from a mass invariant cut, as one can see from the parabola plot in Figure 4.7 (an invariant mass cut at 14 TeV reveals a better sensitivity than at 30 TeV center of mass energy without any cut). This process does not suffer from small cross section and a satisfactory number of events may be obtained at a muon collider already at 14 TeV center of mass energy.

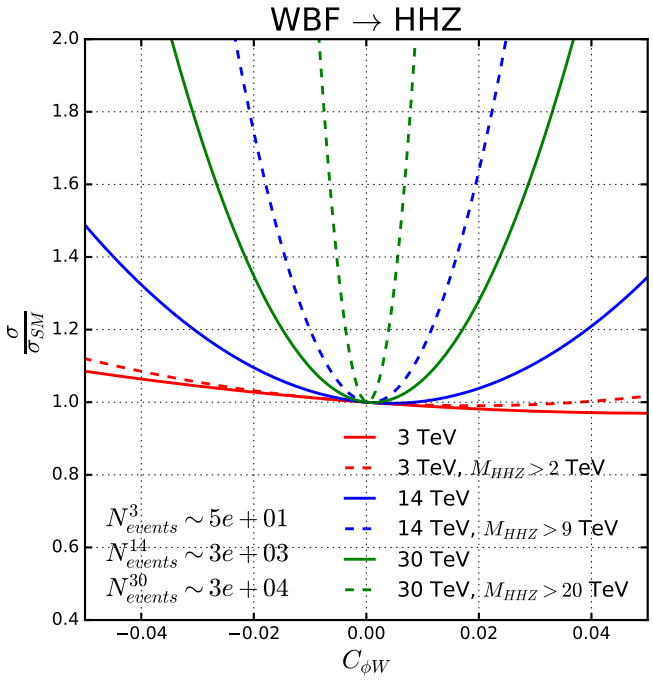

(a)

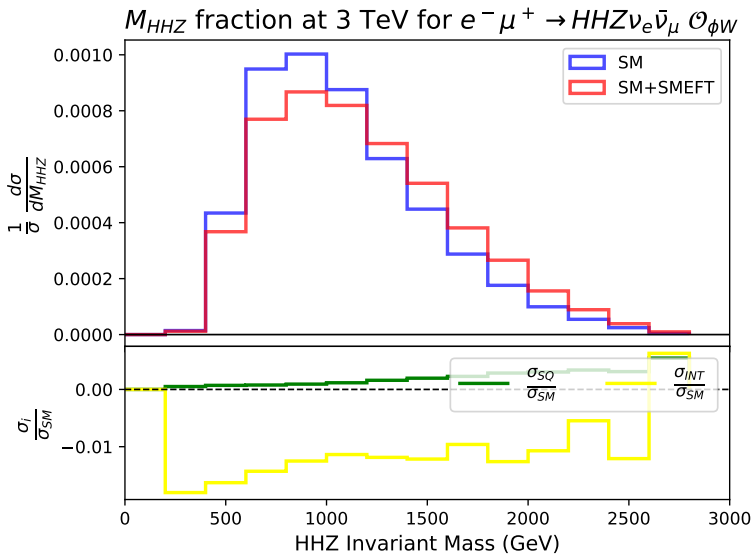

(b)

Figure 4.7: Fig. a: WBF to HHZ sensitivity to the $\mathcal{O}_\phi W$ operator with and without invariant mass cut at 3, 14, 30 TeV. Fig. b upper: Differential cross section as a function of M_{HHZ} normalised to one to show the impact of the dimension six term. Fig. b lower: Sensitivity ratios r_{INT} and r_{SQ} as M_{HHZ} function for $c_{\phi W} = 0.01\ TeV^{-2}$.

$W^+W^- \to W^+W^-H$

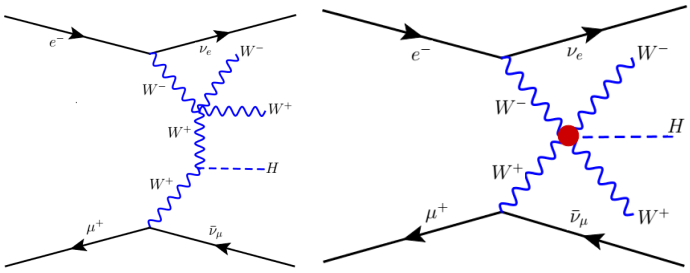

Figure 4.8: The same as in Fig. 4.2 for $W^+W^- \to W^+W^-H$.

This process involves all the seven bosonic operators of the study. It is the simplest extension to the 2 to 3 case of the WW scattering and from its helicity tables it is possible to see that all the helicity amplitude which behaved like a constant E^0 in the 2 to 2 case in this process behave like E^{-2} due to tree-level unitarity in the 2 to 3 case and the even nature of these amplitudes under the parity symmetry discussed in 4.3.
At the helicity amplitude level it is interesting to observe that the operators $\mathcal{O}_{\phi W}$ and $\mathcal{O}_W$ are the operators which violates tree-unitarity in most helicity amplitudes. Also the fact that the $\mathcal{O}_\phi$ violates tree-unitarity only in the fully longitudinal amplitude is remarkable.
The process was embedded in the lepton collider $e^-\mu^+ \to W^+W^-H\nu_e\bar{\nu}_\mu$ and it is rather sensitive to all the operators. Here the $\mathcal{O}_W$ plots are presented. Again, the operator involves derivatives and contributes most at high energies. The contribute due to the interference term is relatively small and oscillates around zero.

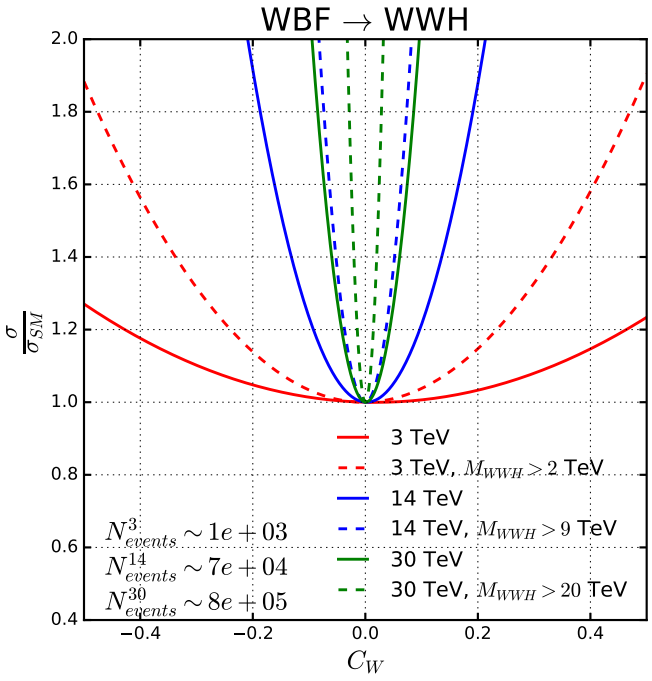

(a)

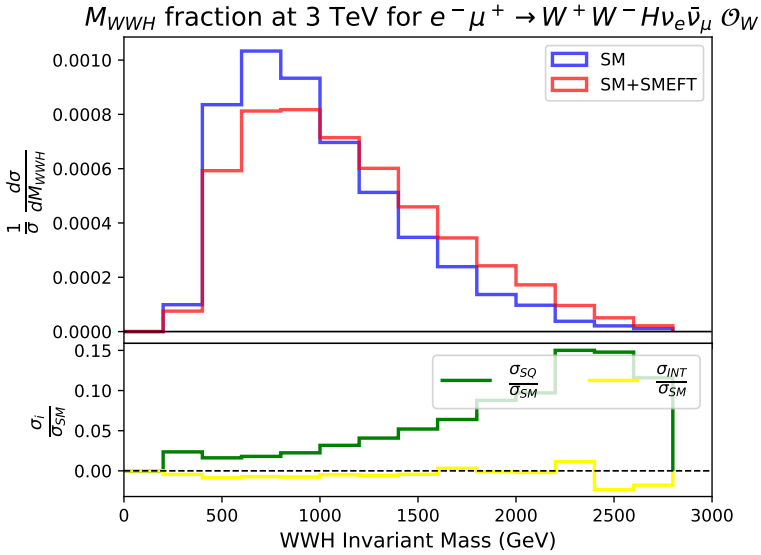

(b)

Figure 4.9: Fig. a: WBF to W^+W^-H sensitivity to the $\mathcal{O}_W$ operator with and without invariant mass cut at 3, 14, 30 TeV. Fig. b upper: Differential cross section as a function of M_{WWH} normalised to one to show the impact of the dimension six term. Fig. b lower: Sensitivity ratios r_{INT} and r_{SQ} as M_{WWH} function for $c_W = 0.18\ TeV^{-2}$.

$W^+W^- \to W^+W^-Z$

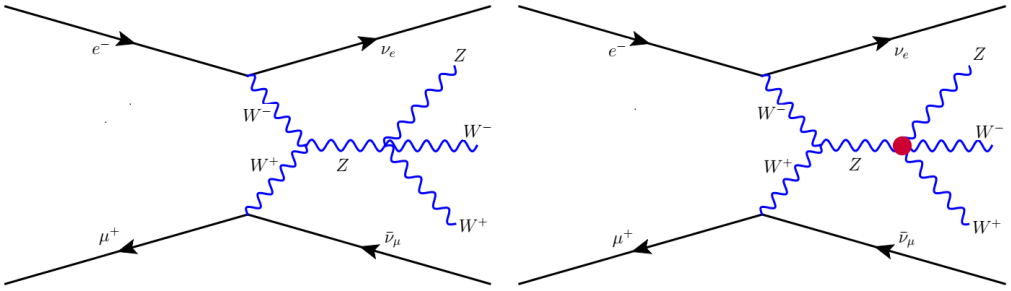

(a) **(b)**

Figure 4.10: The same as in Fig. 4.2 for $W^+W^- \to W^+W^-Z$.

This process was the most challenging to study from a computational point of view, with its 243 helicity amplitudes and the many diagrams arising when embedded in the process $e^-\mu^+ \to W^+W^-Z\nu_e\bar{\nu}_\mu$. However this is also the process which, according to the benchmark luminosities used, will give the highest number of events during a future muon collider study, shown in Figure 4.11. At the helicity amplitude level, the main sources of unitarity violation are again the $\mathcal{O}_W$ and $\mathcal{O}_{\phi W}$ and when the Z boson is longitudinally polarised, the results obtained for the $W^+W^- \to W^+W^-H$ process are recovered in the SM. When embedded in the lepton collider process written above, the process reveals itself to be the one which can give the strongest constraints to the operator $\mathcal{O}_W$ as one can see in Figure 4.25. Even without any cut, its sensitivity to this operator is better than that of the $W^+W^- \to W^+W^-H$ process in Figure 4.9. For what concerns the plot with the sensitivity ratios as invariant mass function, one can notice that the interference contribution is very similar to the one of $W^+W^- \to W^+W^-H$ in the considered phase space region. Moreover, with respect to $W^+W^- \to W^+W^-H$, the square dimension six ratio sensitivity has a cleaner growth to the peak at high-energies.

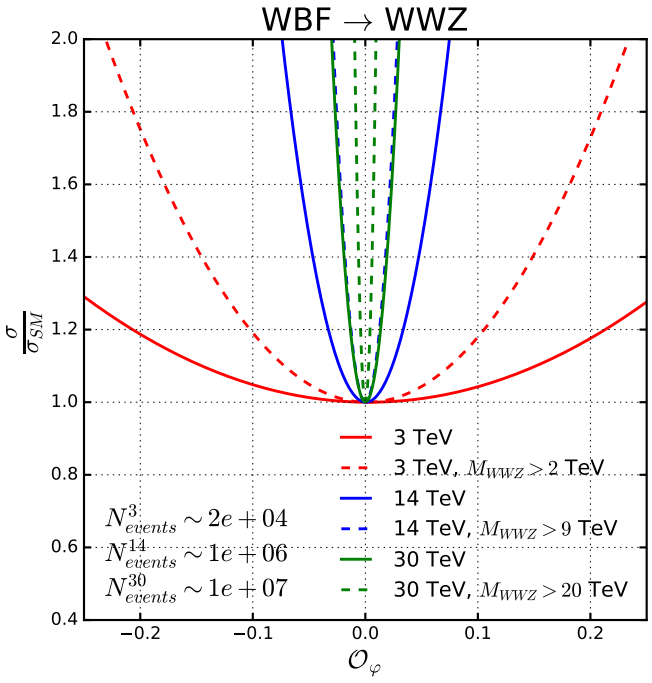

(a)

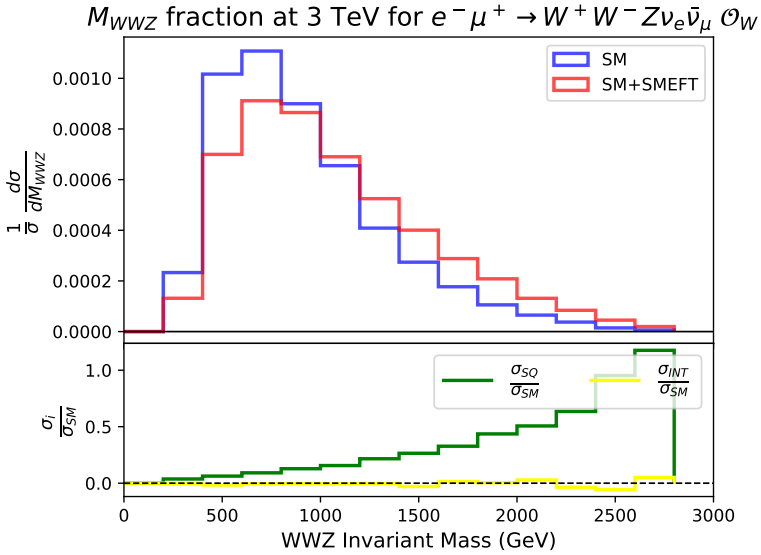

(b)

Figure 4.11: Fig. a: WBF to W^+W^-Z sensitivity to the $\mathcal{O}_W$ operator with and without invariant mass cut at 3, 14, 30 TeV. Fig. b upper: Differential cross section as a function of M_{WWZ} normalised to one to show the impact of the dimension six term. Fig. b lower: Sensitivity ratios r_{INT} and r_{SQ} as M_{WWZ} function for $c_W = 0.18\ TeV^{-2}$.

$W^+W^- \to ZZH$

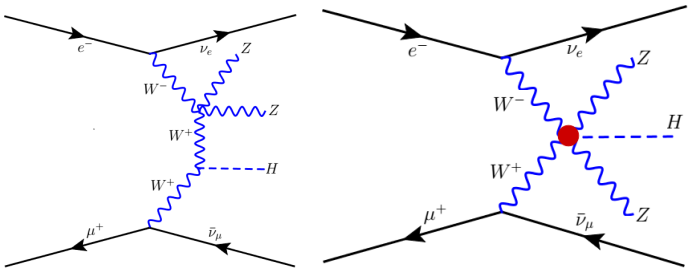

(a) **(b)**

Figure 4.12: The same as in Fig. 4.2 for $W^+W^- \to ZZH$.

This process involves again all the seven operators and all the electroweak sector bosons and may give important information about how this particles interact.
At the helicity amplitude level (Table B.6) it has the same SM behaviour as $W^+W^- \to W^+W^-H$ and again many tree-unitarity violating behaviours appear when including the dimension six operators.
The process was embedded in the $e^-\mu^+ \to ZZH\nu_e\bar{\nu}_\mu$ and showed interesting sensitivity to relatively weakly constrained operators $\mathcal{O}_\phi$, $\mathcal{O}_{\phi d}$ and $\mathcal{O}_W$. Here the sensitivity plots for the operator $\mathcal{O}_{\phi d}$ are illustrated. From the parabola plot is it possible to argue that at low energies the SMEFT contribution to the process comes mostly from the interference term between the SM and the dimension six operator, while the square term dominates at high energies (the 3 TeV parabola does not have the minimum in 1). This is confirmed from the 3 TeV plot with the sensitivity ratios as the invariant mass function.
As in the $W^+W^- \to W^+W^-H$ case, this process can be observed significantly at a future muon collider already starting from 3 TeV center of mass energy.

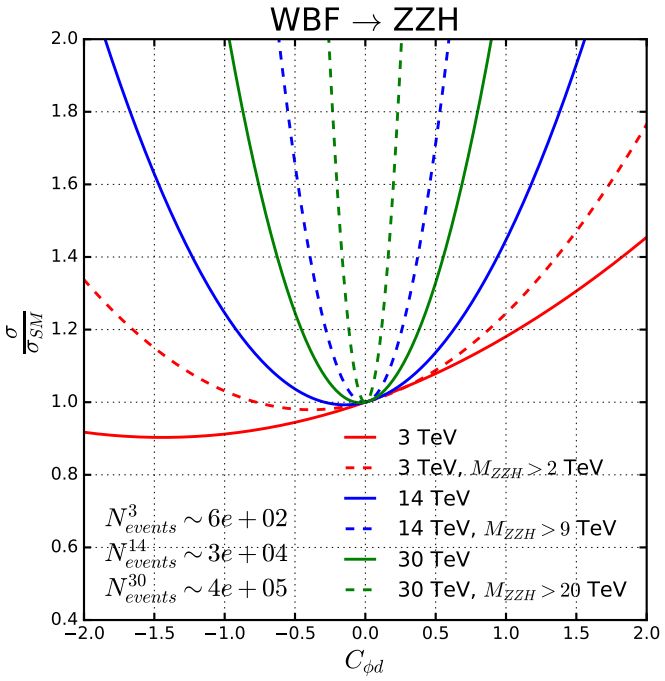

(a)

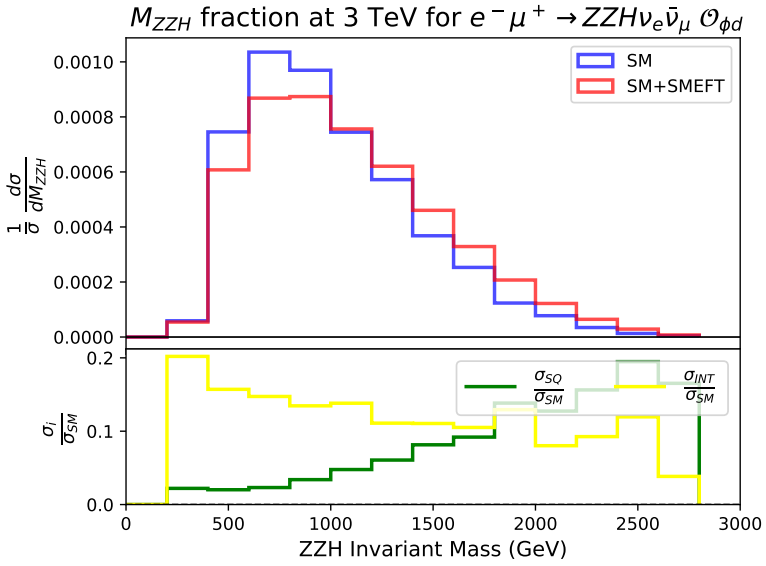

(b)

Figure 4.13: Fig. a: WBF to ZZH sensitivity to the $\mathcal{O}_{\phi d}$ operator with and without invariant mass cut at 3, 14, 30 TeV. Fig. b upper: Differential cross section as a function of M_{ZZH} normalised to one to show the impact of the dimension six term. Fig. b lower: Sensitivity ratios r_{INT} and r_{SQ} as M_{ZZH} function for $c_{\phi d} = 1\ TeV^{-2}$.

$W^+W^- \to ZZZ$

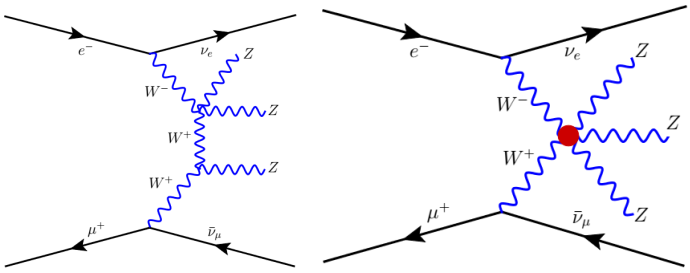

(a) **(b)**

Figure 4.14: The same as in Fig. 4.2 for $W^+W^- \to ZZZ$.

For the same reasons as for $W^+W^- \to W^+W^-Z$, this process was very challenging to study from a computational point of view, with its 243 helicity amplitudes and the many diagrams arising when embedded in the process $e^-\mu^+ \to ZZH\nu_e\bar{\nu}_\mu$. The contributions to the cross section after cuts are therefore not illustrated. It offers the possibility to study the interactions between the W and Z boson and it can produce a rather high number of events already at 3 TeV center of mass energy when compared to the other processes studied here and employing the benchmark integrated luminosities introduced previously.
At the helicity amplitude level, one can observe that one of the three Z in the final state, the SM amplitudes behaves like in the $W^+W^- \to ZZH$ case and that the most tree-level violating operators are $\mathcal{O}_{\phi W}$, $\mathcal{O}_{\phi WB}$ and $\mathcal{O}_W$.
When embedded in the lepton collider process written above, the process reveals to be the one which can give the strongest constraints to the operator $\mathcal{O}_{\phi d}$ as one can see in Figure 4.25. Comparing the parabola plot 4.15 with the one 4.13 for the $W^+W^- \to ZZH$ process, it is clear that already without any cuts, this process will be able to give much more information about the $\mathcal{O}_{\phi d}$ operator. For what concerns instead the plot with the sensitivity ratios as invariant mass function, one can notice that in this case the contribute of the interference term is more or less stable and always positive in the considered phase space region. Moreover, with respect to $W^+W^- \to ZZH$, the sensitivity ratio for the squared dimension is more peaked at high-energies.

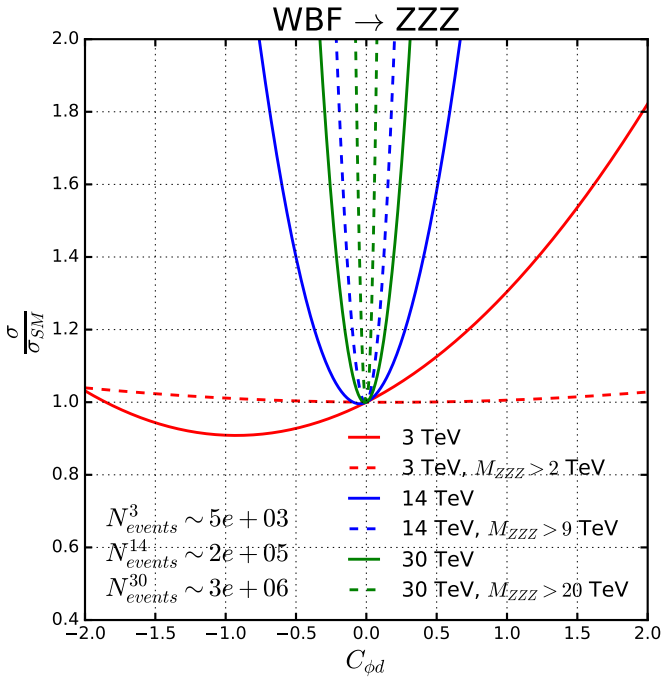

(a)

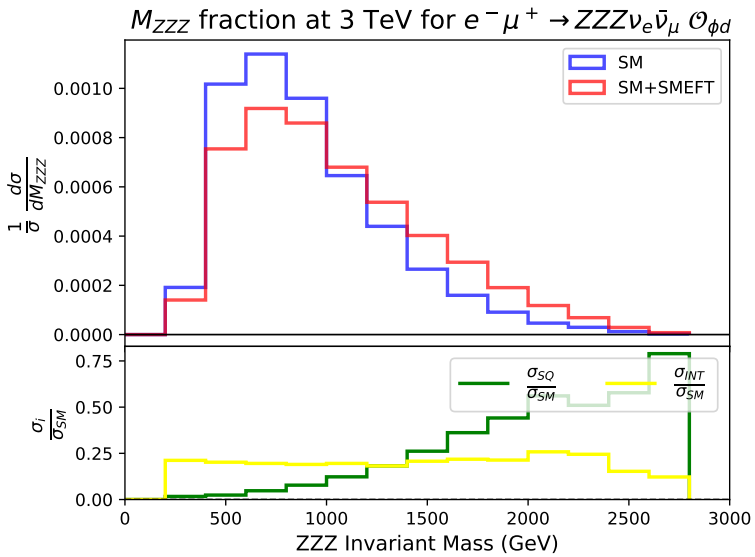

(b)

Figure 4.15: Fig. a: WBF to ZZZ sensitivity to the $\mathcal{O}_{\phi d}$ operator with and without invariant mass cut at 3, 14, 30 TeV. Fig. b upper: Differential cross section as a function of M_{ZZZ} normalised to one to show the impact of the dimension six term. Fig. b lower: Sensitivity ratios r_{INT} and r_{SQ} as M_{ZZZ} function for $c_{\phi d} = 1\ TeV^{-2}$.

4.5.2 Top-quark processes

$W^+W^- \to t\bar{t}H$

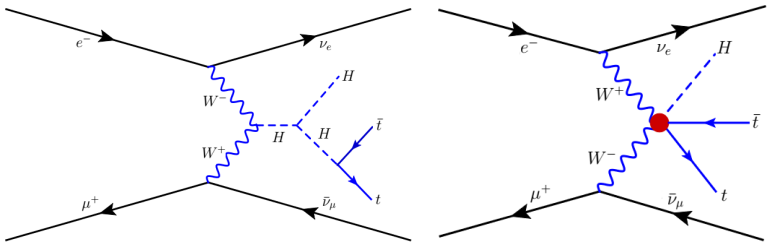

(a) **(b)**

Figure 4.16: The same as in Fig. 4.2 for $W^+W^- \to t\bar{t}H$.

This process involves three important particles: the W, the top-quark and the Higgs boson. The last two particles are the most heavy and less known particles of the SM and this process allows to study their interaction.
At the helicity amplitude level (Table B.8), one can observe that among the top quark operators the most tree-level unitary violating ones are the dipole operator $\mathcal{O}_{tW}$ and the currents operators.
When embedded in the lepton collider process $e^-\mu^+ \to t\bar{t}H\nu_e\bar{\nu}_\mu$, it turn out that this process is the most sensitive (Figure 4.26, 4.27, 4.28) to the current operators $\mathcal{O}_{\phi Q}^{(1)}$ and $\mathcal{O}_{\phi Q}^{(3)}$ and the operators $\mathcal{O}_{\phi t}$ and $\mathcal{O}_{t\phi}$. Moreover, the interference contribution of $\mathcal{O}_{\phi Q}^{(3)}$ appears to go down with the energy: this could be due to a phase space cancellation, since from Table B.8 it is expected to have a similar behaviour to the other current operators.
If one uses the actual constraints on the Wilson coefficients one has in general a better sensitivity as one can see from the radar plot in Figure 4.17.
From the radar plot it is clear that important contribution to the cross-section can come from the squared term. This process is accessible at a future muon collider since employing the benchmark luminosity at 14 TeV center of mass energy previously introduced, one can estimate a number of events of order 10^3.

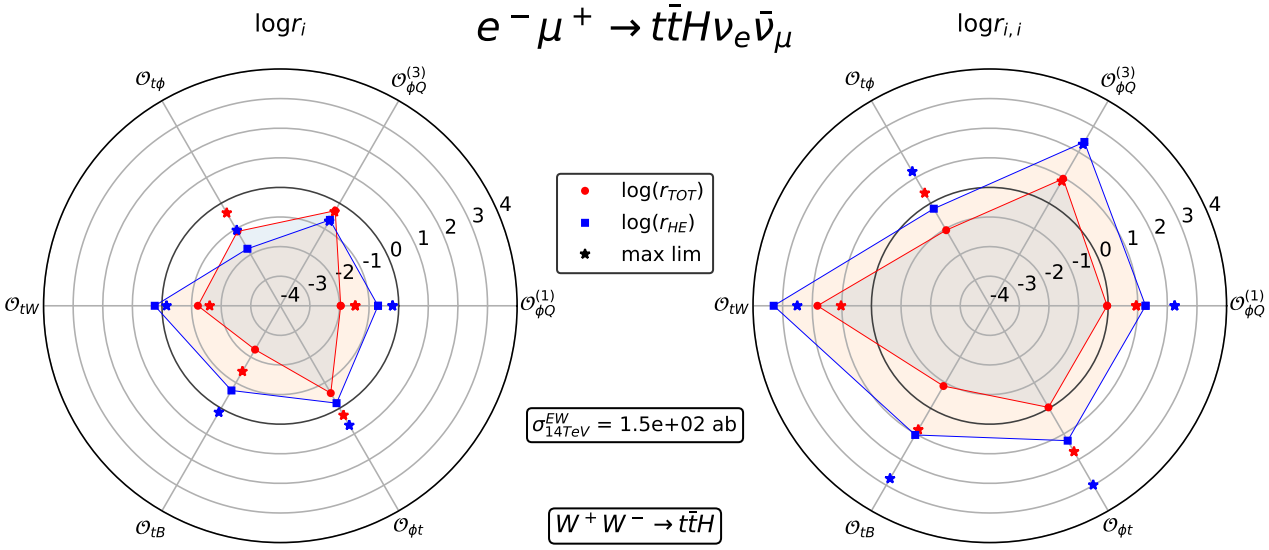

Figure 4.17: Radar plot for the WBF to $t\bar{t}H$ at 14 TeV for a lepton collider. The impacts of every operator with a Wilson's coefficient of 1 TeV^{-2} for the (absolute value) interference term and SMEFT squared term are illustrated in the left and right figure, respectively. Relative impacts at inclusive level and in a high energy region of phase space are depicted by the blue and red dots, respectively. The stars denote the corresponding prediction when saturating the individual limits on the coefficients summarised in Tab.4.3.

$W^+W^- \to t\bar{t}Z$

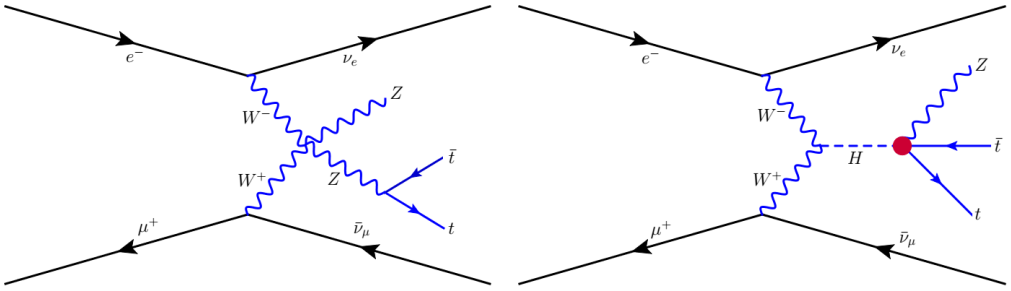

(a) **(b)**

Figure 4.18: The same as in Fig. 4.2 for $W^+W^- \to t\bar{t}Z$.

In this process the electroweak vector bosons and the top quark are involved and can be used to get important information about how these particles interacts each other.
At the helicity amplitudes level, the top-quark operators which have the highest number of tree-unitarity violating behaviours are the dipole operators $\mathcal{O}_{tW}$ and $\mathcal{O}_{tB}$. When the Z boson is longitudinally polarised, the same results of the SM of $W^+W^- \to t\bar{t}H$ are recovered.
The process was embedded in the lepton collider $e^-\mu^+ \to t\bar{t}Z\nu_e\bar{\nu}_\mu$ and showed to be the best one when one looks to the improvement of the Wilson's coefficient constraints of all operators (Figure 4.24). As one can see from the radar plot in Figure 4.19, the same does not hold for the sensitivity: the interference contribution does not appear to grow with the energy and the relative impact of the squared term does not appear as large as in other processes.
This process is easily accessible at 14 TeV center of mass energy for a future muon collider: from the SM cross-section and using the corresponding benchmark luminosity, one can estimate an event number of order 10^4. The higher number of events with respect to other process may be the reason why this process gives the best sensitivity to the Wilson's coefficients.

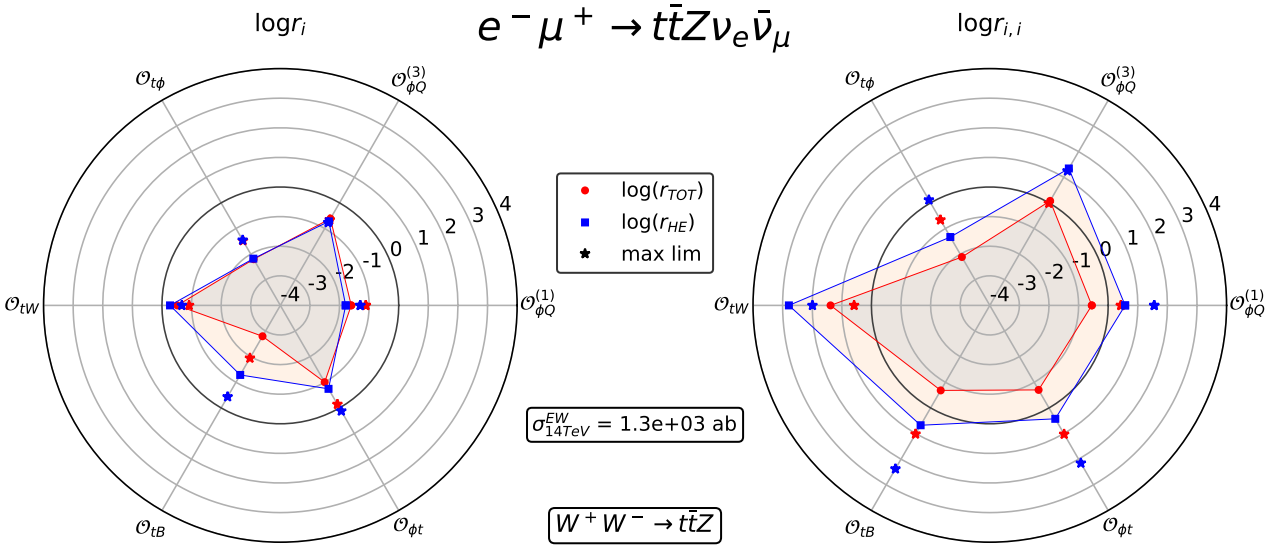

Figure 4.19: The same as Fig. 4.17 for WBF to $t\,\bar{t}\,Z$.

$ZZ \to t\bar{t}H$

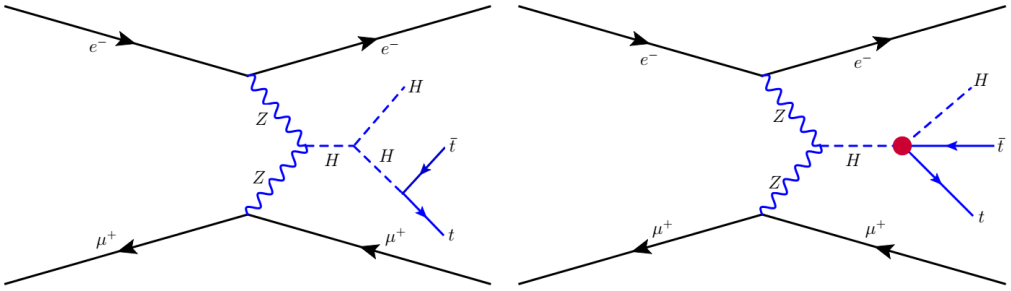

(a) **(b)**

Figure 4.20: The same as in Fig. 4.2 for $ZZ \to t\bar{t}H$.

This process allows to study the interaction between the Higgs boson, the top quark and the Z boson.
At the helicity amplitude level (Table B.10), one has a different behaviour with respect to the WW fusion when looking at the SM helicity amplitudes: this is because of the chiral nature of the W coupling to the fermions. When one includes the dimension six operators, the most tree-unitarity violating ones is again the dipole operator $\mathcal{O}_{tW}$.
The process has been embedded in the lepton collider process $e^-\mu^+ \to t\bar{t}He^-\mu^+$ and it is the most sensitive one to the dipole operators among the studied processes. By comparing the radar plot 4.21 with the corresponding WW one (4.17) it is possible to see how different the sensitivities are.
Unfortunately this process is not accessible even to a future muon collider when one consider the SM cross-section and the benchmark luminosities, since one get less than one event. However it can be still used to put some constraints on the Wilson's coefficients of the dimension six operators, if they predict large enhancements of the total cross section, like in the dipole operators case.

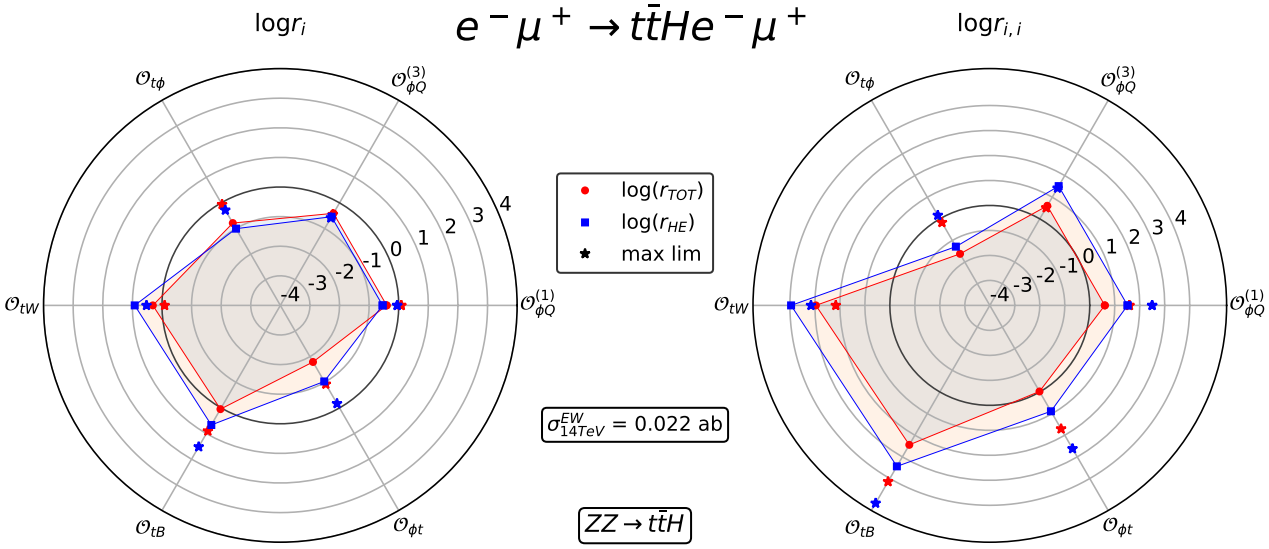

Figure 4.21: The same as Fig. 4.17 for ZBF to $t\,\bar{t}\,H$.

$ZZ \to t\bar{t}Z$

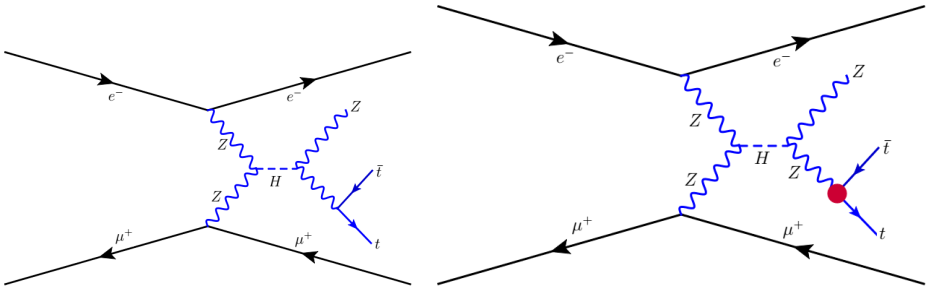

(a) **(b)**

Figure 4.22: The same as in Fig. 4.2 for $ZZ \to t\bar{t}Z$.

In this process only the Z boson and the top quark are involved and it may be used to better study their interactions.
For what concerns the helicity tables, it is possible to notice that the most of the helicity amplitudes where the dipole operators $\mathcal{O}_{tB}$ and $\mathcal{O}_{tW}$ are involved, manifest unitarity violating behaviours at high energies.
The process has been embedded in the lepton collider process $e^-\mu^+ \to t\bar{t}Ze^-\mu^+$ and it is very sensitive to the dipole operators. By comparing the radar plot 4.23 with the corresponding WW one (4.19) it is possible to see how different the sensitivities to the same operators are. The interference contribution of the currents operators seems to go down with energy, while one would expect it to be a constant from the helicity Table B.11: this may be again due to a cancellation in phase space. Unfortunately this process is not accessible even to a future muon collider when one consider the SM cross-section and the benchmark luminosities, since one get less than one event. However it can be still used to put some constrained on the Wilson's coefficients of the dimension six operators, like in the dipole operators case, where they predict a large enhancement of the cross section.

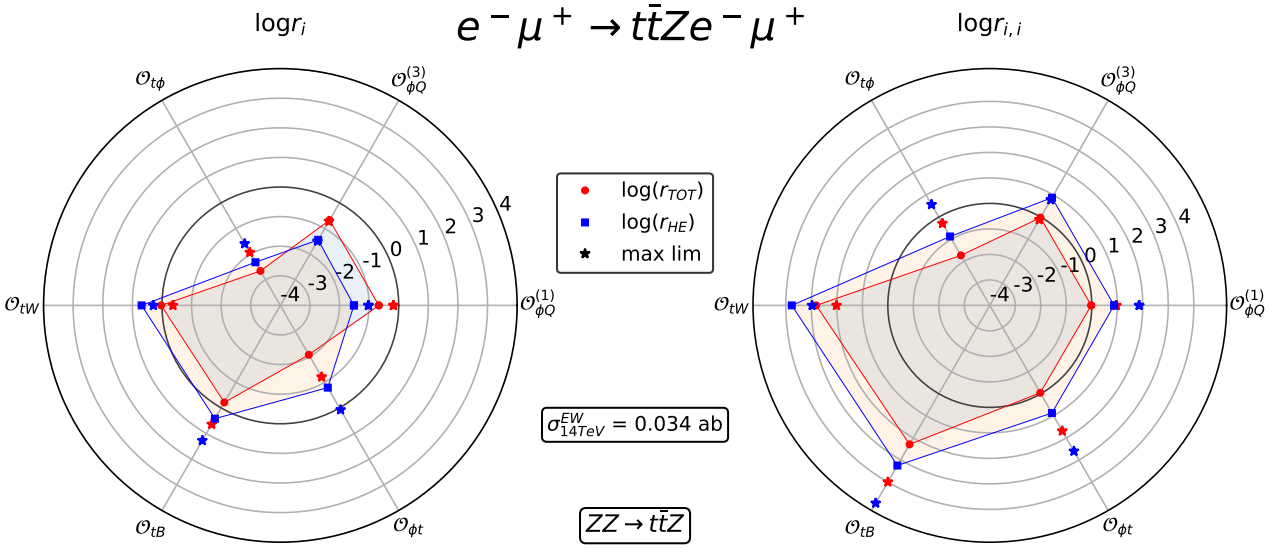

Figure 4.23: The same as 4.17 for ZBF to $t\,\bar{t}\,Z$.

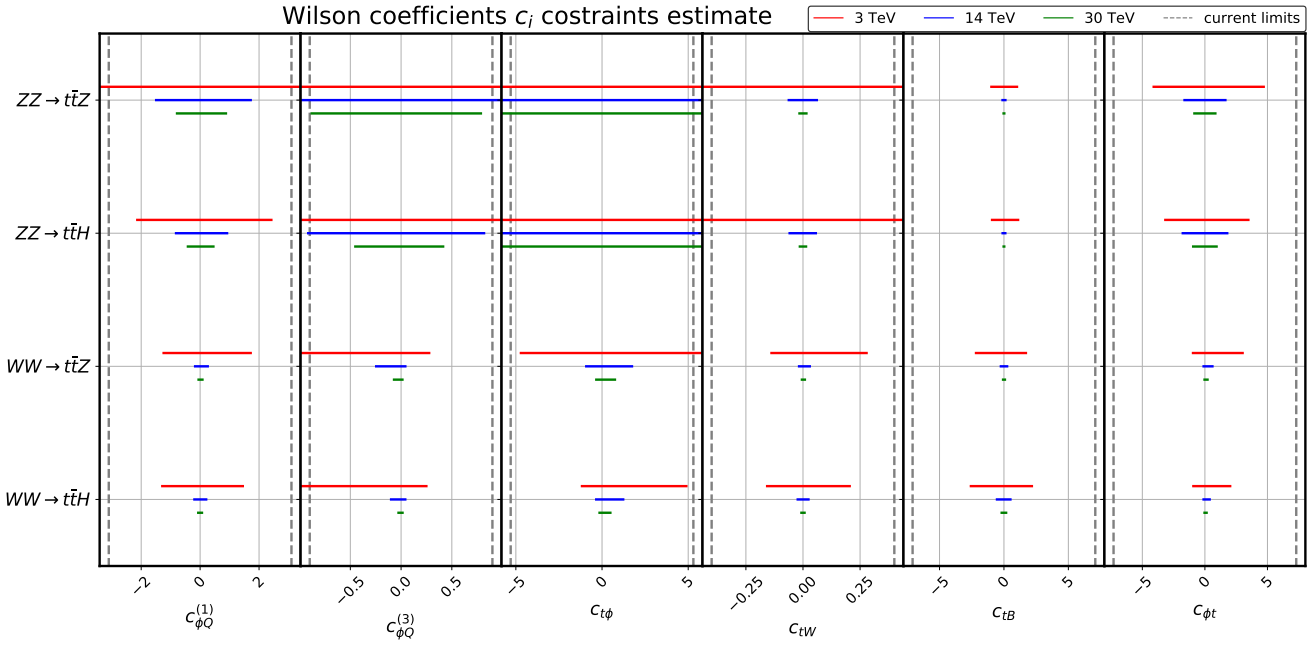

Figure 4.24: Summary plot with an estimate of the individual constraints over the Wilson's coefficients of the top-quark operators from the top-quark processes at 3, 14 and 30 TeV center of mass energy. The grey dashed vertical lines are the current individual limits on the operators Wilson's coefficients.

4.5.3 Summary plots

Here the previously quoted summary plots are presented. In plots 4.26, 4.27 and 4.28 the sensitivity of the top-quark processes to a given operator are summarised, while in plots 4.24 and 4.25 a crude estimate of a possible improvement of the constraints over the Wilson's coefficients are illustrated for all the processes. This estimate for the sensitivity to a Wilson's coefficient c_i has been obtained using the condition

$$2 < \frac{s(c_i)}{\sqrt{b}}, \tag{4.5.1}$$

where the signal is $s(c_i) = L(\sigma_{SM} + c_i\sigma_{INT} + c_i^2\sigma_{SQ})$ and the background is $b = L\sigma_{SM}$, assuming $s >> b$ (L is the benchmark integrated luminosity). This represents the 95% confidence level exclusion limit corresponding to the value of the coefficient that provides a 2σ discovery significance in the absence of decay branching fractions and other backgrounds.

As one can see, according to the estimations, all the Wilson's coefficients of the operators where the top quark is present may be better constrained than the actual individual constraints (see Table 4.3), especially at 14 TeV and 30 TeV center of mass energies. From this point of view (see Fig. 4.24), it is possible to see that the $W^+W^- \to t\bar{t}H$ is the best for all the operators but the dipole $\mathcal{O}_{tB}$, which the best processes are the ZBF for. The $W^+W^- \to t\bar{t}Z$ process is not as suitable as the other processes for a single operator, but can give useful information overall and is easier to access with respect to the others (see the relative paragraph). From plots 4.26, 4.27 and 4.28, it is possible to compare the impact of the operators on different processes and see how it changes with the center of mass energy and with the invariant mas cuts. In general, it is possible to see how the W/ZBF with the Higgs boson in the final state are more sensitive than the corresponding ones with the Z boson in the final state. Moreover, the ZBF processes are the most sensitive ones to the dipole operators $\mathcal{O}_{tB}$ and $\mathcal{O}_{tW}$, giving huge contribution with the squared term (see 4.27). The WBF processes are the most sensitive to the other operators for what concerns the squared terms, while for what concerns the interference term, sometimes the ZBF reveal to be the best. The invariant mass cuts play a fundamental role in enhancing the sensitivity, which grows for every operator in almost every process. The operators which are most affected from such cuts are the dipole operators, whose contributes increase of almost two magnitude orders when cuts at 14 and 30 TeV are considered in the squared terms, while in the interference terms their contribute in the ZBF processes become relevant. In some cases the cuts are not very helpful, like in the interference terms of the operators $\mathcal{O}^{(1)}_{\phi Q}$ and $\mathcal{O}_{t\phi}$ in Figg. 4.26 and 4.28.

For what concerns the bosonic operators, from Figure 4.25 the Higgs self-coupling operator $\mathcal{O}_\phi$ (which is poorly constrained nowadays) would benefit from the VBF process $W^+W^- \to HHH$ to be strongly constrained. The same holds for the operators $\mathcal{O}_{\phi d}$ and $\mathcal{O}_W$, which many processes are sensitive to. Even the sensitivity to the already strongly constrained operator $\mathcal{O}_{\phi W}$ could be slightly improved studying the process $W^+W^- \to HHZ$.
However, one must remember that this is a very crude estimate, which does not take in account any possible backgrounds.

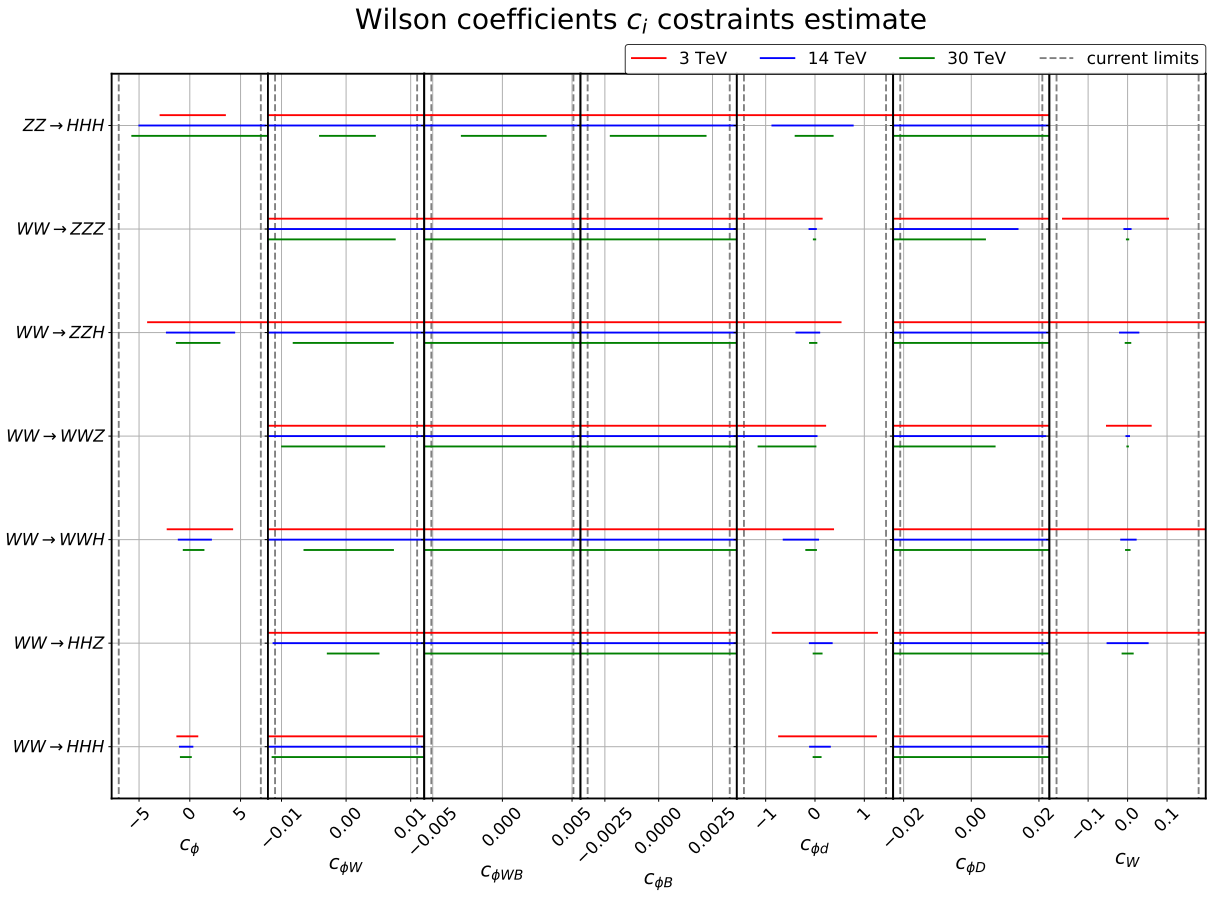

Figure 4.25: Summary plot with an estimate of the individual constraints over the Wilson's coefficients of the bosonic operators from the bosonic processes at 3, 14 and 30 TeV center of mass energy. The grey dashed vertical lines are the current individual limits on the operators Wilson's coefficients.

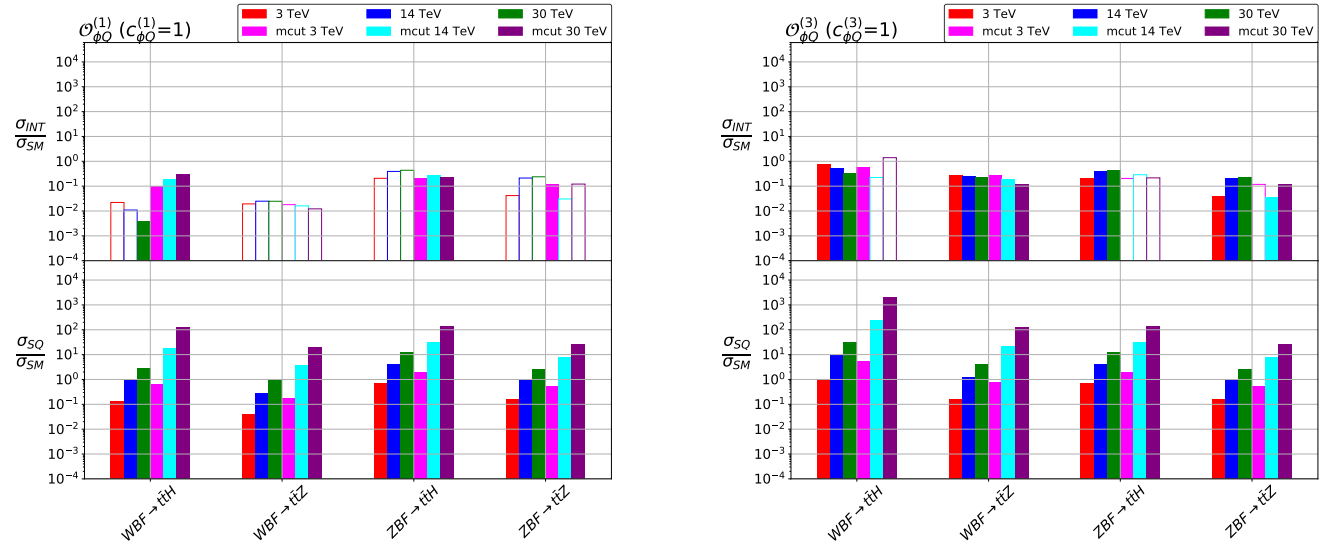

(a) **(b)**

Figure 4.26: Summary of relative impact on collider processes for the operators $\mathcal{O}_{\phi Q}^{(1)}$ and $\mathcal{O}_{\phi Q}^{(1)}$. The interference and quadratic contributions are shown in the upper and lower row, respectively. The multiple data points per process denote, from left to right, the impact of the operators with the energy growth without cuts and with cuts on the invariant mass of the particles in the final state. Filled and unfilled bars denote constructive and destructive interference terms respectively, according to the sign conventions in Table 4.2.

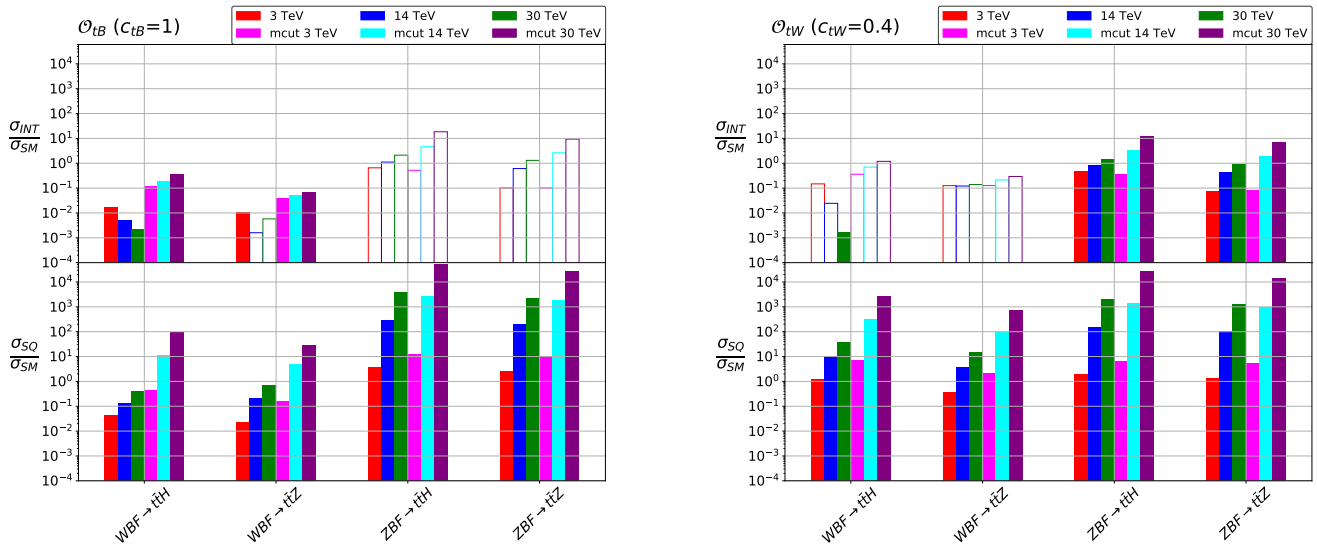

(a) **(b)**

Figure 4.27: The same as in Figure 4.26, but for the operators $\mathcal{O}_{tB}$ and $\mathcal{O}_{tW}$.

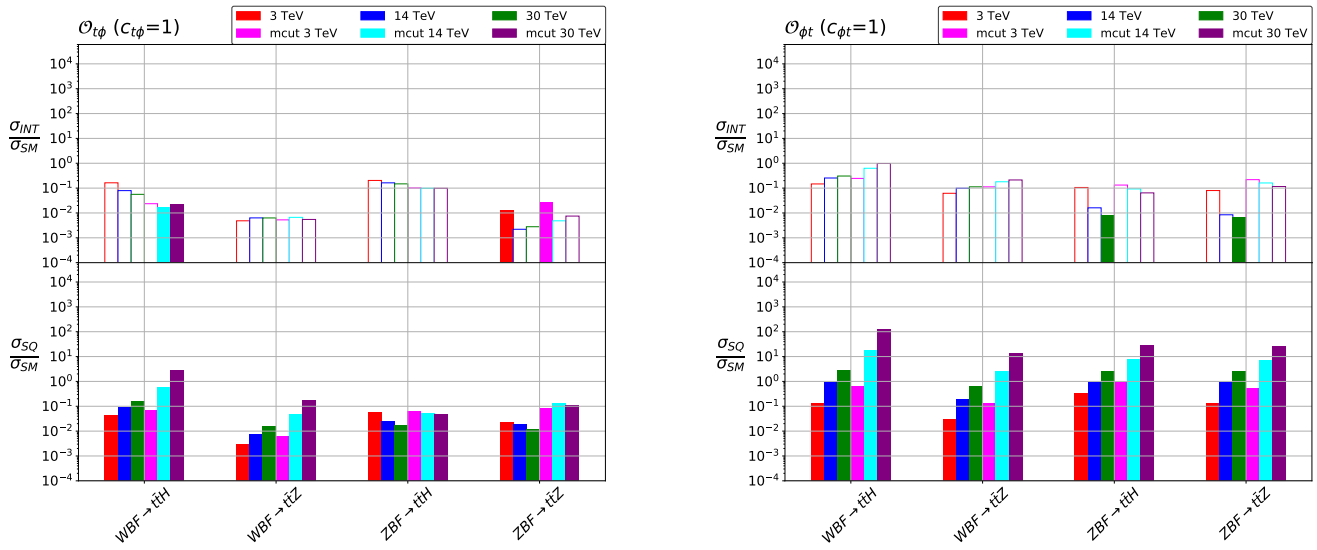

(a) **(b)**

Figure 4.28: The same as in Figure 4.26, but for the operators $\mathcal{O}_{t\phi}$ and $\mathcal{O}_{\phi t}$.

	$\mathcal{O}_{\phi\mathcal{D}}$	$\mathcal{O}_{\phi d}$	$\mathcal{O}_{\phi BB}$	$\mathcal{O}_{\phi W}$	$\mathcal{O}_{\phi WB}$	$\mathcal{O}_{W}$	$\mathcal{O}_{t\phi}$	$\mathcal{O}_{tB}$	$\mathcal{O}_{tW}$	$\mathcal{O}_{\phi Q}^{(1)}$	$\mathcal{O}_{\phi Q}^{(3)}$	$\mathcal{O}_{\phi t}$	$\mathcal{O}_{\phi tb}$
$bW \to tZ$	E	–	–	–	E	E^2	–	E^2	E^2	E	E^2	E	E^2
$bW \to t\gamma$	–	–	–	–	E	E^2	–	E^2	E^2	–	–	–	–
$bW \to th$	–	–	–	E	–	–	E	–	E^2	–	E^2	–	E^2
$tW \to tW$	E	E	–	E	E	E^2	E	E	E^2	E^2	E^2	E^2	–
$tZ \to tZ$	E	E	E	E	E	–	E	E^2	E^2	E	E	E	–
$tZ \to t\gamma$	–	–	E	E	E	–	–	E^2	E^2	–	E	–	–
$t\gamma \to t\gamma$	–	–	E	E	E	–	–	E	E	–	–	–	–
$tZ \to th$	E	–	E	E	E	–	E	E^2	E^2	E^2	E^2	E^2	–
$t\gamma \to th$	–	–	E	E	E	–	–	E^2	E^2	–	–	–	–
$th \to th$	E	E	–	–	–	–	E	–	–	–	–	–	–

Table 4.6: Maximal energy growths induced by each operator on the set of scattering amplitudes considered in [32]. "–" denotes either no contribution or no energy growth and the red entries denote the fact that the interference between the SMEFT and the SM amplitudes also grows with energy.

	$\mathcal{O}_{\phi\mathcal{D}}$	$\mathcal{O}_{\phi d}$	$\mathcal{O}_{\phi BB}$	$\mathcal{O}_{\phi W}$	$\mathcal{O}_{\phi WB}$	$\mathcal{O}_{W}$	$\mathcal{O}_{t\phi}$	$\mathcal{O}_{tB}$	$\mathcal{O}_{tW}$	$\mathcal{O}_{\phi Q}^{(1)}$	$\mathcal{O}_{\phi Q}^{(3)}$	$\mathcal{O}_{\phi t}$	$\mathcal{O}_{\phi}$
$WW \to HHH$	E^2	E^2	–	E^2	–	–	–	–	–	–	–	–	E
$ZZ \to HHH$	E^2	E^2	–	E^2	–	–	–	–	–	–	–	–	E
$WW \to HHZ$	E^2	E^2	E^2	E^2	E^2	E^2	–	–	–	–	–	–	–
$WW \to WWH$	E^2	E^2	E	E^2	E^2	E^2	–	–	–	–	–	–	E
$WW \to WWZ$	E^2	E^2	E^2	E^2	E^2	E^2	–	–	–	–	–	–	–
$WW \to ZZH$	E^2	E^2	E^2	E^2	E^2	E^2	–	–	–	–	–	–	E
$WW \to ZZZ$	E^2	E^2	E^2	E^2	E^2	E^2	–	–	–	–	–	–	–
$WW \to t\bar{t}H$	E^2	E^2	E^2	E^2	E^2	E^2	E^2	E^2	E^2	E^2	E^2	E^2	–
$WW \to t\bar{t}Z$	E^2	E^2	E^2	E^2	E^2	E^2	E^2	E^2	E^2	E^2	E^2	E^2	–
$ZZ \to t\bar{t}H$	E^2	E^2	E^2	E^2	E^2	E^2	E^2	E^2	E^2	E^2	E^2	E^2	–
$ZZ \to t\bar{t}Z$	E^2	E^2	E^2	E^2	E^2	E^2	E^2	E^2	E^2	E^2	E^2	E^2	–

Table 4.7: Maximal energy growths with respect to the SM induced by each operator on the set of scattering amplitudes considered in this work. "–" denotes either no contribution or no energy behaviour violating tree-unitarity, while the red entries denote the fact that the interference between the SMEFT and the SM amplitudes also exhibit a relative energy growth with respect to the SM.

4.5.4 Comparison with previous work

In this paragraph, some obtained results are compared with those of the 2 to 2 processes studied in [32] in order to see whether more sensitivity can be gained by employing the processes here considered.
Hereafter the processes studied in [32] are reported in the summary table Tab. 4.6, while in Tab. 4.7 analogous results are reported for the processes of this work.
As one can see, the two tables have a completely different aspect, but before comparing them it is useful to do the following remark: in Table 4.7 the maximal absolute growths of the operators among the helicity amplitudes of a process is reported, while in Table 4.6 the relative growths of the maximal energy behaviour of the operators among the helicity amplitudes of a process with respect to the maximal SM energy behaviour appear. It

is important to remark this, since it would have been possible to report the absolute maximal energy behaviour also in Table 4.7 and using the tree-unitarity argument for the 2 to 3 processes to mark in red the maximal absolute behaviours which imply tree-unitarity violation even in the interference term. In the 2 to 2 case, instead, using the relative energy growth with respect to the SM is equivalent to the use of the absolute growth, since from tree-unitarity the SM ampltudes can behave at most as a constant at high-energies.
After this long remark, it is possible to proceed with the two tables comparison. It is possible to see that in Tab. 4.6 the cases where also the interference term violates tree-unitarity are rather rare, while in Tab. 4.7 this seems to be rather common. How to interpret this result? could it have been expected?
If one reads with attention the article [32], one will notice that the interference terms of the black coloured energy growth, behave almost always as a constant. The same happens (cfr. Appendix B) for the interference terms related to the behaviours of Tab. 4.7. From this, it seems rather common that the most frequent dominant high-energy behaviour of the interference term between SM and SMEFT is a constant behaviour with the energy. However, the key point is to compare this behaviour with the maximal SM one, which is a constant for a 2 to 2 scattering amplitude, while it is E^{-1} for a 2 to 3 scattering amplitude (owing to tree-unitarity, see Section 3.1.1). Therefore when dividing a constant interference term for the maximal SM behaviour, no relative energy growth is present in the 2 to 2 case, while there is clearly one in the 2 to 3 case.
Since the relative energy growth with respect to the SM is connected to tree-unitarity violating behaviour, it is worthy asking why those behaviours are so in the 2 to 3 case, even at interference level. There may be several motivations for this. The first one is the complexity of a 2 to 3 process with respect to a 2 to 2 one: more particles are involved and the number of Feynman diagram grows of a factor 10 already at the tree-level (considering the SM ones only). This complexity grows much more when one includes also the dimension six operators of the SMEFT: with fixed particles kinds, an operator which does not contribute significantly to a 2 to 2 process can do it for a 2 to 3 process. The examples one can do from these two tables, are the comparison between the operators involved in the $tZ \to tZ$ process and the $ZZ \to t\bar{t}Z$ or between $tZ \to tH$ process and the $ZZ \to t\bar{t}H$ (in the first case only Z boson and the top quark are involved, while in the second case also the Higgs boson appears). It is possible to see that the operator $\mathcal{O}_W$ is not involved at the amplitude level in the 2 to 2 case, while it is in the 2 to 3 case (the same holds for the $\mathcal{O}_{\phi d}$ for the two processes where also the Higgs is involved).
Another important point in the 2 to 3 case is the reduction of vev insertions number in a diagram. This is especially relevant for contact term diagrams which play an important role in spoiling unitarity cancellations of the SM. If one excludes the $\mathcal{O}_\phi$ contact term which still can have a vev insertion in a very rare five Higgs boson scattering, all other operators are very unlikely to exhibit any vev insertion in a five points contact term,

being in this way maximally energy-growing (cfr. Section 4.1).
This is an important point for future studies of this kind. One could, as example, study a 2 to 4 and 2 to 5 scattering amplitudes, but this would be a very demanding work, since the complexity of the processes grows such rapidly and their cross sections would be very small. However, if it is possible to show that beyond the 2 to 3 case (excluding $\mathcal{O}_\phi$) the sensitivity of the processes to a unitarity-violating behaviour of a given operator cannot be further improved (as it seems to be), one can avoid doing those studies and stopping to the 2 to 2 and the 2 to 3 case.

Conclusions

In this conclusive section, the work done is briefly summarised and the main results highlighted.
In Chapter 1, some basic concepts such as spontaneous symmetry breaking and the Higgs mechanism have been presented and applied in order to build the standard model lagrangian, underlining the main points of this procedure. It concludes with the question of the existence of new physics beyond the standard model and the main open problems facing the standard model.
In Chapter 2, the "no-lose theorems" which ensured historic discoveries in particle physics were introduced. However, the main topic of the chapter were effective field theories, whose philosophy and main procedure methods have been highlighted with some applications. At the end of the chapter the standard model effective field theory is introduced and the 2499 dimension six operators presented together with some phenomenological implications.
In Chapter 3, some advanced concepts connected to the standard model have been illustrated, in order to better understand what has been done in Chapter 4. In the first section the ξ gauge and the tree-level unitarity have been shown together with the intricate cancellations in the SM scattering amplitudes needed in order to preserve the unitarity. In the second section, the Goldstone boson equivalence theorem, which connects the longitudinally polarised gauge vector bosons to the Goldstone bosons of the theory, has been derived. Finally, in the third section, an application of the previously introduced concepts has been presented in the case of the fully longitudinal WW scattering.
In the first section of Chapter 4, the 2 to 3 scattering processes and the operators studied were introduced, together with the intention of focusing on the interactions among the bosons of the electroweak sector and the top-quark and to look for processes which could better constrain the Wilson's coefficients considered.
Starting from the 2 to 2 scattering processes studied in [32], some helicity selection rules for the SM helicity amplitudes were found and tested in the 2 to 2 case. These rules apply also to the 2 to 3 case in the SM, provided that constrains from tree-unitarity are included when one evaluate the minimal energy suppression of an helicity amplitude.It was found that not all of the same rules could be applied in the SMEFT case, even if

some similar patterns have been observed. This is somehow expected, since new Lorentz structures appear, together with contact terms which give helpful indications of where to find maximum energy growth.
Next, the helicity amplitude structure of eleven 2 to 3 scattering processes was studied looking for unitarity-violating behaviours at high-energies. It was observed that the occurrence of this behaviours is more frequent in the 2 to 3 studied processes than in the 2 to 2 case, probably due to the higher number of diagrams involved in each process.
The main features, advantages and perspectives of employing lepton colliders in the next colliders generation in order to study better the electroweak sector and the top-quark have been highlighted. After that, the previously analysed processes have been embedded in different muon collider processes and a naive sensitivity study to the various operators has been performed at 3, 14 and 30 TeV center of mass energy. Also a crude estimate of a possible improvement in the Wilson's coefficients constrains of the operators has been presented, with encouraging perspectives.
The analysis has shown that, among the processes considered, the ZZ fusion ones are more sensitive to the operators, but unfortunately they are not accessible (at least considering the SM contribution) even to a future muon collider. Nonetheless, these processes can still be used to improve the constrains over the Wilson's coefficients. Moreover, considering the estimates over the improvements of the Wilson's coefficients constrains, it seems that it may be possible to improve the constrains over those corresponding to every top-quark operator which has been considered. In some cases, it may be possible to improve those constrains also for some purely bosonic operators like $\mathcal{O}_\phi$, $\mathcal{O}_{\phi d}$ and $\mathcal{O}_W$.
This study can be considered as the generalisation/extension of the very first one considering the 2 to 2 case in [32], following a suggestion also proposed in [51]. Our systematic study can now be employed to consider the most promising and interesting processes in more detail and perform dedicated phenomenology studies. For example, here no background nor decay products were considered. Another interesting line of exploration would also be done in the context of hadron colliders and in particular of a future 100 TeV proton-proton collider ([50]) and then compare the results with those obtained for a future lepton collider. This is left to forthcoming investigations.

Appendix A

Dimension six operator basis in SMEFT

In this Appendix the complete basis of dimension six operators in SMEFT is built following the discussion of [12]. Dimensional analysis together with the requirement of Lorentz and gauge invariance will play an important role for a first classification of the operators. Additionally, Equations of Motion (EOMs) and Fierz identities will be widely used to find independent operators. At the end, one will obtain the set of operators in Tab. 2.1 and Tab. 2.2.

A.1 Bosonic operators

For what concerns purely bosonic operators, one has important constraints from the $SU(2)_L$ structure and Lorenz invariance: the former implies that only an even number of Higgs field can appear in purely bosonic operators, the second limits the appearances of covariant derivatives to an even number.
Looking at the canonical mass dimension of the fields ($[\phi] = 1 = [\mathcal{D}]$, $[X] = 2$) and at the above requirements, it is clear that no dimension five operator is present in the bosonic sector. The dimension six operators instead are collected in the following classes:

$$\left\{X^3, X^2\phi^2, X^2\mathcal{D}^2, X\phi^4, X\mathcal{D}^4, X\phi^2\mathcal{D}^2, \phi^6, \phi^4\mathcal{D}^2, \phi^2\mathcal{D}^4\right\}.$$

One can immediately notice that $X\phi^4$ is empty($X^\mu_\mu = 0$) and can discard $X\mathcal{D}^4$ as well, which is absorbed into the class $X^2\mathcal{D}$ (the field strength tensor is contracted with two covariant derivatives, therefore for symmetry $[\mathcal{D}_\mu, \mathcal{D}_\nu] \propto X_{\mu\nu}$).
Now one uses the EOMs and other restrictions to show that $\phi^2\mathcal{D}^4, \phi^2 X\mathcal{D}^2, X^2\mathcal{D}^2$ operators can be expressed as $X^3, X^2\phi^2, \phi^6, \phi^4\mathcal{D}^2$ or operators with fermions. What are the EOMs which are involved?
By remembering that here one is interested in $O\left(\frac{1}{\Lambda^2}\right)$, the classical SM EOMs can be

used (terms of $O(\frac{1}{\Lambda})$ order generate $O(\frac{1}{\Lambda^3})$ effects and can be discarded).
Then the EOMs are ($j = 1, 2$; $I = 1, 2, 3$; $A = 1, 2, ...8$)

$$(\mathcal{D}_\mu \mathcal{D}^\mu \phi)^j = m^2 \phi^j - \lambda \left(\phi^\dagger \phi\right) \phi^j - \bar{e} \Upsilon_e^\dagger \ell^j + \epsilon^{jk} \bar{q}_k \Upsilon_u u - \bar{d} \Upsilon_d^\dagger q^j \tag{A.1.1}$$

$$(\mathcal{D}_\nu G^{\nu\mu})^A = g_s \left(\bar{q} \gamma^\mu T^A q + \bar{u} \gamma^\mu T^A u + \bar{d} \gamma^\mu T^A d\right) \tag{A.1.2}$$

$$(\mathcal{D}_\nu W^{\nu\mu})^I = \frac{g}{2} \left(\phi^\dagger i \overset{\leftrightarrow}{D^\mu} \phi + \bar{\ell} \gamma^\mu \tau^I \ell + \bar{q} \gamma^\mu \tau^I q\right) \tag{A.1.3}$$

$$\partial_\nu B^{\nu\mu} = g' Y_\phi \phi^\dagger i \overset{\leftrightarrow}{D^\mu} \phi + g' \sum_{\psi \in \{l,e,q,u,d\}} Y_\psi \bar{\psi} \gamma^\mu \psi, \tag{A.1.4}$$

where Y_p is the hypercharge of the particle p, Υ the Yukawa matrices and τ^I the Pauli's matrices.

$\phi^2\mathcal{D}^4$: Discarding four-divergences, one can make all the covariant derivatives act on a single ϕ. If one contracts the Lorentz indices with the Levi-Civita tensor $\epsilon^{\mu\nu\rho\sigma}$, one ends in classes where X appears, discussed in the following. If one contracts two derivatives ($\mathcal{D}^2 \mathcal{D}_\mu \mathcal{D}^\mu \phi$), the EOMs allow to end in the $\phi^4\mathcal{D}^2$ and $\psi^2\phi\mathcal{D}^2$ classes together with dimension four operators times m^2.

$\phi^2 X \mathcal{D}^2$: The dual strength tensor $\tilde{X}$ can appear (so that one can ignore $\epsilon^{\mu\nu\rho\sigma}$ contractions). X must be contracted with covariant derivatives, otherwise one gets null terms. There are three cases:

(i) $X_{\mu\nu} \mathcal{D}^\mu \phi^\dagger \mathcal{D}^\nu \phi$ can be eliminated "by part";

(ii) the two derivative act on a single field $\Rightarrow [\mathcal{D}_\mu, \mathcal{D}_\nu] \propto X_{\mu\nu}$ and one ends in $\phi^2 X^2$;

(iii) $\mathcal{D}^\mu X_{\mu\nu} \phi^\dagger \mathcal{D}^\nu \phi$ can be reduced to $\phi^4\mathcal{D}^2$ and $\psi^2\phi^2\mathcal{D}$ classes using the EOMs for the strength field tensor or Bianchi identities ($\mathcal{D}_\mu \tilde{X}^{\mu\nu} = 0$) for the dual strength tensor case.

$X^2\mathcal{D}^2$: Discarding four-divergences, one can make the two derivatives act on a single X (or $\tilde{X}$). If both derivatives are contracted with the same X, one ends in the X^3 class ($[\mathcal{D}_\mu, \mathcal{D}_\nu] \propto X_{\mu\nu}$). If the derivatives are contracted with two different Xs, one uses again $[\mathcal{D}_\mu, \mathcal{D}_\nu] \propto X_{\mu\nu}$ to create terms proportional to $\mathcal{D}_\mu X^{\mu\nu}$ and can use the EOMs to end into $\phi^2 X \mathcal{D}^2$ and $\psi^2 X \mathcal{D}$ classes. The last case with derivatives contracted each other $X^{\mu\nu} \mathcal{D}^\rho \mathcal{D}_\rho X_{\mu\nu}$ can be reduced to the classes X^3, $\phi^2 X \mathcal{D}^2$, $\psi^2 X \mathcal{D}$ and operator proportional to EOMs by using first the Bianchi Identities $\mathcal{D}_{[\rho} X_{\mu\nu]} = 0$ and next the EOMs.

Now one has to show that the remaining bosonic operator classes $X^3, X^2\phi^2, \phi^6, \phi^4\mathcal{D}^2$ form a complete basis for the boson operators.

X^3: Allowing the presence of dual tensors, the only non vanishing and independent Lorentz contraction involves three different strength field tensor $X^\nu_\mu Y^\rho_\nu Z^\mu_\rho$ (by "different", one here means also that $Y = \tilde{X}$ produces a vanishing term). The only gauge singlet combinations can be obtained only by using the $SU(2)_L$ and $SU(3)_C$ structure constants and one gets the operators in Tab. 2.1.

$X^2\phi^2$: Owing to the hypercharge invariance, the Higgs field can form only $SU(2)_L$ singlets or triplets as $\phi^\dagger\phi$ or $\phi^\dagger\tau^I\phi$. The possible contractions among field strength tensors which form singlets or triplet of $SU(2)_L$ or singlets of $SU(3)_C$ form the operators in Tab. 2.1.

ϕ^6: In order to get a zero hypercharge operator, one must organise the Higgs fields in the couples $\phi^\dagger\phi$ and consider tensor product of singlets and triplets of $SU(2)_L$. It turns out that the only surviving operator is given by $\left(\phi^\dagger\phi\right)^3$ (because $\epsilon^{IJK}(\phi^\dagger\tau^I\phi)(\phi^\dagger\tau^J\phi)(\phi^\dagger\tau^K\phi) = 0$ and $(\phi^\dagger\tau^I\phi)(\phi^\dagger\tau^I\phi)(\phi^\dagger\phi) = (\phi^\dagger\phi)^3$ because of the Fierz identities $\tau^I_{jk}\tau^I_{mn} = 2\delta_{jn}\delta_{km} - \delta_{jk}\delta_{mn}$).

$\phi^4\mathcal{D}$: The Higgs fields are organised again in couples $\phi^\dagger\phi$ and the covariant derivatives are contracted each other. They must act on two different fields, otherwise one uses EOMs two move to other operator classes. If they act on two (un)conjugated fields, they can be eliminated "by parts". The case where one derivative acts on a ϕ and the other one on a $\phi^\dagger$ implies the existence of only two independent $SU(2)_L$ singlets, which give rise to the following operators:

$$\left(\phi^\dagger\tau^I\phi\right)\left[\left(\mathcal{D}_\mu\phi\right)^\dagger\tau_I\left(\mathcal{D}^\mu\phi\right)\right] = 2\left(\phi^\dagger\mathcal{D}_\mu\phi\right)^*\left(\phi^\dagger\mathcal{D}^\mu\phi\right) - \left(\phi^\dagger\phi\right)\left[\left(\mathcal{D}_\mu\phi\right)^\dagger\left(\mathcal{D}^\mu\phi\right)\right], \quad \text{(A.1.5)}$$

$$\left(\phi^\dagger\phi\right)\left[\left(\mathcal{D}_\mu\phi\right)^\dagger\left(\mathcal{D}^\mu\phi\right)\right] = \frac{1}{2}\left(\phi^\dagger\phi\right)\Box\left(\phi^\dagger\phi\right) + \psi^2\phi^3 + \phi^6 + m^2\phi^4 + E, \quad \text{(A.1.6)}$$

where in the first equation one has used the Fierz identities and in the second the EOM.

A.2 Fermionic operators

Now, one wants to classify the dimension six operators containing fermions. It is useful to split them in two categories: single-fermion-current operators and four-fermions operators. In order to simplify the classification, it emerges that it is better working with left-handed fermion fields: this can be done by using the charge conjugated of the $SU(2)_L$ singlets as fundamental fields. In this way, the fermion fields are $\psi \in \{\ell, e^c, q, u^c, d^c\}$.

A.2.1 Single-fermion-current operators

Up to hermitian conjugation, one has three currents: $\bar{\psi}_1\gamma^\mu\psi_2$, $\psi_1^T C\psi_2$ and $\psi_1^T C\sigma^{\mu\nu}\psi_2$. If one now considers bosonic objects with the right number of Lorentz indices (ignoring $X^\mu{}_\mu = 0$), one gets the operator classes for each current:

$$\begin{aligned} \bar{\psi}_1\gamma^\mu\psi_2 \quad &\longleftrightarrow \quad \left\{X\mathcal{D}, \phi^2\mathcal{D}, \mathcal{D}^3\right\} \\ \psi_1^T C\psi_2 \quad &\longleftrightarrow \quad \left\{\phi^3, \phi\mathcal{D}^2\right\} \\ \psi_1^T C\sigma^{\mu\nu}\psi_2 \quad &\longleftrightarrow \quad \left\{X\phi, \phi\mathcal{D}^2\right\}. \end{aligned} \tag{A.2.1}$$

Before proceeding further, it is useful to collect the EOMs for the fermions:

$$i\not{\mathcal{D}}\ell = \Upsilon_e e\phi \quad i\not{\mathcal{D}}e = \Upsilon_\ell^\dagger \ell\phi^\dagger \quad i\not{\mathcal{D}}q = \Upsilon_u u\tilde{\phi} + \Upsilon_d d\phi \quad i\not{\mathcal{D}}u = \Upsilon_u^\dagger \tilde{\phi}^\dagger q \quad i\not{\mathcal{D}}d = \Upsilon_d^\dagger \phi^\dagger q. \tag{A.2.2}$$

Moreover, the following Dirac-algebra identities will be used:

$$\gamma^\mu\gamma^\nu = g^{\mu\nu} - i\sigma^{\mu\nu} \qquad \gamma^\mu\gamma^\nu\gamma^\rho = g^{\mu\nu}\gamma^\rho - g^{\mu\rho}\gamma^\nu + g^{\rho\nu}\gamma^\mu - i\epsilon^{\mu\nu\rho\sigma}\gamma_\sigma\gamma_5. \tag{A.2.3}$$

Before starting the analysis, one last observation: in the scalar and tensorial currents cases, the Higgs field number is always odd. This means that these two currents must form isospin doublets. Concerning the vectorial currents, only even numbers of Higgs fields appear. Consequently, these currents will form only isospin singlets or triplets. Now one discusses the six operator classes found above.

$\psi^2\mathcal{D}^3$: This operator class contains vector currents. "By parts" and by choosing a specifical order for the derivatives, one can always get $\bar{\psi}\mathcal{D}_\mu\mathcal{D}^\mu\not{\mathcal{D}}\psi$. By using the EOMs, one ends in the $\psi^2\phi\mathcal{D}^2$ operator class.

$\psi^2\phi\mathcal{D}^2$: This operator class involves scalar and tensor currents. "By parts" one can make no derivative act on $\bar{\psi}$. One immediately notices that $\mathcal{D}_\mu\mathcal{D}_\nu\phi\bar{\psi}\sigma^{\mu\nu}\psi$ and $\phi\bar{\psi}\sigma^{\mu\nu}\mathcal{D}_\mu\mathcal{D}_\nu\psi$ belong to the $\psi^2 X\phi$ class operator (as usual because $[\mathcal{D}_\mu, \mathcal{D}_\nu] \propto X_{\mu\nu}$). Four cases have to be treated by using EOMs and some Dirac's algebra: $(\mathcal{D}_\mu\mathcal{D}^\mu\phi)\bar{\psi}\psi$, $\phi\bar{\psi}\mathcal{D}_\mu\mathcal{D}^\mu\psi$, $(\mathcal{D}_\mu\phi)\bar{\psi}\sigma^{\mu\nu}\mathcal{D}_\nu\psi$ and $(\mathcal{D}_\mu\phi)\bar{\psi}\mathcal{D}_\mu\psi$.

$$
\begin{aligned}
(\mathcal{D}_\mu\mathcal{D}^\mu\phi)\bar\psi\psi &\overset{(A.1.1)}{\sim} \psi^4+\psi^2\phi^3+m^2\psi^2\phi+E;\\
\phi\bar\psi\mathcal{D}_\mu\mathcal{D}^\mu\psi &\overset{(A.2.3)}{\sim} \phi\bar\psi\not{\mathcal{D}}\not{\mathcal{D}}\psi+\psi^2X\phi \overset{(A.2.2)}{\sim} \psi^2X\phi+\psi^2\phi^2\mathcal{D}+E;\\
(\mathcal{D}_\mu\phi)\bar\psi\sigma^{\mu\nu}\mathcal{D}_\nu\psi &= \frac{i}{2}(\mathcal{D}_\mu\phi)\bar\psi(\gamma^\mu\not{\mathcal{D}}-\not{\mathcal{D}}\gamma^\mu)\psi = i(\mathcal{D}_\mu\phi)\bar\psi\gamma^\mu\not{\mathcal{D}}\psi-i(\mathcal{D}_\mu\phi)\bar\psi\mathcal{D}^\mu\psi \overset{(A.2.2)}{\sim}\\
&\overset{(A.2.2)}{\sim} -i(\mathcal{D}^\mu\phi)\bar\psi\mathcal{D}_\mu\psi+\psi^2\phi^2\mathcal{D}+E;\\
2(\mathcal{D}_\mu\phi)\bar\psi\mathcal{D}^\mu\psi &= (\mathcal{D}_\mu\phi)\bar\psi(\gamma^\mu\not{\mathcal{D}}+\not{\mathcal{D}}\gamma^\mu)\psi \overset{Leib.}{=}\\
&\overset{Leib.}{=} (\mathcal{D}_\mu\phi)\bar\psi\gamma^\mu\not{\mathcal{D}}\psi-(\mathcal{D}_\mu\phi)\bar\psi\overleftarrow{\not{\mathcal{D}}}\gamma^\mu\psi-\bar\psi\gamma^\nu\gamma^\mu\psi\mathcal{D}_\nu\mathcal{D}_\mu\phi+T \overset{EOMs}{\sim}\\
&\overset{EOMs}{\sim} \psi^2\phi^2\mathcal{D}+\psi^4+\psi^2\phi^3+m^2\psi^2\phi+\psi^2X\phi+E+T,
\end{aligned}
$$

where E and T are respectively operators proportional to EOMs and total derivatives.

$\psi^2X\mathcal{D}$: This operator class appears only for vector currents. The derivative is contracted with X or $\tilde X$. Moreover if the derivative acts on X ($\tilde X$), one can use the EOMs for the field strength tensor (or the Bianchi Identities for the dual one) to pass to the classes $\psi^2\phi^2\mathcal{D}$ and ψ^4. The other possibility is the action of the derivative over ψ. In this case

$$
X_{\mu\nu}\bar\psi\gamma^\mu\mathcal{D}^\nu\psi = \frac{1}{2}X_{\mu\nu}\bar\psi(\gamma^\mu\gamma^\nu\not{\mathcal{D}}+\gamma^\mu\not{\mathcal{D}}\gamma^\nu)\psi = \frac{1}{2}(\gamma^\mu\gamma\nu\not{\mathcal{D}}-\not{\mathcal{D}}\gamma^\mu\gamma^\nu)\psi+X_{\mu\nu}\bar\psi\gamma^\nu\mathcal{D}^\mu\psi.
$$

The last term is the term on the l.h.s. but with opposite sign. Therefore one gets

$$
\begin{aligned}
X_{\mu\nu}\bar\psi\gamma^\mu\mathcal{D}^\nu\psi = \frac{1}{4}X_{\mu\nu}\bar\psi\gamma^\mu\mathcal{D}^\nu\psi &\overset{Leib.}{=} \frac{1}{4}(X_{\mu\nu}\bar\psi\gamma^\mu\gamma^\nu\not{\mathcal{D}}\psi+X_{\mu\nu}\bar\psi\overleftarrow{\not{\mathcal{D}}}\gamma^\mu\gamma^\nu\psi+\mathcal{D}_\rho X_{\mu\nu}\bar\psi\gamma^\rho\gamma^\mu\gamma^\nu\psi)+T\\
&\overset{(A.2.2)}{\sim} \psi^2X\phi+\psi^2\phi^2\mathcal{D}+\psi^4+E+T,
\end{aligned}
$$

where in the last step one has also considered that

$$
\bar\psi\gamma^\rho\gamma^\mu\gamma^\nu\psi\mathcal{D}_\rho X_{\mu\nu} = 2\bar\psi\gamma^\mu\psi\mathcal{D}^\rho X_{\mu\nu}-i\epsilon_{\rho\mu\nu\rho}\bar\psi\gamma^\sigma\gamma_5\psi\mathcal{D}^\rho X_{\mu\nu}\sim\psi^2\phi\mathcal{D}+\psi^4+E,
$$

thanks to Dirac's algebra and EOMs and Bianchi identities for the field strength tensor.

$\psi^2\phi^3$: This operator class is associated with scalar currents. The scalar current $\psi_1^TC\psi_2$ must be an isospin doublet and a colour singlet like $\bar\psi_1\psi_2$. Moreover, the number of (un)conjugated Higgs fields ϕ is fixed by means of hypercharge constraints. The combination of the scalar fields in isospin doublets is unique, since the combination $\phi^\dagger\tilde\phi=0$. As a consequence, the only possibility for this class operator is to be a Yukawa term multiplied by $\phi^\dagger\phi$.

$\psi^2 X\phi$: This operator class contains tensor currents. The tensor current must be an isospin doublet of the form $\bar{\psi}_1\sigma^{\mu\nu}\psi_2$ because of the antisymmetry of X and the single Higgs field presence. Moreover, a combination with null hypercharge can be obtained only if the Higgs field couples with the currents like in the Yukawa case. In the case of $W^I_{\mu\nu}$ and $G^A_{\mu\nu}$, these two must be combined with isospin triplets and colour octects as shown in Table 2.2. Replacing strength field tensors with their duals would not change anything thanks to the identities $\epsilon_{\mu\nu\rho\sigma}\sigma^{\rho\sigma} = 2i\sigma_{\mu\nu}\gamma_5$ and $\gamma_5\psi_{L/R} = \mp\psi_{L/R}$.

$\psi^2\phi^2\mathcal{D}$: This operator involves only vector currents. If the derivative acts over a fermion field, it is easy to see that one ends in the $\psi^2\phi^3$ class by using the EOMs. Therefore one analyses when the derivative acts over a Higgs field. The Higgs fields can be isospin singlets or triplets and colour singlet, so must be the current as well. Hypercharge constrains imply how many (un)conjugated Higgs fields appear. "By parts" one can form isospin singlets and triplets through ϕ_1 and $\mathcal{D}_\mu\phi_2$ products and a precise structure is obtained according to the structure of fermion currents. Requiring hermiticity, one has finally the operators in Tab. 2.2.

This ends the classification of single-fermion-current operator. Now only the four-fermion operators are left.

A.2.2 Four-fermion operators

Despite their high number, the classification of four-fermion operators is the easiest one. Once again one starts working with only left-handed fermions. Combination such as $\bar{\psi}\psi\psi\psi$ and $\bar{\psi}\bar{\psi}\bar{\psi}\psi$ are not allowed by Lorentz singlets products of the currents previously used. Looking for relevant null hypercharge possibilities, one ends with the following operators (also trivial products of two zero hypercharge currents can be found):

$$\left\{\bar{\ell}\bar{e}^c d^c q,\ q u^c q d^c,\ \ell e^c q u^c,\ qqq\ell,\ d^c u^c u^c e^c,\ qq\bar{u}^c\bar{e}^c,\ q\ell\bar{u}^c\bar{d}^c\right\},$$

and their Hermitian conjugated. The last four of them do not conserve the Baryon number.
Operators with equal number of ψ and $\bar{\psi}$ are organised in product of currents $\bar{\psi}_L\gamma^\mu\psi_L$, which result in to an overall $SU(2)_L$ singlets. As far as $SU(3)_C$ is concerned, one has only one colour singlet $3\otimes\bar{3}$ for non B-violating operators and a singlet $3\otimes 3\otimes 3$ for B-violating ones. Turning back to the usual notation with $SU(2)_L$ right-handed singlets, one find the operators Q_{ledq}, Q_{duq}, Q_{qqu} in Tab. 2.2.
Now, only the four left-handed ψ operators have to be analysed. One can pair the fermions in products of scalar and tensor currents. A simplification can be done by using the following Fierz identities for the tensor currents:

$$\left(\psi^T_{1L}C\sigma^{\mu\nu}\psi_{2L}\right)\left(\psi^T_{3L}C\sigma_{\mu\nu}\psi_{4L}\right) = -4\left(\psi^T_{1L}C\psi_{2L}\right)\left(\psi^T_{3L}C\psi_{4L}\right) - 8\left(\psi^T_{1L}C\psi_{4L}\right)\left(\psi^T_{3L}C\psi_{2L}\right).$$

Once the fields are paired into currents, one can determine possible isospin and colour contractions.
This allows to find a basis for operators which cannot be written as a product of zero hypercharge currents, i.e. the classes $(\bar{L}R)(\bar{R}L)$, $(\bar{L}R)(\bar{L}R)$ and B-violating in Tab. 2.2. Similarly, one gets the operators classes $(\bar{L}L)(\bar{L}L)$, $(\bar{R}R)(\bar{R}R)$ and $(\bar{L}L)(\bar{R}R)$.
One could now show that those operators form a complete basis for the various classes. Essentially, one considers the product of currents which form isospin singlets or triplets and colour singlets or octects and eliminates many of them by using the Fierz identities for $SU(2)_L$ and $SU(3)_C$.

$$\tau^I_{jk}\tau^I_{mn} = 2\delta_{jn}\delta_{mk} - \delta_{jk}\delta_{mn}, \qquad T^A_{\alpha\beta}T^A_{\kappa\gamma} = \frac{1}{2}\delta_{\alpha\gamma}\delta_{\kappa\beta} - \frac{1}{6}\delta_{\alpha\beta}\delta_{\kappa\gamma} \tag{A.2.4}$$

In this way, one can show that:

$$\left(\bar{u}\gamma_\mu T^A u\right)\left(\bar{u}T^A\gamma^\mu u\right) = \frac{1}{2}\mathcal{O}^{ptsr}_{uu} - \frac{1}{6}\mathcal{O}^{prst}_{uu} \tag{A.2.5}$$

$$\left(\bar{d}\gamma_\mu T^A d\right)\left(\bar{d}T^A\gamma^\mu d\right) = \frac{1}{2}\mathcal{O}^{ptsr}_{dd} - \frac{1}{6}\mathcal{O}^{prst}_{dd} \tag{A.2.6}$$

$$\left(\bar{q}\gamma_\mu T^A q\right)\left(\bar{q}T^A\gamma^\mu q\right) = \frac{1}{4}\mathcal{O}^{(3)ptsr}_{qq} + \frac{1}{4}\mathcal{O}^{(1)ptsr}_{qq} - \frac{1}{6}\mathcal{O}^{(1)prst}_{qq} \tag{A.2.7}$$

$$\left(\bar{q}\gamma_\mu T^A \tau^I q\right)\left(\bar{q}T^A\tau_I\gamma^\mu q\right) = -\frac{1}{4}\mathcal{O}^{(3)ptsr}_{qq} + \frac{3}{4}\mathcal{O}^{(1)ptsr}_{qq} - \frac{1}{6}\mathcal{O}^{(3)prst}_{qq} \tag{A.2.8}$$

This ends the classification of the 59 dimension six operators in the SMEFT.

Appendix B

Helicity tables

In this Appendix the helicity tables of the processes studied in Chapter 4 are presented and some more detail about the phase space parameterisation is illustrated.

B.1 Phase space parametrisation

The helicity amplitudes have been computed using the following explicit parameterisation of spinor and polarisation vectors

$$u_+(p) = \sqrt{E_p+m}\left(\cos\tfrac{\theta}{2},\ e^{i\varphi}\sin\tfrac{\theta}{2},\ \tfrac{p_z}{E_p+m}\cos\tfrac{\theta}{2},\ e^{i\varphi}\tfrac{p_z}{E_p+m}\sin\tfrac{\theta}{2}\right), \tag{B.1.1}$$

$$u_-(p) = \sqrt{E_p+m}\left(-\sin\tfrac{\theta}{2},\ e^{i\varphi}\cos\tfrac{\theta}{2},\ \tfrac{p_z}{E_p+m}\sin\tfrac{\theta}{2},\ -e^{i\varphi}\tfrac{p_z}{E_p+m}\cos\tfrac{\theta}{2}\right), \tag{B.1.2}$$

$$v_+(p) = \sqrt{E_p+m}\left(\tfrac{p_z}{E_p+m}\sin\tfrac{\theta}{2},\ -e^{i\varphi}\tfrac{p_z}{E_p+m}\cos\tfrac{\theta}{2},\ \sin\tfrac{\theta}{2},\ e^{-i\varphi}\cos\tfrac{\theta}{2}\right), \tag{B.1.3}$$

$$v_-(p) = \sqrt{E_p+m}\left(\tfrac{p_z}{E_p+m}\cos\tfrac{\theta}{2},\ e^{i\varphi}\tfrac{p_z}{E_p+m}\sin\tfrac{\theta}{2},\ \cos\tfrac{\theta}{2},\ e^{i\varphi}\sin\tfrac{\theta}{2}\right) \tag{B.1.4}$$

$$\epsilon_0^\mu = \left(\frac{|\vec{p}|}{M}, \frac{E\hat{p}}{M}\right) = \left(\frac{|\vec{p}|}{M}, \frac{E}{M}\sin\theta\cos\varphi, \frac{E}{M}\sin\theta\sin\varphi, \frac{E}{M}cos\theta\right), \tag{B.1.5}$$

$$\epsilon_\pm^\mu = \frac{1}{\sqrt{2}}\left(0,\ \cos\varphi\cos\theta \mp i\sin\varphi,\ \sin\varphi\cos\theta \pm i\cos\varphi,\ -\sin\theta\right), \tag{B.1.6}$$

where m, M, E and $\vec{p}$ are the particles masses, energy and 3-momentum, while θ is the polar angle between the z-axis and $\vec{p}$ and ϕ azimuthal angle in the x-y plan. The z-axis has been chosen along the direction of one of the two incoming particle in the center of mass frame $2 \to 3$. u and v are the eigenspinors of the helicity operator, labelled by their eigenvalues, while $\epsilon_\pm$ and ϵ are the left/right-handed and longitudinal polarisation vectors.

The configuration studied is the one where the three particles in the final state have a relative angle of $\frac{2}{3}\pi$ each other and therefore their momenta modula are the same and the energy only energy dependence is the center of mass energy.
Starting from the configuration where the three final state particle are in on the x-y plan with one moving along the y-axis, the studied one is reached by rotating the final state particle plan by $-\frac{\pi}{4}$ around the x-axis.
The results are presented in table form, containing the SM prediction and the contribution of each operator from Table 4.2 that displays at least one configuration that grows with energy. Only the center of mass energy dependence up to a constant is kept and it is labelled with E, while a constant behaviour with the energy is indicated with E^0.

B.2 Helicity tables

λ_W, λ_W	SM	$\mathcal{O}_\phi$	$\mathcal{O}_{\phi W}$	$\mathcal{O}_{\phi d}$	$\mathcal{O}_{\phi D}$
$\pm\ \mp$	E^{-2}	–	E^0	E^0	E^0
$\pm\ 0$	E^{-1}	–	E^1	E^1	E^1
$\pm\ \pm$	E^{-2}	–	E^0	E^0	E^0
$0\ \mp$	E^{-1}	–	E^1	E^1	E^1
$0\ 0$	E^{-2}	E^0	E^0	E^0	E^0

Table B.1: Helicity amplitudes in the high-energy limit ($s >> v$) for $W^+W^- \to HHH$.

λ_Z, λ_Z	SM	$\mathcal{O}_\phi$	$\mathcal{O}_{\phi W}$	$\mathcal{O}_{\phi WB}$	$\mathcal{O}_{\phi BB}$	$\mathcal{O}_{\phi d}$	$\mathcal{O}_{\phi D}$
$\mp\ \mp$	E^{-2}	–	E^0	E^0	E^0	E^0	E^0
$\mp\ 0$	E^{-1}	–	E^1	E^1	E^1	E^1	E^1
$\mp\ \pm$	E^{-2}	–	E^0	E^0	E^0	E^0	E^0
$0\ \mp$	E^{-1}	–	E^1	E^1	E^1	E^1	E^1
$0\ 0$	E^{-2}	E^0	E^0	E^0	E^0	E^0	E^0

Table B.2: Helicity amplitudes in the high-energy limit ($s >> v$) for $ZZ \to HHH$.

$\lambda_W, \lambda_W, \lambda_Z$	SM	$\mathcal{O}_{\phi W}$	$\mathcal{O}_{\phi WB}$	$\mathcal{O}_{\phi BB}$	$\mathcal{O}_{\phi d}$	$\mathcal{O}_{\phi D}$	$\mathcal{O}_W$
$+\ -\ -$	E^{-1}	E^1	E^1	–	–	–	E^1
$+\ -\ 0$	E^{-2}	E^0	–	–	E^0	E^0	E^0
$+\ -\ +$	E^{-1}	E^1	E^1	–	–	–	E^1
$+\ 0\ -$	E^{-2}	E^0	E^0	E^0	E^0	E^0	E^0
$+\ 0\ 0$	E^{-1}	E^1	E^1	–	E^1	E^1	E^1
$+\ 0\ +$	E^{-2}	E^0	E^0	E^0	E^0	E^0	E^0
$+\ +\ -$	E^{-3}	E^1	E^1	–	–	–	E^1
$+\ +\ 0$	E^{-2}	E^0	E^0	–	–	E^0	E^0
$+\ +\ +$	E^{-1}	E^1	–	–	–	–	E^1
$0\ -\ -$	E^{-2}	E^0	E^0	E^0	E^0	E^0	E^0
$0\ -\ 0$	E^{-1}	E^1	E^1	–	E^1	E^1	E^1
$0\ -\ +$	E^{-2}	E^0	E^0	E^0	E^0	E^0	E^0
$0\ 0\ -$	E^{-1}	E^1	E^1	E^1	E^1	E^1	–
$0\ 0\ 0$	E^{-2}	E^0	E^0	E^0	E^0	E^0	E^0

Table B.3: Helicity amplitudes in the high-energy limit ($s >> v$) for $W^+W^- \to HHZ$. The missing helicity amplitudes behaviours are obtained by sending $\pm \to \mp$.

$\lambda_W, \lambda_W, \lambda_W, \lambda_W$	SM	$\mathcal{O}_\phi$	$\mathcal{O}_{\phi W}$	$\mathcal{O}_{\phi WB}$	$\mathcal{O}_{\phi BB}$	$\mathcal{O}_{\phi d}$	$\mathcal{O}_{\phi D}$	$\mathcal{O}_W$
$+\,-\,-\,+$	E^{-2}	–	E^0	–	–	–	–	E^0
$+\,-\,-\,0$	E^{-1}	–	E^1	–	–	–	–	E^1
$+\,-\,-\,-$	E^{-2}	–	E^0	–	–	–	–	E^0
$+\,-\,0\,+$	E^{-1}	–	E^1	–	–	–	–	E^1
$+\,-\,0\,0$	E^{-2}	–	E^0	E^0	–	E^0	E^0	E^0
$+\,-\,0\,-$	E^{-1}	–	–	–	–	–	–	E^1
$+\,-\,+\,+$	E^{-2}	–	E^0	–	–	–	–	E^0
$+\,-\,+\,0$	E^{-1}	–	–	–	–	–	–	E^1
$+\,-\,+\,-$	E^{-2}	–	E^0	–	–	–	–	E^0
$+\,0\,-\,+$	E^{-1}	–	E^1	–	–	–	–	E^1
$+\,0\,-\,0$	E^{-2}	–	E^0	E^0	–	E^0	E^0	E^0
$+\,0\,-\,-$	E^{-3}	–	E^1	–	–	–	–	E^1
$+\,0\,0\,+$	E^{-2}	–	E^0	E^0	–	E^0	E^0	E^0
$+\,0\,0\,0$	E^{-1}	–	E^1	E^1	–	E^1	E^1	E^1
$+\,0\,0\,-$	E^{-2}	–	E^0	E^0	–	E^0	E^0	E^0
$+\,0\,+\,+$	E^{-1}	–	E^1	–	–	–	–	E^1
$+\,0\,+\,0$	E^{-2}	–	E^0	E^0	–	E^0	E^0	E^0
$+\,0\,+\,-$	E^{-1}	–	–	–	–	–	–	E^1
$+\,+\,-\,+$	E^{-2}	–	E^0	–	–	–	–	E^0
$+\,+\,-\,0$	E^{-3}	–	E^1	–	–	–	–	E^1
$+\,+\,-\,-$	E^{-4}	–	E^0	–	–	–	–	E^0
$+\,+\,0\,+$	E^{-1}	–	E^1	–	–	–	–	E^1
$+\,+\,0\,0$	E^{-2}	–	E^0	E^0	–	E^0	E^0	E^0
$+\,+\,0\,-$	E^{-3}	–	E^1	–	–	–	–	E^1
$+\,+\,+\,+$	E^{-2}	–	E^0	–	–	–	–	E^0
$+\,+\,+\,0$	E^{-1}	–	E^1	–	–	–	–	E^1
$+\,+\,+\,-$	E^{-2}	–	E^0	–	–	–	–	E^0
$0\,-\,-\,+$	E^{-1}	–	E^1	–	–	–	–	E^1
$0\,-\,-\,0$	E^{-2}	–	E^0	E^0	–	E^0	E^0	E^0
$0\,-\,-\,-$	E^{-1}	–	E^1	–	–	–	–	E^1
$0\,-\,0\,+$	E^{-2}	–	E^0	E^0	–	E^0	E^0	E^0
$0\,-\,0\,0$	E^{-1}	–	E^1	E^1	–	E^1	E^1	E^1
$0\,-\,0\,-$	E^{-2}	–	E^0	E^0	–	E^0	E^0	E^0
$0\,-\,+\,+$	E^{-3}	–	E^1	–	–	–	–	E^1
$0\,-\,+\,0$	E^{-2}	–	E^0	E^0	–	E^0	E^0	E^0
$0\,-\,+\,-$	E^{-1}	–	–	–	–	–	–	E^1
$0\,0\,-\,+$	E^{-2}	–	E^0	E^0	–	E^0	E^0	E^0
$0\,0\,-\,0$	E^{-1}	–	E^1	E^1	–	E^1	E^1	E^1
$0\,0\,-\,-$	E^{-2}	–	E^0	E^0	–	E^0	E^0	E^0
$0\,0\,0\,+$	E^{-1}	–	E^1	E^1	–	E^1	E^1	E^1
$0\,0\,0\,0$	E^{-2}	E^0	E^0	E^0	E^0	E^0	E^0	E^0

Table B.4: Helicity amplitudes in the high-energy limit ($s >> v$) for $W^+W^- \to W^+W^-H$. The missing helicity amplitudes behaviours are obtained by sending $\pm \to \mp$.

$\lambda_W, \lambda_W, \lambda_W, \lambda_W, \lambda_Z$	SM	$\mathcal{O}_{\phi W}$	$\mathcal{O}_{\phi WB}$	$\mathcal{O}_{\phi BB}$	$\mathcal{O}_{\phi d}$	$\mathcal{O}_{\phi D}$	$\mathcal{O}_W$
$+\,-\,-\,+\,-$	E^{-1}	–	–	–	–	–	E^1
$+\,-\,-\,+\,0$	E^{-2}	E^0	–	–	–	–	E^0
$+\,-\,-\,+\,+$	E^{-1}	–	–	–	–	–	E^1
$+\,-\,-\,0\,-$	E^{-2}	E^0	E^0	–	–	–	E^0
$+\,-\,-\,0\,0$	E^{-1}	E^1	–	–	–	–	E^1
$+\,-\,-\,0\,+$	E^{-2}	E^0	E^0	–	–	–	E^0
$+\,-\,-\,-\,-$	E^{-3}	–	–	–	–	–	E^1
$+\,-\,-\,-\,0$	E^{-2}	E^0	–	–	–	–	E^0

$\lambda_W, \lambda_W, \lambda_W, \lambda_W, \lambda_Z$	SM	$\mathcal{O}_{\phi W}$	$\mathcal{O}_{\phi WB}$	$\mathcal{O}_{\phi BB}$	$\mathcal{O}_{\phi d}$	$\mathcal{O}_{\phi D}$	$\mathcal{O}_W$
$+\,-\,-\,-\,+$	E^{-1}	–	–	–	–	–	E^1
$+\,-\,0\,+\,-$	E^{-2}	E^0	E^0	–	–	–	E^0
$+\,-\,0\,+\,0$	E^{-1}	E^1	–	–	–	–	E^1
$+\,-\,0\,+\,+$	E^{-2}	E^0	E^0	–	–	–	E^0
$+\,-\,0\,0\,-$	E^{-1}	E^1	E^1	–	–	–	E^1
$+\,-\,0\,0\,0$	E^{-2}	E^0	E^0	–	E^0	E^0	E^0
$+\,-\,0\,0\,+$	E^{-1}	E^1	E^1	–	–	–	E^1
$+\,-\,0\,-\,-$	E^{-2}	E^0	E^0	–	–	–	E^0
$+\,-\,0\,-\,0$	E^{-1}	–	–	–	–	–	E^1
$+\,-\,0\,-\,+$	E^{-2}	E^0	E^0	–	–	–	E^0
$+\,-\,+\,+\,-$	E^{-1}	–	–	–	–	–	E^1
$+\,-\,+\,+\,0$	E^{-2}	E^0	–	–	–	–	E^0
$+\,-\,+\,+\,+$	E^{-3}	–	–	–	–	–	E^1
$+\,-\,+\,0\,-$	E^{-2}	E^0	E^0	–	–	–	E^0
$+\,-\,+\,0\,0$	E^{-1}	–	–	–	–	–	E^1
$+\,-\,+\,0\,+$	E^{-2}	E^0	E^0	–	–	–	E^0
$+\,-\,+\,-\,-$	E^{-1}	–	–	–	–	–	E^1
$+\,-\,+\,-\,0$	E^{-2}	–	–	–	–	–	E^0
$+\,-\,+\,-\,+$	E^{-1}	–	–	–	–	–	E^1
$+\,0\,-\,+\,-$	E^{-2}	E^0	E^0	–	–	–	E^0
$+\,0\,-\,+\,0$	E^{-1}	E^1	–	–	–	–	E^1
$+\,0\,-\,+\,+$	E^{-2}	E^0	E^0	–	–	–	E^0
$+\,0\,-\,0\,-$	E^{-3}	E^1	E^1	–	–	–	E^1
$+\,0\,-\,0\,0$	E^{-2}	E^0	E^0	–	E^0	E^0	E^0
$+\,0\,-\,0\,+$	E^{-1}	E^1	–	–	–	–	E^1
$+\,0\,-\,-\,-$	E^{-4}	E^0	E^0	–	–	–	E^0
$+\,0\,-\,-\,0$	E^{-3}	E^1	–	–	–	–	E^1
$+\,0\,-\,-\,+$	E^{-2}	E^0	–	–	–	–	E^0
$+\,0\,0\,+\,-$	E^{-3}	–	–	–	–	–	–
$+\,0\,0\,+\,0$	E^{-2}	E^0	E^0	–	E^0	E^0	E^0
$+\,0\,0\,+\,+$	E^{-3}	–	–	–	–	–	–
$+\,0\,0\,0\,-$	E^{-2}	E^0	E^0	E^0	E^0	E^0	E^0
$+\,0\,0\,0\,0$	E^{-1}	E^1	E^1	–	E^1	E^1	E^1
$+\,0\,0\,0\,+$	E^{-2}	E^0	E^0	E^0	E^0	E^0	E^0
$+\,0\,0\,-\,-$	E^{-3}	–	–	–	–	–	–
$+\,0\,0\,-\,0$	E^{-2}	E^0	E^0	–	E^0	E^0	E^0
$+\,0\,0\,-\,+$	E^{-3}	–	–	–	–	–	–
$+\,0\,+\,+\,-$	E^{-2}	E^0	E^0	–	–	–	E^0
$+\,0\,+\,+\,0$	E^{-1}	E^1	–	–	–	–	E^1
$+\,0\,+\,+\,+$	E^{-2}	E^0	E^0	–	–	–	E^0
$+\,0\,+\,0\,-$	E^{-1}	E^1	E^1	–	–	–	E^1
$+\,0\,+\,0\,0$	E^{-2}	E^0	E^0	–	E^0	E^0	E^0
$+\,0\,+\,0\,+$	E^{-1}	E^1	E^1	–	–	–	E^1
$+\,0\,+\,-\,-$	E^{-2}	E^0	E^0	–	–	–	E^0
$+\,0\,+\,-\,0$	E^{-1}	–	–	–	–	–	E^1
$+\,0\,+\,-\,+$	E^{-2}	E^0	E^0	–	–	–	E^0
$+\,+\,-\,+\,-$	E^{-3}	–	–	–	–	–	E^1
$+\,+\,-\,+\,0$	E^{-2}	E^0	–	–	–	–	E^0
$+\,+\,-\,+\,+$	E^{-1}	–	–	–	–	–	E^1
$+\,+\,-\,0\,-$	E^{-4}	E^0	E^0	–	–	–	E^0
$+\,+\,-\,0\,0$	E^{-3}	E^1	–	–	–	–	E^1
$+\,+\,-\,0\,+$	E^{-2}	E^0	–	–	–	–	E^0
$+\,+\,-\,-\,-$	–	–	–	–	–	–	E^1
$+\,+\,-\,-\,0$	E^{-4}	E^0	–	–	–	–	E^0
$+\,+\,-\,-\,+$	E^{-3}	–	–	–	–	–	E^1
$+\,+\,0\,+\,-$	E^{-2}	E^0	E^0	–	–	–	E^0
$+\,+\,0\,+\,0$	E^{-1}	E^1	–	–	–	–	E^1
$+\,+\,0\,+\,+$	E^{-2}	E^0	E^0	–	–	–	E^0
$+\,+\,0\,0\,-$	E^{-3}	E^1	E^1	–	–	–	E^1
$+\,+\,0\,0\,0$	E^{-2}	E^0	E^0	–	E^0	E^0	E^0

$\lambda_W, \lambda_W, \lambda_W, \lambda_W, \lambda_Z$	SM	$\mathcal{O}_{\phi W}$	$\mathcal{O}_{\phi WB}$	$\mathcal{O}_{\phi BB}$	$\mathcal{O}_{\phi d}$	$\mathcal{O}_{\phi D}$	$\mathcal{O}_W$
+ + 0 0 +	E^{-1}	E^1	–	–	–	–	E^1
+ + 0 − −	E^{-4}	E^0	E^0	–	–	–	E^0
+ + 0 − 0	E^{-3}	E^1	–	–	–	–	E^1
+ + 0 − +	E^{-2}	E^0	–	–	–	–	E^0
+ + + + −	E^{-1}	–	–	–	–	–	E^1
+ + + + 0	E^{-2}	–	–	–	–	–	E^0
+ + + + +	E^{-1}	–	–	–	–	–	E^1
+ + + 0 −	E^{-2}	E^0	E^0	–	–	–	E^0
+ + + 0 0	E^{-1}	E^1	–	–	–	–	E^1
+ + + 0 +	E^{-2}	E^0	E^0	–	–	–	E^0
+ + + − −	E^{-3}	–	–	–	–	–	E^1
+ + + − 0	E^{-2}	E^0	–	–	–	–	E^0
+ + + − +	E^{-1}	–	–	–	–	–	E^1
0 − − + −	E^{-2}	E^0	E^0	–	–	–	E^0
0 − − + 0	E^{-1}	E^1	–	–	–	–	E^1
0 − − + +	E^{-2}	E^0	E^0	–	–	–	E^0
0 − − 0 −	E^{-3}	–	–	–	–	–	–
0 − − 0 0	E^{-2}	E^0	E^0	–	E^0	E^0	E^0
0 − − 0 +	E^{-3}	–	–	–	–	–	–
0 − − − −	E^{-2}	E^0	E^0	–	–	–	E^0
0 − − − 0	E^{-1}	E^1	–	–	–	–	E^1
0 − − − +	E^{-2}	E^0	E^0	–	–	–	E^0
0 − 0 + −	E^{-1}	E^1	–	–	–	–	E^1
0 − 0 + 0	E^{-2}	E^0	E^0	–	E^0	E^0	E^0
0 − 0 + +	E^{-3}	E^1	E^1	–	–	–	E^1
0 − 0 0 −	E^{-2}	E^0	E^0	E^0	E^0	E^0	E^0
0 − 0 0 0	E^{-1}	E^1	E^1	–	E^1	E^1	E^1
0 − 0 0 +	E^{-2}	E^0	E^0	E^0	E^0	E^0	E^0
0 − 0 − −	E^{-1}	E^1	E^1	–	–	–	E^1
0 − 0 − 0	E^{-2}	E^0	E^0	–	E^0	E^0	E^0
0 − 0 − +	E^{-1}	E^1	E^1	–	–	–	E^1
0 − + + −	E^{-2}	E^0	–	–	–	–	E^0
0 − + + 0	E^{-3}	E^1	–	–	–	–	E^1
0 − + + +	E^{-4}	E^0	E^0	–	–	–	E^0
0 − + 0 −	E^{-3}	–	–	–	–	–	–
0 − + 0 0	E^{-2}	E^0	E^0	–	E^0	E^0	E^0
0 − + 0 +	E^{-3}	–	–	–	–	–	–
0 − + − −	E^{-2}	E^0	E^0	–	–	–	E^0
0 − + − 0	E^{-1}	–	–	–	–	–	E^1
0 − + − +	E^{-2}	E^0	E^0	–	–	–	E^0
0 0 − + −	E^{-1}	E^1	E^1	–	–	–	E^1
0 0 − + 0	E^{-2}	E^0	E^0	–	E^0	E^0	E^0
0 0 − + +	E^{-1}	E^1	E^1	–	–	–	E^1
0 0 − 0 −	E^{-2}	E^0	E^0	E^0	E^0	E^0	E^0
0 0 − 0 0	E^{-1}	E^1	E^1	–	E^1	E^1	E^1
0 0 − 0 +	E^{-2}	E^0	E^0	E^0	E^0	E^0	E^0
0 0 − − −	E^{-3}	E^1	E^1	–	–	–	E^1
0 0 − − 0	E^{-2}	E^0	E^0	–	E^0	E^0	E^0
0 0 − − +	E^{-1}	E^1	–	–	–	–	E^1
0 0 0 + −	E^{-2}	E^0	E^0	E^0	E^0	E^0	E^0
0 0 0 + 0	E^{-1}	E^1	E^1	–	E^1	E^1	E^1
0 0 0 + +	E^{-2}	E^0	E^0	E^0	E^0	E^0	E^0
0 0 0 0 −	E^{-1}	E^1	–	E^1	E^1	E^1	–
0 0 0 0 0	E^{-2}	E^0	E^0	E^0	E^0	E^0	E^0

Table B.5: Helicity amplitudes in the high-energy limit ($s >> v$) for $W^+W^- \to W^+W^-Z$. The missing helicity amplitudes behaviours are obtained by sending $\pm \to \mp$.

$\lambda_W, \lambda_W, \lambda_Z, \lambda_Z$	SM	$\mathcal{O}_\phi$	$\mathcal{O}_{\phi W}$	$\mathcal{O}_{\phi WB}$	$\mathcal{O}_{\phi BB}$	$\mathcal{O}_{\phi d}$	$\mathcal{O}_{\phi D}$	$\mathcal{O}_W$
$+\,-\,-\,-$	E^{-2}	–	E^0	E^0	E^0	–	–	E^0
$+\,-\,-\,0$	E^{-1}	–	–	E^1	–	–	–	E^1
$+\,-\,-\,+$	E^{-2}	–	E^0	E^0	–	–	–	E^0
$+\,-\,0\,-$	E^{-1}	–	–	E^1	–	–	–	E^1
$+\,-\,0\,0$	E^{-2}	–	E^0	E^0	–	E^0	E^0	E^0
$+\,-\,0\,+$	E^{-1}	–	–	E^1	–	–	–	E^1
$+\,-\,+\,-$	E^{-2}	–	E^0	E^0	–	–	–	E^0
$+\,-\,+\,0$	E^{-1}	–	–	E^1	–	–	–	E^1
$+\,-\,+\,+$	E^{-2}	–	E^0	E^0	E^0	–	–	E^0
$+\,0\,-\,-$	E^{-3}	–	E^1	E^1	E^1	–	–	E^1
$+\,0\,-\,0$	E^{-2}	–	E^0	E^0	E^0	E^0	E^0	E^0
$+\,0\,-\,+$	E^{-1}	–	–	E^1	–	–	–	E^1
$+\,0\,0\,-$	E^{-2}	–	E^0	E^0	E^0	E^0	E^0	E^0
$+\,0\,0\,0$	E^{-1}	–	E^1	E^1	–	E^1	E^1	E^1
$+\,0\,0\,+$	E^{-2}	–	E^0	E^0	E^0	E^0	E^0	E^0
$+\,0\,+\,-$	E^{-1}	–	–	E^1	–	–	–	E^1
$+\,0\,+\,0$	E^{-2}	–	E^0	E^0	E^0	E^0	E^0	E^0
$+\,0\,+\,+$	E^{-1}	–	E^1	E^1	E^1	–	–	E^1
$+\,+\,-\,-$	E^{-4}	–	E^0	E^0	E^0	–	–	E^0
$+\,+\,-\,0$	E^{-3}	–	E^1	E^1	–	–	–	E^1
$+\,+\,-\,+$	E^{-2}	–	E^0	E^0	–	–	–	E^0
$+\,+\,0\,-$	E^{-3}	–	E^1	E^1	–	–	–	E^1
$+\,+\,0\,0$	E^{-2}	–	E^0	E^0	–	E^0	E^0	E^0
$+\,+\,0\,+$	E^{-1}	–	E^1	–	–	–	–	E^1
$+\,+\,+\,-$	E^{-2}	–	E^0	E^0	–	–	–	E^0
$+\,+\,+\,0$	E^{-1}	–	E^1	–	–	–	–	E^1
$+\,+\,+\,+$	E^{-2}	–	E^0	E^0	E^0	–	–	E^0
$0\,-\,-\,-$	E^{-1}	–	E^1	E^1	E^1	–	–	E^1
$0\,-\,-\,0$	E^{-2}	–	E^0	E^0	E^0	E^0	E^0	E^0
$0\,-\,-\,+$	E^{-1}	–	–	E^1	–	–	–	E^1
$0\,-\,0\,-$	E^{-2}	–	E^0	E^0	E^0	E^0	E^0	E^0
$0\,-\,0\,0$	E^{-1}	–	E^1	E^1	–	E^1	E^1	E^1
$0\,-\,0\,+$	E^{-2}	–	E^0	E^0	E^0	E^0	E^0	E^0
$0\,-\,+\,-$	E^{-1}	–	–	E^1	–	–	–	E^1
$0\,-\,+\,0$	E^{-2}	–	E^0	E^0	E^0	E^0	E^0	E^0
$0\,-\,+\,+$	E^{-3}	–	E^1	E^1	E^1	–	–	E^1
$0\,0\,-\,-$	E^{-2}	–	E^0	E^0	E^0	E^0	E^0	E^0
$0\,0\,-\,0$	E^{-1}	–	E^1	E^1	E^1	E^1	E^1	E^1
$0\,0\,-\,+$	E^{-2}	–	E^0	E^0	E^0	E^0	E^0	E^0
$0\,0\,0\,-$	E^{-1}	–	E^1	E^1	E^1	E^1	E^1	E^1
$0\,0\,0\,0$	E^{-2}	E^0	E^0	E^0	–	E^0	E^0	E^0

Table B.6: Helicity amplitudes in the high-energy limit ($s >> v$) for $W^+W^- \to ZZH$. The missing helicity amplitudes behaviours are obtained by sending $\pm \to \mp$.

$\lambda_W, \lambda_W, \lambda_Z, \lambda_Z, \lambda_Z$	SM	$\mathcal{O}_{\phi W}$	$\mathcal{O}_{\phi WB}$	$\mathcal{O}_{\phi BB}$	$\mathcal{O}_{\phi d}$	$\mathcal{O}_{\phi D}$	$\mathcal{O}_W$
$+\,-\,-\,-\,-$	E^{-3}	–	–	–	–	–	E^1
$+\,-\,-\,-\,0$	E^{-2}	E^0	E^0	E^0	–	–	E^0
$+\,-\,-\,-\,+$	E^{-1}	–	–	–	–	–	E^1
$+\,-\,-\,0\,-$	E^{-2}	E^0	E^0	E^0	–	–	E^0
$+\,-\,-\,0\,0$	E^{-1}	E^1	E^1	–	–	–	E^1
$+\,-\,-\,0\,+$	E^{-2}	E^0	E^0	–	–	–	E^0
$+\,-\,-\,+\,-$	E^{-1}	–	–	–	–	–	E^1
$+\,-\,-\,+\,0$	E^{-2}	E^0	E^0	–	–	–	E^0

$\lambda_W, \lambda_W, \lambda_Z, \lambda_Z, \lambda_Z$	SM	$\mathcal{O}_{\phi W}$	$\mathcal{O}_{\phi WB}$	$\mathcal{O}_{\phi BB}$	$\mathcal{O}_{\phi d}$	$\mathcal{O}_{\phi D}$	$\mathcal{O}_W$
$+\,-\,-\,+\,+$	E^{-1}	–	–	–	–	–	E^1
$+\,-\,0\,-\,-$	E^{-2}	E^0	E^0	E^0	–	–	E^0
$+\,-\,0\,-\,0$	E^{-1}	E^1	E^1	–	–	–	E^1
$+\,-\,0\,-\,+$	E^{-2}	E^0	E^0	–	–	–	E^0
$+\,-\,0\,0\,-$	E^{-1}	E^1	E^1	–	–	–	E^1
$+\,-\,0\,0\,0$	E^{-2}	E^0	E^0	–	E^0	E^0	E^0
$+\,-\,0\,0\,+$	E^{-1}	E^1	E^1	–	–	–	E^1
$+\,-\,0\,+\,-$	E^{-2}	E^0	E^0	–	–	–	E^0
$+\,-\,0\,+\,0$	E^{-1}	E^1	E^1	–	–	–	E^1
$+\,-\,0\,+\,+$	E^{-2}	E^0	E^0	E^0	–	–	E^0
$+\,-\,+\,-\,-$	E^{-1}	–	–	–	–	–	E^1
$+\,-\,+\,-\,0$	E^{-2}	E^0	E^0	–	–	–	E^0
$+\,-\,+\,-\,+$	E^{-1}	–	–	–	–	–	E^1
$+\,-\,+\,0\,-$	E^{-2}	E^0	E^0	–	–	–	E^0
$+\,-\,+\,0\,0$	E^{-1}	E^1	E^1	–	–	–	E^1
$+\,-\,+\,0\,+$	E^{-2}	E^0	E^0	E^0	–	–	E^0
$+\,-\,+\,+\,-$	E^{-1}	–	–	–	–	–	E^1
$+\,-\,+\,+\,0$	E^{-2}	E^0	E^0	E^0	–	–	E^0
$+\,-\,+\,+\,+$	E^{-3}	–	–	–	–	–	E^1
$+\,0\,-\,-\,-$	E^{-4}	E^0	E^0	E^0	–	–	E^0
$+\,0\,-\,-\,0$	E^{-3}	E^1	E^1	E^1	–	–	E^1
$+\,0\,-\,-\,+$	E^{-2}	E^0	E^0	E^0	–	–	E^0
$+\,0\,-\,0\,-$	E^{-3}	E^1	E^1	E^1	–	–	E^1
$+\,0\,-\,0\,0$	E^{-2}	E^0	E^0	E^0	E^0	E^0	E^0
$+\,0\,-\,0\,+$	E^{-1}	–	E^1	–	–	–	E^1
$+\,0\,-\,+\,-$	E^{-2}	E^0	E^0	E^0	–	–	E^0
$+\,0\,-\,+\,0$	E^{-1}	–	E^1	–	–	–	E^1
$+\,0\,-\,+\,+$	E^{-2}	E^0	E^0	E^0	–	–	E^0
$+\,0\,0\,-\,-$	E^{-3}	E^1	E^1	E^1	–	–	E^1
$+\,0\,0\,-\,0$	E^{-2}	E^0	E^0	E^0	E^0	E^0	E^0
$+\,0\,0\,-\,+$	E^{-1}	–	E^1	–	–	–	E^1
$+\,0\,0\,0\,-$	E^{-2}	E^0	E^0	E^0	E^0	E^0	E^0
$+\,0\,0\,0\,0$	E^{-1}	E^1	–	–	E^1	E^1	–
$+\,0\,0\,0\,+$	E^{-2}	E^0	E^0	E^0	E^0	E^0	E^0
$+\,0\,0\,+\,-$	E^{-1}	–	E^1	–	–	–	E^1
$+\,0\,0\,+\,0$	E^{-2}	E^0	E^0	E^0	E^0	E^0	E^0
$+\,0\,0\,+\,+$	E^{-1}	E^1	E^1	E^1	–	–	E^1
$+\,0\,+\,-\,-$	E^{-2}	E^0	E^0	E^0	–	–	E^0
$+\,0\,+\,-\,0$	E^{-1}	–	E^1	–	–	–	E^1
$+\,0\,+\,-\,+$	E^{-2}	E^0	E^0	E^0	–	–	E^0
$+\,0\,+\,0\,-$	E^{-1}	–	E^1	–	–	–	E^1
$+\,0\,+\,0\,0$	E^{-2}	E^0	E^0	E^0	E^0	E^0	E^0
$+\,0\,+\,0\,+$	E^{-1}	E^1	E^1	E^1	–	–	E^1
$+\,0\,+\,+\,-$	E^{-2}	E^0	E^0	E^0	–	–	E^0
$+\,0\,+\,+\,0$	E^{-1}	E^1	E^1	E^1	–	–	E^1
$+\,0\,+\,+\,+$	E^{-2}	E^0	E^0	E^0	–	–	E^0
$+\,+\,-\,-\,-$	–	–	–	–	–	–	E^1
$+\,+\,-\,-\,0$	E^{-4}	E^0	E^0	–	–	–	E^0
$+\,+\,-\,-\,+$	E^{-3}	–	–	–	–	–	E^1
$+\,+\,-\,0\,-$	E^{-4}	E^0	E^0	–	–	–	E^0
$+\,+\,-\,0\,0$	E^{-3}	E^1	E^1	–	–	–	E^1
$+\,+\,-\,0\,+$	E^{-2}	E^0	E^0	–	–	–	E^0
$+\,+\,-\,+\,-$	E^{-3}	–	–	–	–	–	E^1
$+\,+\,-\,+\,0$	E^{-2}	E^0	E^0	–	–	–	E^0
$+\,+\,-\,+\,+$	E^{-1}	–	–	–	–	–	E^1
$+\,+\,0\,-\,-$	E^{-4}	E^0	E^0	–	–	–	E^0
$+\,+\,0\,-\,0$	E^{-3}	E^1	E^1	–	–	–	E^1
$+\,+\,0\,-\,+$	E^{-2}	E^0	E^0	–	–	–	E^0
$+\,+\,0\,0\,-$	E^{-3}	E^1	E^1	–	–	–	E^1
$+\,+\,0\,0\,0$	E^{-4}	E^0	–	–	–	–	–

$\lambda_W, \lambda_W, \lambda_Z, \lambda_Z, \lambda_Z$	SM	$\mathcal{O}_{\phi W}$	$\mathcal{O}_{\phi WB}$	$\mathcal{O}_{\phi BB}$	$\mathcal{O}_{\phi d}$	$\mathcal{O}_{\phi D}$	$\mathcal{O}_W$
+ + 0 0 +	E^{-1}	E^1	–	–	–	–	E^1
+ + 0 + −	E^{-2}	E^0	E^0	–	–	–	E^0
+ + 0 + 0	E^{-1}	E^1	–	–	–	–	E^1
+ + 0 + +	E^{-2}	E^0	E^0	–	–	–	E^0
+ + + − −	E^{-3}	–	–	–	–	–	E^1
+ + + − 0	E^{-2}	E^0	E^0	–	–	–	E^0
+ + + − +	E^{-1}	–	–	–	–	–	E^1
+ + + 0 −	E^{-2}	E^0	E^0	–	–	–	E^0
+ + + 0 0	E^{-1}	E^1	–	–	–	–	E^1
+ + + 0 +	E^{-2}	E^0	E^0	–	–	–	E^0
+ + + + −	E^{-1}	–	–	–	–	–	E^1
+ + + + 0	E^{-2}	E^0	E^0	–	–	–	E^0
+ + + + +	E^{-1}	–	–	–	–	–	E^1
0 − − − −	E^{-2}	E^0	E^0	E^0	–	–	E^0
0 − − − 0	E^{-1}	E^1	E^1	E^1	–	–	E^1
0 − − − +	E^{-2}	E^0	E^0	E^0	–	–	E^0
0 − − 0 −	E^{-1}	E^1	E^1	E^1	–	–	E^1
0 − − 0 0	E^{-2}	E^0	E^0	E^0	E^0	E^0	E^0
0 − − 0 +	E^{-1}	–	E^1	–	–	–	E^1
0 − − + −	E^{-2}	E^0	E^0	E^0	–	–	E^0
0 − − + 0	E^{-1}	–	E^1	–	–	–	E^1
0 − − + +	E^{-2}	E^0	E^0	E^0	–	–	E^0
0 − 0 − −	E^{-1}	E^1	E^1	E^1	–	–	E^1
0 − 0 − 0	E^{-2}	E^0	E^0	E^0	E^0	E^0	E^0
0 − 0 − +	E^{-1}	–	E^1	–	–	–	E^1
0 − 0 0 −	E^{-2}	E^0	E^0	E^0	E^0	E^0	E^0
0 − 0 0 0	E^{-1}	E^1	–	–	E^1	E^1	–
0 − 0 0 +	E^{-2}	E^0	E^0	E^0	E^0	E^0	E^0
0 − 0 + −	E^{-1}	–	E^1	–	–	–	E^1
0 − 0 + 0	E^{-2}	E^0	E^0	E^0	E^0	E^0	E^0
0 − 0 + +	E^{-3}	E^1	E^1	E^1	–	–	E^1
0 − + − −	E^{-2}	E^0	E^0	E^0	–	–	E^0
0 − + − 0	E^{-1}	–	E^1	–	–	–	E^1
0 − + − +	E^{-2}	E^0	E^0	E^0	–	–	E^0
0 − + 0 −	E^{-1}	–	E^1	–	–	–	E^1
0 − + 0 0	E^{-2}	E^0	E^0	E^0	E^0	E^0	E^0
0 − + 0 +	E^{-3}	E^1	E^1	E^1	–	–	E^1
0 − + + −	E^{-2}	E^0	E^0	E^0	–	–	E^0
0 − + + 0	E^{-3}	E^1	E^1	E^1	–	–	E^1
0 − + + +	E^{-4}	E^0	E^0	E^0	–	–	E^0
0 0 − − −	E^{-3}	E^1	E^1	E^1	–	–	–
0 0 − − 0	E^{-2}	E^0	E^0	E^0	E^0	E^0	E^0
0 0 − − +	E^{-1}	E^1	E^1	E^1	–	–	–
0 0 − 0 −	E^{-2}	E^0	E^0	E^0	E^0	E^0	E^0
0 0 − 0 0	E^{-1}	E^1	E^1	E^1	E^1	E^1	E^1
0 0 − 0 +	E^{-2}	E^0	E^0	E^0	E^0	E^0	E^0
0 0 − + −	E^{-1}	E^1	E^1	E^1	–	–	–
0 0 − + 0	E^{-2}	E^0	E^0	E^0	E^0	E^0	E^0
0 0 − + +	E^{-1}	E^1	E^1	E^1	–	–	–
0 0 0 − −	E^{-2}	E^0	E^0	E^0	E^0	E^0	E^0
0 0 0 − 0	E^{-1}	E^1	E^1	E^1	E^1	E^1	E^1
0 0 0 − +	E^{-2}	E^0	E^0	E^0	E^0	E^0	E^0
0 0 0 0 −	E^{-1}	E^1	E^1	E^1	E^1	E^1	–
0 0 0 0 0	E^{-2}	–	–	–	E^0	E^0	–

Table B.7: Helicity amplitudes in the high-energy limit ($s >> v$) for $W^+W^- \to ZZZ$. The missing helicity amplitudes behaviours are obtained by sending $\pm \to \mp$.

$\lambda_W, \lambda_W, \lambda_t, \lambda_t$	SM	$\mathcal{O}_{\phi Q}^{(1)}$	$\mathcal{O}_{\phi Q}^{(3)}$	$\mathcal{O}_{tB}$	$\mathcal{O}_{tW}$	$\mathcal{O}_{t\phi}$	$\mathcal{O}_{\phi t}$	$\mathcal{O}_{\phi W}$	$\mathcal{O}_{\phi WB}$	$\mathcal{O}_{\phi BB}$	$\mathcal{O}_{\phi d}$	$\mathcal{O}_{\phi D}$	$\mathcal{O}_W$
$+--+$	E^{-2}	E^0	E^0	–	E^0	–	–	E^0	E^0	–	–	–	E^0
$+---$	E^{-1}	–	–	–	E^1	–	–	–	–	–	–	–	–
$+-++$	E^{-1}	–	–	–	E^1	–	–	–	–	–	–	–	–
$+-+-$	E^{-2}	–	–	–	E^0	–	E^0	–	E^0	–	–	–	–
$+0-+$	E^{-1}	E^1	E^1	–	E^1	–	–	–	E^1	–	–	–	E^1
$+0--$	E^{-2}	E^0	E^0	E^0	E^0	E^0	E^0	E^0	E^0	–	E^0	E^0	E^0
$+0++$	E^{-2}	E^0	E^0	E^0	E^0	E^0	E^0	E^0	E^0	–	E^0	E^0	E^0
$+0+-$	E^{-1}	–	–	–	E^1	–	E^1	–	E^1	–	–	–	–
$++-+$	E^{-2}	E^0	E^0	–	E^0	–	–	E^0	E^0	–	–	–	E^0
$++--$	E^{-3}	–	–	–	E^1	–	–	E^1	–	–	–	–	E^1
$+++-$	E^{-1}	–	–	–	–	–	–	E^1	–	–	–	–	E^1
$+++-$	E^{-2}	–	–	–	E^0	–	E^0	–	E^0	–	–	–	E^0
$0--+$	E^{-1}	E^1	E^1	–	E^1	–	–	–	E^1	–	–	–	E^1
$0---$	E^{-2}	E^0	E^0	E^0	E^0	E^0	E^0	E^0	E^0	–	E^0	E^0	E^0
$0-++$	E^{-2}	E^0	E^0	E^0	E^0	E^0	E^0	E^0	E^0	–	E^0	E^0	E^0
$0-+-$	E^{-1}	–	–	–	E^1	–	E^1	–	E^1	–	–	–	–
$00-+$	E^{-2}	E^0	E^0	E^0	E^0	–	E^0	E^0	E^0	E^0	–	E^0	E^0
$00--$	E^{-1}	E^1	E^1	E^1	E^1	E^1	E^1	–	–	–	E^1	E^1	–
$00++$	E^{-1}	E^1	E^1	E^1	E^1	E^1	E^1	–	–	–	E^1	E^1	–
$00+-$	E^{-2}	E^0	E^0	E^0	E^0	E^0	E^0	–	E^0	E^0	–	E^0	–
$0+-+$	E^{-1}	E^1	E^1	–	–	–	–	–	E^1	–	–	–	E^1
$0+--$	E^{-2}	E^0	E^0	E^0	E^0	E^0	E^0	E^0	E^0	–	E^0	E^0	E^0
$0+++$	E^{-2}	E^0	E^0	E^0	E^0	E^0	E^0	E^0	E^0	–	E^0	E^0	E^0
$0++-$	E^{-1}	–	–	–	E^1	–	E^1	–	E^1	–	–	–	–
$---+$	E^{-2}	E^0	E^0	–	E^0	–	–	E^0	E^0	–	–	–	E^0
$----$	E^{-1}	–	–	–	–	–	–	E^1	–	–	–	–	E^1
$--++$	E^{-3}	–	–	–	E^1	–	–	E^1	–	–	–	–	E^1
$--+-$	E^{-2}	–	–	–	E^0	–	E^0	–	E^0	–	–	–	E^0
$-0-+$	E^{-1}	E^1	E^1	–	–	–	–	–	E^1	–	–	–	E^1
$-0--$	E^{-2}	E^0	E^0	E^0	E^0	E^0	E^0	E^0	E^0	–	E^0	E^0	E^0
$-0++$	E^{-2}	E^0	E^0	E^0	E^0	E^0	E^0	E^0	E^0	–	E^0	E^0	E^0
$-0+-$	E^{-1}	–	–	–	E^1	–	E^1	–	E^1	–	–	–	–
$-+-+$	E^{-2}	E^0	E^0	–	E^0	–	–	E^0	E^0	–	–	–	E^0
$-+--$	E^{-1}	–	–	–	E^1	–	–	–	–	–	–	–	–
$-+++$	E^{-1}	–	–	–	E^1	–	–	–	–	–	–	–	–
$-++-$	E^{-2}	–	–	–	E^0	–	E^0	–	E^0	–	–	–	–

Table B.8: Helicity amplitudes in the high-energy limit ($s >> v$) for $W^+W^- \to t\bar{t}H$.

$\lambda_W, \lambda_W, \lambda_t, \lambda_t, \lambda_Z$	SM	$\mathcal{O}_{\phi Q}^{(1)}$	$\mathcal{O}_{\phi Q}^{(3)}$	$\mathcal{O}_{tB}$	$\mathcal{O}_{tW}$	$\mathcal{O}_{t\phi}$	$\mathcal{O}_{\phi t}$	$\mathcal{O}_{\phi W}$	$\mathcal{O}_{\phi WB}$	$\mathcal{O}_{\phi BB}$	$\mathcal{O}_{\phi d}$	$\mathcal{O}_{\phi D}$	$\mathcal{O}_W$
$+--+-$	E^{-1}	–	–	–	–	–	–	–	–	–	–	–	E^1
$+--+0$	E^{-2}	E^0	E^0	–	E^0	–	–	–	E^0	–	–	–	E^0
$+--++$	E^{-1}	–	–	–	–	–	–	–	–	–	–	–	E^1
$+----$	E^{-2}	–	–	E^0	E^0	–	–	E^0	–	–	–	–	E^0
$+---0$	E^{-1}	–	–	–	E^1	–	–	–	–	–	–	–	–
$+----+$	E^{-2}	–	–	–	E^0	–	–	E^0	E^0	–	–	–	E^0
$+-++-$	E^{-2}	–	–	–	E^0	–	–	E^0	E^0	–	–	–	E^0
$+-++0$	E^{-1}	–	–	–	E^1	–	–	–	–	–	–	–	–
$+-+++$	E^{-2}	–	–	E^0	E^0	–	–	E^0	–	–	–	–	E^0
$+-+--$	E^{-3}	–	–	–	–	–	–	–	–	–	–	–	–
$+-+-0$	E^{-2}	–	–	–	E^0	–	E^0	–	E^0	–	–	–	–
$+-+-+$	E^{-3}	–	–	–	–	–	–	–	–	–	–	–	–
$+0-+-$	E^{-2}	E^0	E^0	E^0	E^0	–	–	–	E^0	–	–	–	E^0
$+0-+0$	E^{-1}	E^1	E^1	–	E^1	–	–	–	E^1	–	–	–	E^1

$\lambda_W, \lambda_W, \lambda_t, \lambda_t, \lambda_Z$	SM	$\mathcal{O}_{\phi Q}^{(1)}$	$\mathcal{O}_{\phi Q}^{(3)}$	$\mathcal{O}_{tB}$	$\mathcal{O}_{tW}$	$\mathcal{O}_{t\phi}$	$\mathcal{O}_{\phi t}$	$\mathcal{O}_{\phi W}$	$\mathcal{O}_{\phi WB}$	$\mathcal{O}_{\phi BB}$	$\mathcal{O}_{\phi d}$	$\mathcal{O}_{\phi D}$	$\mathcal{O}_W$
$+\,0\,-\,+\,+$	E^{-2}	E^0	E^0	E^0	E^0	–	–	–	E^0	–	–	–	E^0
$+\,0\,-\,-\,-$	E^{-3}	–	–	E^1	E^1	–	–	–	E^1	–	–	–	E^1
$+\,0\,-\,-\,0$	E^{-2}	E^0	E^0	E^0	E^0	E^0	E^0	E^0	E^0	–	E^0	E^0	E^0
$+\,0\,-\,-\,+$	E^{-1}	–	–	–	E^1	–	–	–	–	–	–	–	–
$+\,0\,+\,+\,-$	E^{-3}	–	–	–	–	–	–	–	–	–	–	–	–
$+\,0\,+\,+\,0$	E^{-2}	E^0	E^0	E^0	E^0	E^0	E^0	E^0	E^0	–	E^0	E^0	E^0
$+\,0\,+\,+\,+$	E^{-3}	–	–	–	–	–	–	–	–	–	–	–	–
$+\,0\,+\,-\,-$	E^{-2}	–	–	E^0	E^0	–	E^0	–	E^0	–	–	–	E^0
$+\,0\,+\,-\,0$	E^{-1}	–	–	–	E^1	–	E^1	–	E^1	–	–	–	–
$+\,0\,+\,-\,+$	E^{-2}	–	–	–	E^0	–	E^0	–	E^0	–	–	–	–
$+\,+\,-\,+\,-$	E^{-3}	–	–	–	–	–	–	–	–	–	–	–	E^1
$+\,+\,-\,+\,0$	E^{-2}	E^0	E^0	–	E^0	–	–	E^0	E^0	–	–	–	E^0
$+\,+\,-\,+\,+$	E^{-1}	–	–	–	–	–	–	–	–	–	–	–	E^1
$+\,+\,-\,-\,-$	E^{-4}	–	–	E^0	E^0	–	–	E^0	E^0	–	–	–	E^0
$+\,+\,-\,-\,0$	E^{-3}	–	–	–	E^1	–	–	E^1	–	–	–	–	E^1
$+\,+\,-\,-\,+$	E^{-2}	–	–	–	E^0	–	–	E^0	–	–	–	–	E^0
$+\,+\,+\,+\,-$	E^{-2}	–	–	–	–	–	–	E^0	E^0	–	–	–	E^0
$+\,+\,+\,+\,0$	E^{-1}	–	–	–	–	–	–	E^1	–	–	–	–	E^1
$+\,+\,+\,+\,+$	E^{-2}	–	–	E^0	E^0	–	–	E^0	–	–	–	–	E^0
$+\,+\,+\,-\,-$	E^{-3}	–	–	–	–	–	–	–	–	–	–	–	–
$+\,+\,+\,-\,0$	E^{-2}	–	–	–	E^0	–	E^0	E^0	E^0	–	–	–	–
$+\,+\,+\,-\,+$	E^{-3}	–	–	–	–	–	–	–	–	–	–	–	–
$0\,-\,-\,+\,-$	E^{-2}	E^0	E^0	E^0	E^0	–	–	–	E^0	–	–	–	E^0
$0\,-\,-\,+\,0$	E^{-1}	E^1	E^1	–	E^1	–	–	–	E^1	–	–	–	E^1
$0\,-\,-\,+\,+$	E^{-2}	E^0	E^0	E^0	E^0	–	–	–	E^0	–	–	–	E^0
$0\,-\,-\,-\,-$	E^{-3}	–	–	–	–	–	–	–	–	–	–	–	–
$0\,-\,-\,-\,0$	E^{-2}	E^0	E^0	E^0	E^0	E^0	E^0	E^0	E^0	–	E^0	E^0	E^0
$0\,-\,-\,-\,+$	E^{-3}	–	–	–	–	–	–	–	–	–	–	–	–
$0\,-\,+\,+\,-$	E^{-1}	–	–	–	E^1	–	–	–	–	–	–	–	–
$0\,-\,+\,+\,0$	E^{-2}	E^0	E^0	E^0	E^0	E^0	E^0	E^0	E^0	–	E^0	E^0	E^0
$0\,-\,+\,+\,+$	E^{-3}	–	–	E^1	E^1	–	–	–	E^1	–	–	–	E^1
$0\,-\,+\,-\,-$	E^{-2}	–	–	–	E^0	–	E^0	–	E^0	–	–	–	–
$0\,-\,+\,-\,0$	E^{-1}	–	–	–	E^1	–	E^1	–	E^1	–	–	–	–
$0\,-\,+\,-\,+$	E^{-2}	–	–	E^0	E^0	–	E^0	–	E^0	–	–	–	E^0
$0\,0\,-\,+\,-$	E^{-1}	E^1	E^1	–	–	–	–	E^1	E^1	E^1	–	–	–
$0\,0\,-\,+\,0$	E^{-2}	E^0	E^0	–	E^0	E^0	–	E^0	E^0	E^0	E^0	E^0	E^0
$0\,0\,-\,+\,+$	E^{-1}	E^1	E^1	–	–	–	–	E^1	E^1	E^1	–	–	–
$0\,0\,-\,-\,-$	E^{-2}	E^0	E^0	E^0	E^0	E^0	E^0	E^0	E^0	E^0	E^0	E^0	E^0
$0\,0\,-\,-\,0$	E^{-1}	E^1	E^1	E^1	E^1	E^1	E^1	–	–	–	E^1	E^1	–
$0\,0\,-\,-\,+$	E^{-2}	E^0	E^0	E^0	E^0	E^0	E^0	E^0	E^0	E^0	E^0	E^0	E^0
$0\,0\,+\,+\,-$	E^{-2}	E^0	E^0	E^0	E^0	E^0	E^0	E^0	E^0	E^0	E^0	E^0	E^0
$0\,0\,+\,+\,0$	E^{-1}	E^1	E^1	E^1	E^1	E^1	E^1	–	–	–	E^1	E^1	–
$0\,0\,+\,+\,+$	E^{-2}	E^0	E^0	E^0	E^0	E^0	E^0	E^0	E^0	E^0	E^0	E^0	E^0
$0\,0\,+\,-\,-$	E^{-1}	–	–	E^1	E^1	–	E^1	–	E^1	E^1	–	–	–
$0\,0\,+\,-\,0$	E^{-2}	E^0	E^0	E^0	E^0	E^0	E^0	–	E^0	E^0	E^0	E^0	–
$0\,0\,+\,-\,+$	E^{-1}	–	–	E^1	E^1	–	E^1	–	E^1	E^1	–	–	–
$0\,+\,-\,+\,-$	E^{-2}	E^0	E^0	E^0	E^0	–	–	–	E^0	–	–	–	E^0
$0\,+\,-\,+\,0$	E^{-1}	E^1	E^1	–	–	–	–	–	E^1	–	–	–	E^1
$0\,+\,-\,+\,+$	E^{-2}	E^0	E^0	E^0	E^0	–	–	–	E^0	–	–	–	E^0
$0\,+\,-\,-\,-$	E^{-3}	–	–	–	–	–	–	–	–	–	–	–	–
$0\,+\,-\,-\,0$	E^{-2}	E^0	E^0	E^0	E^0	E^0	E^0	E^0	E^0	–	E^0	E^0	E^0
$0\,+\,-\,-\,+$	E^{-3}	–	–	–	–	–	–	–	–	–	–	–	–
$0\,+\,+\,+\,-$	E^{-1}	–	–	–	–	–	–	–	E^1	–	–	–	E^1
$0\,+\,+\,+\,0$	E^{-2}	E^0	E^0	E^0	E^0	E^0	E^0	E^0	E^0	–	E^0	E^0	E^0
$0\,+\,+\,+\,+$	E^{-1}	–	–	E^1	E^1	–	–	–	–	–	–	–	–
$0\,+\,+\,-\,-$	E^{-2}	–	–	E^0	E^0	–	E^0	–	E^0	–	–	–	E^0
$0\,+\,+\,-\,0$	E^{-1}	–	–	–	E^1	–	E^1	–	E^1	–	–	–	–
$0\,+\,+\,-\,+$	E^{-2}	–	–	E^0	E^0	–	E^0	–	E^0	–	–	–	–
$-\,-\,-\,+\,-$	E^{-1}	–	–	–	–	–	–	–	–	–	–	–	E^1

$\lambda_W, \lambda_W, \lambda_t, \lambda_t, \lambda_Z$	SM	$\mathcal{O}_{\phi Q}^{(1)}$	$\mathcal{O}_{\phi Q}^{(3)}$	$\mathcal{O}_{tB}$	$\mathcal{O}_{tW}$	$\mathcal{O}_{t\phi}$	$\mathcal{O}_{\phi t}$	$\mathcal{O}_{\phi W}$	$\mathcal{O}_{\phi WB}$	$\mathcal{O}_{\phi BB}$	$\mathcal{O}_{\phi d}$	$\mathcal{O}_{\phi D}$	$\mathcal{O}_W$
$- - - + 0$	E^{-2}	E^0	E^0	–	E^0	–	–	E^0	E^0	–	–	–	E^0
$- - - + +$	E^{-3}	–	–	–	–	–	–	–	–	–	–	–	E^1
$- - - - -$	E^{-2}	–	–	E^0	E^0	–	–	E^0	–	–	–	–	E^0
$- - - - 0$	E^{-1}	–	–	–	–	–	–	E^1	–	–	–	–	E^1
$- - - - +$	E^{-2}	–	–	–	–	–	–	E^0	E^0	–	–	–	E^0
$- - + + -$	E^{-2}	–	–	–	E^0	–	–	E^0	–	–	–	–	E^0
$- - + + 0$	E^{-3}	–	–	–	E^1	–	–	E^1	–	–	–	–	E^1
$- - + + +$	E^{-4}	–	–	E^0	E^0	–	–	E^0	E^0	–	–	–	E^0
$- - + - -$	E^{-3}	–	–	–	–	–	–	–	–	–	–	–	–
$- - + - 0$	E^{-2}	–	–	–	E^0	–	E^0	E^0	E^0	–	–	–	–
$- - + - +$	E^{-3}	–	–	–	–	–	–	–	–	–	–	–	–
$- 0 - + -$	E^{-2}	E^0	E^0	E^0	E^0	–	–	–	E^0	–	–	–	E^0
$- 0 - + 0$	E^{-1}	E^1	E^1	–	–	–	–	–	E^1	–	–	–	E^1
$- 0 - + +$	E^{-2}	E^0	E^0	E^0	E^0	–	–	–	E^0	–	–	–	E^0
$- 0 - - -$	E^{-1}	–	–	E^1	E^1	–	–	–	–	–	–	–	–
$- 0 - - 0$	E^{-2}	E^0	E^0	E^0	E^0	E^0	E^0	E^0	E^0	–	E^0	E^0	E^0
$- 0 - - +$	E^{-1}	–	–	–	–	–	–	–	E^1	–	–	–	E^1
$- 0 + + -$	E^{-3}	–	–	–	–	–	–	–	–	–	–	–	–
$- 0 + + 0$	E^{-2}	E^0	E^0	E^0	E^0	E^0	E^0	E^0	E^0	–	E^0	E^0	E^0
$- 0 + + +$	E^{-3}	–	–	–	–	–	–	–	–	–	–	–	–
$- 0 + - -$	E^{-2}	–	–	E^0	E^0	–	E^0	–	E^0	–	–	–	–
$- 0 + - 0$	E^{-1}	–	–	–	E^1	–	E^1	–	E^1	–	–	–	–
$- 0 + - +$	E^{-2}	–	–	E^0	E^0	–	E^0	–	E^0	–	–	–	E^0
$- + - + -$	E^{-1}	–	–	–	–	–	–	–	–	–	–	–	E^1
$- + - + 0$	E^{-2}	E^0	E^0	–	E^0	–	–	–	E^0	–	–	–	E^0
$- + - + +$	E^{-1}	–	–	–	–	–	–	–	–	–	–	–	E^1
$- + - - -$	E^{-2}	–	–	E^0	E^0	–	–	E^0	E^0	–	–	–	E^0
$- + - - 0$	E^{-1}	–	–	–	E^1	–	–	–	–	–	–	–	–
$- + - - +$	E^{-2}	–	–	–	E^0	–	–	E^0	–	–	–	–	E^0
$- + + + -$	E^{-2}	–	–	–	E^0	–	–	E^0	–	–	–	–	E^0
$- + + + 0$	E^{-1}	–	–	–	E^1	–	–	–	–	–	–	–	–
$- + + + +$	E^{-2}	–	–	E^0	E^0	–	–	E^0	E^0	–	–	–	E^0
$- + + - -$	E^{-3}	–	–	–	–	–	–	–	–	–	–	–	–
$- + + - 0$	E^{-2}	–	–	–	E^0	–	E^0	–	E^0	–	–	–	–
$- + + - +$	E^{-3}	–	–	–	–	–	–	–	–	–	–	–	–

Table B.9: Helicity amplitudes in the high-energy limit ($s >> v$) for $W^+W^- \to t\bar{t}Z$.

$\lambda_Z, \lambda_Z, \lambda_t, \lambda_t$	SM	$\mathcal{O}_{\phi Q}^{(1)}$	$\mathcal{O}_{\phi Q}^{(3)}$	$\mathcal{O}_{tB}$	$\mathcal{O}_{tW}$	$\mathcal{O}_{t\phi}$	$\mathcal{O}_{\phi t}$	$\mathcal{O}_{\phi W}$	$\mathcal{O}_{\phi WB}$	$\mathcal{O}_{\phi BB}$	$\mathcal{O}_{\phi d}$	$\mathcal{O}_{\phi D}$
$- - - +$	E^{-2}	E^0	E^0	E^0	E^0	–	–	E^0	E^0	E^0	–	–
$- - - -$	E^{-1}	–	–	–	–	–	–	E^1	E^1	E^1	–	–
$- - + +$	E^{-3}	–	–	E^1	E^1	–	–	E^1	E^1	E^1	–	–
$- - + -$	E^{-2}	–	–	E^0	E^0	–	E^0	–	E^0	E^0	–	–
$- 0 - +$	E^{-1}	E^1	E^1	E^1	E^1	–	–	–	–	–	–	–
$- 0 - -$	E^{-2}	E^0	E^0	E^0	E^0	E^0	E^0	E^0	E^0	E^0	E^0	E^0
$- 0 + +$	E^{-2}	E^0	E^0	E^0	E^0	E^0	E^0	E^0	E^0	E^0	E^0	E^0
$- 0 + -$	E^{-1}	–	–	E^1	E^1	–	E^1	–	–	–	–	–
$- + - +$	E^{-2}	E^0	E^0	E^0	E^0	–	–	E^0	E^0	E^0	–	–
$- + - -$	E^{-1}	–	–	E^1	E^1	–	–	–	–	–	–	–
$- + + +$	E^{-1}	–	–	E^1	E^1	–	–	–	–	–	–	–
$- + + -$	E^{-2}	–	–	E^0	E^0	–	E^0	–	E^0	E^0	–	–
$0 - - +$	E^{-1}	E^1	E^1	E^1	E^1	–	–	–	–	–	–	–
$0 - - -$	E^{-2}	E^0	E^0	E^0	E^0	E^0	E^0	E^0	E^0	E^0	E^0	E^0
$0 - + +$	E^{-2}	E^0	E^0	E^0	E^0	E^0	E^0	E^0	E^0	E^0	E^0	E^0
$0 - + -$	E^{-1}	–	–	E^1	E^1	–	E^1	–	–	–	–	–
$0\,0 - +$	–	–	–	–	–	–	–	–	–	–	–	–
$0\,0 - -$	E^{-1}	E^1	E^1	E^1	E^1	E^1	E^1	–	–	–	E^1	E^1

Table B.10: Helicity amplitudes in the high-energy limit ($s >> v$) for $ZZ \to t\bar{t}H$. The missing helicity amplitudes behaviours are obtained by sending $\pm \to \mp$.

$\lambda_Z, \lambda_Z, \lambda_t, \lambda_t, \lambda_Z$	SM	$\mathcal{O}_{\phi Q}^{(1)}$	$\mathcal{O}_{\phi Q}^{(3)}$	$\mathcal{O}_{tB}$	$\mathcal{O}_{tW}$	$\mathcal{O}_{t\phi}$	$\mathcal{O}_{\phi t}$	$\mathcal{O}_{\phi W}$	$\mathcal{O}_{\phi WB}$	$\mathcal{O}_{\phi BB}$	$\mathcal{O}_{\phi d}$	$\mathcal{O}_{\phi D}$
$- - - + -$	E^{-1}	–	–	–	–	–	–	–	–	–	–	–
$- - - + 0$	E^{-2}	E^0	E^0	E^0	E^0	–	–	E^0	E^0	E^0	–	–
$- - - + +$	E^{-3}	–	–	–	–	–	–	–	–	–	–	–
$- - - - -$	E^{-2}	–	–	E^0	E^0	–	–	E^0	E^0	E^0	–	–
$- - - - 0$	E^{-1}	–	–	–	–	–	–	E^1	E^1	E^1	–	–
$- - - - +$	E^{-2}	–	–	–	–	–	–	E^0	E^0	E^0	–	–
$- - + + -$	E^{-2}	–	–	E^0	E^0	–	–	E^0	E^0	E^0	–	–
$- - + + 0$	E^{-3}	–	–	E^1	E^1	–	–	E^1	E^1	E^1	–	–
$- - + + +$	E^{-4}	–	–	E^0	E^0	–	–	E^0	E^0	E^0	–	–
$- - + - -$	E^{-1}	–	–	–	–	–	–	–	–	–	–	–
$- - + - 0$	E^{-2}	–	–	E^0	E^0	–	E^0	E^0	E^0	E^0	–	–
$- - + - +$	E^{-3}	–	–	–	–	–	–	–	–	–	–	–
$- 0 - + -$	E^{-2}	E^0	E^0	E^0	E^0	–	–	E^0	E^0	E^0	–	–
$- 0 - + 0$	E^{-1}	E^1	E^1	E^1	E^1	–	–	E^1	E^1	E^1	–	–
$- 0 - + +$	E^{-2}	E^0	E^0	E^0	E^0	–	–	E^0	E^0	E^0	–	–
$- 0 - - -$	E^{-1}	–	–	E^1	E^1	–	–	–	–	–	–	–
$- 0 - - 0$	E^{-2}	E^0	E^0	E^0	E^0	E^0	E^0	E^0	E^0	E^0	E^0	E^0
$- 0 - - +$	E^{-1}	–	–	–	–	–	–	E^1	E^1	E^1	–	–
$- 0 + + -$	E^{-1}	–	–	E^1	E^1	–	–	–	–	–	–	–
$- 0 + + 0$	E^{-2}	E^0	E^0	E^0	E^0	E^0	E^0	E^0	E^0	E^0	E^0	E^0
$- 0 + + +$	E^{-3}	–	–	E^1	E^1	–	–	E^1	E^1	E^1	–	–
$- 0 + - -$	E^{-2}	–	–	E^0	E^0	–	E^0	–	E^0	E^0	–	–
$- 0 + - 0$	E^{-1}	–	–	E^1	E^1	–	E^1	–	E^1	E^1	–	–
$- 0 + - +$	E^{-2}	–	–	E^0	E^0	–	E^0	E^0	E^0	E^0	–	–
$- + - + -$	E^{-1}	–	–	–	–	–	–	–	–	–	–	–
$- + - + 0$	E^{-2}	E^0	E^0	E^0	E^0	–	–	E^0	E^0	E^0	–	–
$- + - + +$	E^{-1}	–	–	–	–	–	–	–	–	–	–	–
$- + - - -$	E^{-2}	–	–	E^0	E^0	–	–	E^0	E^0	E^0	–	–
$- + - - 0$	E^{-1}	–	–	E^1	E^1	–	–	–	–	–	–	–
$- + - - +$	E^{-2}	–	–	E^0	E^0	–	–	E^0	E^0	E^0	–	–
$- + + + -$	E^{-2}	–	–	E^0	E^0	–	–	E^0	E^0	E^0	–	–

$\lambda_Z, \lambda_Z, \lambda_t, \lambda_t, \lambda_Z$	SM	$\mathcal{O}_{\phi Q}^{(1)}$	$\mathcal{O}_{\phi Q}^{(3)}$	$\mathcal{O}_{tB}$	$\mathcal{O}_{tW}$	$\mathcal{O}_{t\phi}$	$\mathcal{O}_{\phi t}$	$\mathcal{O}_{\phi W}$	$\mathcal{O}_{\phi WB}$	$\mathcal{O}_{\phi BB}$	$\mathcal{O}_{\phi d}$	$\mathcal{O}_{\phi D}$
$-++0$	E^{-1}	–	–	E^1	E^1	–	–	–	–	–	–	–
$-+++$	E^{-2}	–	–	E^0	E^0	–	–	E^0	E^0	E^0	–	–
$-+--$	E^{-1}	–	–	–	–	–	–	–	–	–	–	–
$-+-0$	E^{-2}	–	–	E^0	E^0	–	E^0	–	E^0	E^0	–	–
$-+-+$	E^{-1}	–	–	–	–	–	–	–	–	–	–	–
$0--+-$	E^{-2}	E^0	E^0	E^0	E^0	–	–	E^0	E^0	E^0	–	–
$0--+0$	E^{-1}	E^1	E^1	E^1	E^1	–	–	E^1	E^1	E^1	–	–
$0--++$	E^{-2}	E^0	E^0	E^0	E^0	–	–	E^0	E^0	E^0	–	–
$0---$	E^{-1}	–	–	E^1	E^1	–	–	–	–	–	–	–
$0---0$	E^{-2}	E^0	E^0	E^0	E^0	E^0	E^0	E^0	E^0	E^0	E^0	E^0
$0---+$	E^{-1}	–	–	–	–	–	–	E^1	E^1	E^1	–	–
$0-+-$	E^{-1}	–	–	E^1	E^1	–	–	–	–	–	–	–
$0-+-0$	E^{-2}	E^0	E^0	E^0	E^0	E^0	E^0	E^0	E^0	E^0	E^0	E^0
$0-++$	E^{-3}	–	–	E^1	E^1	–	–	E^1	E^1	E^1	–	–
$0-+--$	E^{-2}	–	–	E^0	E^0	–	E^0	–	E^0	E^0	–	–
$0-+-0$	E^{-1}	–	–	E^1	E^1	–	E^1	–	E^1	E^1	–	–
$0-+-+$	E^{-2}	–	–	E^0	E^0	–	E^0	E^0	E^0	E^0	–	–
$00-+-$	E^{-1}	E^1	E^1	E^1	E^1	–	–	E^1	E^1	E^1	–	–
$00-+0$	E^{-2}	E^0	E^0	E^0	E^0	E^0	E^0	E^0	E^0	E^0	E^0	E^0
$00-++$	E^{-1}	E^1	E^1	E^1	E^1	–	–	E^1	E^1	E^1	–	–
$00---$	E^{-2}	E^0	E^0	E^0	E^0	E^0	E^0	E^0	E^0	E^0	E^0	E^0
$00--0$	E^{-1}	–	–	–	–	E^1	–	–	–	–	E^1	E^1
$00--+$	E^{-2}	E^0	E^0	E^0	E^0	E^0	E^0	E^0	E^0	E^0	E^0	E^0

Table B.11: Helicity amplitudes in the high-energy limit ($s >> v$) for $ZZ \to t\bar{t}Z$. The missing helicity amplitudes behaviours are obtained by sending $\pm \to \mp$.

Bibliography

[1] Michael E. Peskin, Daniel V. Schröder *An Introduction to Quantum Field Theory*, Addinson-Wesley Publishing Company (1995)

[2] R. Soldati, *"Advances in Quantum Field Theory"*, www.robertosoldati.com

[3] I. J. J.Iliopoulos, *"Introduction to the STANDARD MODEL of the Electro-Weak Interactions"*, 2012 CERN Summer School, June 2012, arXiv:1305.6779v1

[4] Y. Nambu, *"Axial Vector Current Conservation in Weak Interactions"*, Physical Review Letters 4 (1960) 380-382

[5] J. Goldstone, *"Field Theories with Superconductor Solutions"*, Il Nuovo Cimento 19 (1961) 154-164

[6] J. Goldstone, A. Salam and S. Weinberg, *"Broken Symmetries"*, Physical Review 127 (1962) 965-970

[7] P. W. Higgs, *Broken Symmetries, Massless Particles and Gauge Fields*,Physics Letters B12 (1964) 132-133;
Broken Symmetries and the Masses of Gauge Bosons, Physical Review Letters 13 (1964) 508-509

[8] R. Brout, F. Englert, *Broken Symmetries and the Mass of Gauge Vector Mesons*, Physical Review Letters 13 (1964) 321-323

[9] S. L. Glashow, *Partial Symmetries of Weak Interactions*, Nuclear Physics 22, 579

[10] M. Kobayashi, T. Maskawa *CP-Violation in the Renormalizable Theory of Weak Interactions*, (1973) Progress of Theoretical Physics 49, 652-657

[11] Andrea Wulzer (2019), *Behind the Standard Model*, https://arxiv.org/abs/1901.01017

[12] Grzadkowski B., Iskrzynski M., Misiak M. and Rosiek J.(2010), *Dimension-Six Terms in the Standard Model Lagrangian*. JHEP, 1010, 085

[13] Aneesh V. Manohar (2018), *Introduction to Effective Field Theories*,https://arxiv.org/abs/1804.05863

[14] Ben Gripaios (2015),*Lectures on Effective Field Theories*, https://arxiv.org/abs/1506.05039

[15] Witold Skiba (2010), *TASI Lectures on Effective Field Theories and Precision Electroweak Measurements*, https://arxiv.org/abs/1006.2142

[16] Lehmann, H., Symanzik, K., and Zimmermann, W. (1955). *On the formulation of quantized field theories*. Nuovo Cim., 1, 205-225.

[17] S. Weinberg, Phys. Rev. Lett.43(1979) 1566

[18] Jenkins E. E., Manohar A. V., Trott M. (2013), *Renormalization Group Evolution of the Standard Model Dimension Six Operators I: Formalism and λ Dependence*, arXiv:1308.2627v3 [hep-ph] 23 Oct 2013

[19] Jenkins E. E., Manohar A. V., Trott M. (2015), *Renormalization Group Evolution of the Standard Model Dimension Six Operators II: Yukawa Dependence*, arXiv:1310.4838v2 [hep-ph] 27 Jul 2015

[20] Jenkins E. E., Manohar A. V., Trott M. (2015), *Renormalization Group Evolution of the Standard Model Dimension Six Operators III: Gauge Coupling Dependence and Phenomenology*, arXiv:1312.2014v3 [hep-ph] 27 Jul 2015

[21] Kobach A. (2016), *Baryon Number, Lepton Number, and Operator Dimension in the Standard Model*, Phys. Lett., B758, 455-457

[22] Buchuller W, Wyler D. (1986), *Effective Lagrangian Analysis of New Interactions and Flavor Conservation*, Nucl. Phys., B268, 621

[23] B. Grinstein, M. B. Wise, *Operator analysis for precision electroweak physics*, Phys. Lett. B265 (1991), 326-334

[24] C. M. Becchi, A.Rouet, Raymond Stora, *The abelian Higgs Kibble model, unitarity of the S-operator*, Physics Letters 52B, 344 ()1974

[25] J. C. Taylor, *Ward identities and charge renormalization of the Yang-Mills Fields*, Nucl.Phys. b££, 173-199 (1971)

[26] J. M. Cornwall, D. N. Levin, G. Tiktopoulos, Phys. Rev. D10, 1145 (1974)

[27] C. E. Vayonakis, Lett. Nuov. Cim. 17, 383 (1976)

[28] M. S. Chanowitz and M. K. Gaillard, Nucl. Phys. B261, 379 (1985)

[29] R. E. Cutkosky, J. Math. Phys. 1, 429 (1960)

[30] J. M. Cornwall, D. N. Levin and G. Tiktopoulos, Phys. Rev. D 10 (1974) 1145.

[31] J. C. Romão, *A resource for signs and Feynman diagrams of the Standard Model*, arXiv: 1209.6213 [hep-ph]

[32] F. Maltoni, L. Mantani, K. Mimasu, *Top-quark electroweak interactions at high-energy*, arXiv:1904.05637v1 [hep-ph], (2019)

[33] http://feynrules.irmp.ucl.ac.be/wiki/SMEFTatNLO

[34] J. Ellis, C. W. Murphy, V. Sanz, and T. You, *Updated Global SMEFT Fit to Higgs, Diboson and Electroweak Data*, JHEP 06 (2018) 146, arXiv:1803.03252 [hep-ph]

[35] N. P. Hartland, F. Maltoni, E. R. Nocera, J. Rojo, E. Slade, E. Vryonidou, and C. Zhang, *A Monte Carlo global analysis of the Standard Model Effective Field Theory: the top quark sector*, arXiv:1901.05965 [hep-ph]

[36] A. Buckley, C. Englert, J. Ferrando, D. J. Miller, L. Moore, M. Russell, and C. D. White, *Constraining top quark effective theory in the LHC Run II era*, JHEP 04 (2016) 015, arXiv:1512.03360 [hep-ph]

[37] A. Butter, O. J. P. Eboli, J. Gonzalez-Fraile, M. C. Gonzalez-Garcia, T. Plehn, and M. Rauch, *The Gauge-Higgs Legacy of the LHC Run I*, JHEP 07 (2016) 152, arXiv:1604.03105 [hep-ph]

[38] J. Alwall, M. Herquet, F. Maltoni, O. Mattelaer, and T. Stelzer, *MadGraph 5 : Going Beyond*, JHEP 06 (2011) 128, arXiv:1106.0522 [hep-ph]

[39] J. Alwall, R. Frederix, S. Frixione, V. Hirschi, F. Maltoni, O. Mattelaer, H. S. Shao, T. Stelzer, P. Torrielli, and M. Zaro, *The automated computation of tree-level and next-to-leading order differential cross sections, and their matching to parton shower simulations*, JHEP 07 (2014) 079, arXiv:1405.0301 [hep-ph].

[40] T. Hahn, Comput. Phys. Commun. 140 (2001) 418 [hep-ph/0012260]

[41] V. Shtabovenko, R. Mertig and F. Orellana, Comput. Phys. Commun., 207C, 432-444, 2016, arXiv:1601.01167; R. Mertig, M. Böhm, and A. Denner, Comput. Phys. Commun., 64, 345-359, 1991

[42] E .Byckling, K. Kajantie, *Particle Kinematics*, John Wiley & Sons, 1973

[43] A. Azatov, R. Contino, C. S. Machado, F. Riva, *Helicity Selection Rules and Non-Interference for BSM Amplitudes* arXiv: 1607.05236v1 [hep-ph], 2016

[44] F. Coradeschi, P. Lodone, *Selection rules for helicity amplitudes in massive gauge theories*, arXiv:1211.1880v3 [hep-ph] (2013)

[45] P. Borel, R. Franceschini, R. Rattazzi and A. Wulzer, JHEP 1206 (2012) 122 arXiv:1202.1904

[46] *The Compact Linear Collider (CLIC) - 2018 Summary Report*, https://arxiv.org/abs/1812.06018

[47] *The CLIC Potential for New Physics*, https://arxiv.org/abs/1812.02093

[48] *Muon Collider*, arXiv:1901.06150v1 [physics.acc-ph] (2019)

[49] *Higgs Boson studies at future particle colliders*, arXiv:1905.03764v1 [hep-ph] (2019)

[50] N. Arkani-Hamed, T. Han, M. Mangano and L. T. Wang, *Physics opportunities of a 100 TeV proton-proton collider*, Phys. Rept. 652 (2016) 1, [arXiv:1511.06495].

[51] B. Henning, D. Lombardo, M. Riembau, and F. Riva *Higgs Couplings without the Higgs*, arXiv:1812.09299v1 [hep-ph] (2018)